2015

RELATIVISTIC CONFIGURATION INTERACTION CALCULATIONS OF THE ATOMIC PROPERTIES OF SELECTED TRANSITION METAL POSITIVE IONS; NI II, V II AND W II

Marwa Hefny Abdalmoneam
Michigan Technological University, mhabdalm@mtu.edu

RELATIVISTIC CONFIGURATION INTERACTION CALCULATIONS OF THE ATOMIC PROPERTIES OF SELECTED TRANSITION METAL POSITIVE IONS; Ni II, V II AND W II

By

Marwa Hefny Abdalmoneam

A DISSERTATION

Submitted in partial fulfillment of the requirements for the degree of

DOCTOR OF PHILOSOPHY

In Physics

MICHIGAN TECHNOLOGICAL UNIVERSITY

2015

This dissertation has been approved in partial fulfillment of the requirements for the Degree of DOCTOR OF PHILOSOPHY in Physics.

Department of Physics

Dissertation Advisor:	*Prof. Dr. Donald R. Beck*
Committee Member:	*Prof. Dr. Ravindra Pandey*
Committee Member:	*Prof. Dr. Ranjit Pati*
Committee Member:	*Prof. Dr. Loredana Valenzano*
Department Chair:	*Prof. Dr. Ravindra Pandey*

Table of Contents

List of Figures

List of Tables

Acknowledgments

I'd like to thank Dr. Beck for accepting me in his research group, for teaching me atomic physics, for being patient with me while learning how to use the RCI codes and for all his guidance while studying the different projects. He supported me going to conferences and presenting our results which had great impact on my confidence as a researcher, as it helped me to compare the RCI methodology to other available computational methods and it helped me to see the importance of our computation methodology and the value of our results in the scientific community. Another help was that Dr. Beck formed his group as a supportive and cooperative not competitive group. Within the group I met Dr. Lin Pan, who was doing her post-doctoral research and lecturing at Michigan Tech, and she was very busy researcher. But she gave me a lot of help, much more than I would expect from any team worker. Her instructions to me when I joined the group and for the first 6 months were so helpful and essential in my learning process. After she moved to Cedarville University she continued helping me through emails and Skype meetings. I would like to acknowledge the National Science Foundation for partial support of the three projects that appear in this study.

Thanks for the committee members for putting the time and effort to read this study and giving their useful comments.

I am so thankful to Dr. Pandey, whose help to me is undeniable. We met in a Solid State International Conference in Cairo, Egypt, in November 2008. As I was planning for a simple friendly discussion with the solid state professor who was visiting Egypt for the first time and having his family with him to see the pyramids he kindly asked me about my masters study and took the discussion into another dimension, telling me about Michigan Tech, and Houghton. On the last day of the conference, as I was giving him a little souvenir and saying good bye, he did not say good-bye. He made a generous offer to support me as a PhD student at Michigan Tech. At that moment I was expecting for a short friendly talk ending our meeting in Egypt. But this smart, kind professor seemed to be one who did not like simple ends. He invited me to start a new chapter in my life as a

researcher and as a person. He explained to me how to apply to the Physics Department in MTU. I replied with hesitation as I did not have the TOEFL Score, or the GRE, and my certificates were all in Arabic. He did not stop at these obstacles, but went through explaining what to do step by step, and he ended his talk by saying “I believe in you”. Now in August 2015 I have to say “Thank you Dr. Pandey, from the deepest point in my heart I am thankful for your encouragement, your support and mentoring for 6 years”.

I’d like to thank Douglas Banyai for his kindness and cooperation; he was always there when I asked for help during studying the courses, practicing for presentations, and computer problems.

I thank Kathy Wollan, for replying to my emails while I was applying in the physics department for the PhD. Her replies were always clearly informative and helpful and I felt so welcomed in the department. I thank Andrea Lappi, she has been always doing more beyond what could be expected from a department coordinator and this had eased many things for me for my 6 years in the physics department.

My very special thanks are to my mum, dad, and my sisters as they have borne the difficulty of my departure away from them. As for my mum, Sondus Mansour, she has my gratitude because she taught me mathematics and science and through her I learned that a woman must be smart, no other option. My father, Hefny, had deeply supported me in my university studies for many years I never needed to take any loans as he was supporting everything. When I told him that I was accepted for a PhD study in USA he just smiled. I appreciate that smile because it was not common or easy for an eastern man to let his daughter travel alone for that long. It was his belief in me as a researcher, his love, support, and smile that made me able to come to The States and do this PhD. Maha and Manar, never blamed their eldest sister for leaving them and have been always kind to me.

Above All I have the absolute gratitude to Allah, as He gave me my heart, my brain, and my eyes and I enjoy life as I see it and understand it through this heart and this brain.

Abstract

Relativistic Configuration Interaction (RCI) method has been used to investigate atomic properties of the singly ionized transition metals including Nickel (Ni II), Vanadium (V II), and Tungsten (W II). The methodology of RCI computations was also improved. Specifically, the method to shift the energy diagonal matrix of the reference configurations was modified which facilitated including the effects of many electronic configurations that used to be difficult to be included in the energy matrix and speeded-up the final calculations of the bound and continuum energy spectrum. RCI results were obtained for three different cases:

i. Atomic moments and polarizabilities of Ni II;
ii. Hyperfine structure constants of V II;
iii. Lifetime, Lande g-values, and Oscillator strength of W II.

Four atomic quantities of Ni II were calculated; scalar dipole polarizability, off-diagonal electric dipole polarizability, non-adiabatic scalar dipole polarizability, and quadrupole polarizability of Ni II. These quantities appear as effective parameters in an effective potential model. These quantities are computed for the first time.

The two hyperfine structure (HFS) constants ; magnetic dipole interaction constant, A, and the electric quadrupole interaction constant, B, have been calculated for the V II $3d^4$, $3d^3$ 4s, and $3d^2$ $4s^2$ J=1 to 5 even parity states . Analysis of the results shows the sum of HFS A of nearby energy levels to be conserved. The Lande g-value and the vector composition percentages for all the wavefunctions of those configurations have also been calculated. RCI results are in good agreement with most of the available experimental data.

Lifetimes of 175 decay branches in W II have been calculated. Also, Lande g-values have been calculated for all measured W II odd parity levels J=1/2-11/2. The RCI oscillator strengths and branching fraction values of the lowest 10 energy levels for each odd parity J are presented. The calculated results are only in semi-quantitative agreement with experiment for the oscillator strength and branching fractions. However the calculated lifetimes and Lande g-values are in very good agreement with the available

measured quantities. We found the sums of lifetimes and the sums of Lande g-values of the nearby levels were almost independent of the calculation stage.

The calculated atomic properties for Ni II, V II, and W II fill in many gaps in the available atomic data for these three ions. Also, they are expected to facilitate the fundamental understanding of electric and magnetic behaviors of most of the transition metal ions and atoms with similar electronic configurations.

Introduction

This is a computational study of some atomic properties of the singly positive ions of Nickel, Vanadium, and Tungsten using the relativistic configuration interaction methodology that is implemented in the computer programs created by Beck and his group. The selection of these ions was based on three criteria; it was interesting to the scientific community, as only a few recent accurate measurements were available on these ions, more accurate data was needed because of large errors were present in the available calculations, and to further develop the atomic relativistic correlation methodology used by Beck's research group. Work on each of these extended for more than 1 year and led to two referred papers and three poster presentations in two annual meetings.

This dissertation includes four chapters. The first one gives a general background about the relativistic configuration interaction method and how it was developed and implemented by Beck in a series of computer programs. Most of the computational studies recently are done using computer packages that hide the mathematical details from the user and focus on the final results. One main advantage of the widely used computer packages is the employment of large matrix sizes for calculations. The disadvantage is the loss of most of the physics during the process of the intermediate calculations, where only the input and final output have physical interpretations. The RCI programs that we use employ matrix sizes of 20K with 60 eigenvalues at most, which is small in comparison to many available programs. The advantage of using our RCI programs is the very direct relations between the physics and most of the steps of calculations. This gives room for improving each step of calculations based on understanding the physics details in each problem. Also, the physical and computational details which might be lost because of the small matrix size can be compensated through different approaches. One approach is by doing separate calculations and using their results to shift the diagonal matrix elements in the final energy matrix. A second approach is splitting the calculation into multiple steps (e.g. splitting the Rydberg states into two parts in Ni II where one set of calculation included 4p to 8p the other included

9p to 14 p sub-shells). Thus the limited number of eigenvalues obtained does not stop us from doing the required physics and getting to the required accuracy.

Singly ionized Nickel, Ni II was studied previously by our group and by Lundeen's experimental group [details and references in chapter 2]. The electronic configuration of this ion makes it a good example for a transition metal that can be used for developing sophisticated computational, empirical, and semi-empirical studies that can be applied for more complex ions (e.g. Th I). By studying Ni II we helped Lundeen's group in developing their potential model. Also, we improved our methodology for including both the localized and continuum parts of the energy spectrum. The potential model includes quantities of small values that result from cancelation of other big quantities. For example assume the three quantities A, B, and C, where A - B = C and C << |A|, |B|. Both of A and B are the main physical quantities that need to be determined. Theoretically we can calculate A and B directly. Experimentally C is the measured quantity. This creates a great stress on the computations as very high accuracy is needed. But since the model itself is empirical it does not provide a direct test for evaluating the accuracy of the theoretical results.

Vanadium atom and positive ions are of high interest to the astrophysics community. We calculated the hyperfine structure constants A and B. Analyzing the spectrum of V II (as one of iron group elements) helps in determining how the Chemically Peculiar stars were formed [more details and references in chapter 3]. To do this requires several accurate oscillator strengths which involve hyperfine structure effects. Hyperfine structure of d^n atomic levels may be strongly affected by the presence of nearby d^{n-1} s levels, as Beck noted in 1992. V II exhibits this effect, which requires accurate computation of the energy differences between the neighboring levels. Through these calculations we improved our calculations with usage of the shift method, chapter 3.

Tungsten ion, W II is another interesting ion for astrophysicists and for the plasma fusion community. Because it is quite refractory it is important for many applications. One of the most important is in plasma fusion devices, as a wall material. During operation W ions are boiled off from the wall and enter the plasma as impurities which affect the efficiency of the device. The efficiency is strongly dependent on W II oscillator

strengths. It is one of the most complex transition metals to study computationally as most of its energy levels are composed of many electronic configurations. Also, it involves strong relativistic and correlation effects. The most required quantity for W II is its oscillator strength (or *f*-value) which can be obtained either directly or through two other quantities; the lifetime and branching fractions. Accurate energy level measurements of W II were provided only in 2010 (contrary to most other atoms and ions that had their energy levels available much earlier). Looking at the literature, from the mid-1980s to 2010, only 28 lifetime measurements are available. This made studying W II interesting for our group as we could provide lifetime values that were (and still are) needed by the scientific community. Producing our results is not as expensive (considering time and financial costs) as experiments. We studied W II and presented our results of the lifetimes of 175 decays in DAMOP conference June 2012. Our results were welcomed by the community as there was good agreement with most of the available experimental data. In the process of assembling a manuscript for publication we found a recently published paper that included experimentally measured branching fractions for nine decays. Although our calculated lifetimes for those nine decays have very good agreement with the measured lifetimes (published in 2010) our calculated branching fractions disagree some with the measured ones (published in 2011). So our group decided not to publish the calculated lifetimes at that time. We think the branching ratios may be improved by improving the even parity wavefunctions, which should not affect our lifetime value very much (see chapter 4).

Although the three projects in this dissertations are completely different there was a common theme in all of them; that is to develop the use of shifts (of diagonal matrix elements) in order to replace some of the correlation effects that are computationally difficult. This work also serves to partially formally justify the semi-empirical Cowan fitting method frequently used by experimentalists and semi-empirical researchers for complex atoms.

1 Development of RCI Method and General Background

1.1 Development of RCI code

1.1.1 Earlier Models and Introduction of RCI code

Reliable computational models have been always needed in order to provide realistic quantum mechanical descriptions of atoms and atomic ions in different conditions; ground states, excited states, highly ionized states, etc., and to form physically meaningful treatments of some problems in atomic physics experiments, e.g. accounting for the Auger cascading process in which inner-shell vacancies are being filled which leads to highly charged atomic states.

In classical mechanics it is well known that the 3-body problem has no formal solution in terms of known functions. So in quantum mechanics we may also expect that for "its" 3 body problem-the He atom there is also no exact formal solution. So some useful approximation scheme that is universal, rapidly convergent (if possible), and easy to computationally implement needed to be found.

Such a scheme was proposed by Hartree in a series of ground breaking papers [1], in the late 1920s [shortly after the Schrödinger equation was put forward!]. It is based on the concept that each electron moved in a potential created from the average field of the other electrons. Mathematically, this was expressed by the operator

$$\hat{h} = -\frac{1}{2}\nabla^2 + V(r) = e \qquad (1.1).$$

Operating on a one particle wavefunction

$$\psi(r) = R(r)Y_{lm}(\theta,\varphi) * \eta_{ms}(\sigma) \qquad (1.2).$$

Where "e" is a Lagrange parameter introduced to insure normalization, and η_{ms} is a function of the spin (σ) , the spin-orbital form was taken the hydrogen atom, and V(r) is due to the Columb repulsion and nuclear attraction term;

$$\frac{-Z}{r_2} + \sum_{k\neq i}^{N} \left\langle k_1\, i_2 \left| \frac{1}{r_{12}} \right| k_1\, i_2 \right\rangle$$

the subscript "*i*" for the one particle function being determined. The N-electron wavefunction was a product of single particle wavefunction, $\Psi_N(1,2,\ldots..,N) = \psi_1(r_1,\sigma_1) * \psi_2(r_2,\sigma_2) * \ldots\ldots\ldots * \psi_N(r_N,\sigma_N),,\sigma$ where the spin which did not make a difference in Hartree approximation because anti-symmetry was not included. This

coupled set of integro-differential eigenvalue radial equations required the potential integrals and differential equations be solved "self-consistently". Though no computers existed at the time, Hartree along with his retired book keeper father was able to manually solve the equations for some few electron problems. Since the boundary conditions for the 2nd order differential equations were "two-point" ($r = 0$ and $r = \infty$), with an unknown constant (e) , they integrated outwards from the origin to a midpoint, and inward from "infinity" to the midpoint, using the midpoint "mismatch" to adjust "e" (and the slope of R at $r = 0$). Great care was needed to avoid numerical errors in the outward integration, as small errors could lead to exponentially increasing terms, as "*r*" increased.

It is fair to say that the work of Hartree and his father [1] forms a common foundation of all quantum calculations on atoms and molecules done from that point until today. His wavefunction approximation, and various extensions (Hartree- Fock [2], Hartree-Fock-Slater [3], etc.) are known as Independent Particle Models (IPM). IPM deal only with the average potential seen by each electron, not its specific potential, i.e. correlation is neglected.

1.1.2 Computation of Bound State Properties

The non-relativistic IPM models, e.g. Hartree-Fock, were inadequate for producing accurate results because they neglected the relativistic and correlation effects. Even in smaller atoms correlation effects cannot be ignored. In He ground state the energy contribution due to correlation is ~ 1.2 eV. Another example is the energy contribution due to exchanging a 3d and a 4s electron in Sc I which ~ 0.1 eV per exchange [4].

For atoms there are few competitive relativistic-correlation methodologies that have been developed and widely applied. The two[1] most common are a relativistic many body perturbation theory approach (Johnson [5])-RMBPT and a relativistic configuration interaction (RCI) approach (Beck and others [6-8]). Each of the two methods has its strengths and weaknesses. Concentrating on the weaknesses, RMBPT has no upper

[1] Large scale MCDF calculations are now being done as well. Though these are frequently competitive in accuracy, they make larger computational demands (energy matrix > 200 K can arise) tend to obscure the physics (e.g. patterns), and are still difficult to apply for many open sub-shell electron cases.

bound property, while methods based on the energy variation principle do, and also is difficult to apply to cases involving more than 2-3 open sub-shell electrons. RCI, on the other hand, has convergence difficulties, i.e. size inconsistency problems [9] which may start to appear when second and higher order effects must be included in the wavefunctions, and treatment of continuum effects is still incomplete. Some work on this last point (Ni II, chapter 2) is presented in this dissertation.

Full application of relativistic methods for molecules is still under development and full application to the condensed matter is more remote. This is because of the extra complications arising from a multi-center problem which essentially precludes the use of numerical (tabular) wave-functions and the reduction in symmetry. Instead more inefficient expansions of radial functions into Gaussian functions (GTOs) are commonly used.

There are two approaches to including relativistic effects in atoms. Both start with the same Hamiltonian. That is the one-electron Dirac operators (Bethe and Salpeter [10]) and the two particle Coulomb operator $\langle\frac{1}{r_{ij}}\rangle$. The two particle relativistic Breit operator [10] may also be included. While QED effects (Lamb shift, vacuum polarization, etc.) [10] need to be included for very accurate work on small atoms (e.g. H, He) or for highly stripped high Z atoms (e.g. Al-like gold [11]), QED treatments are still unable to include exchange effects at the independent particle level [12, 13].

Very early (1935) Bertha Swirles [14] set up the independent particle equations arising from the Dirac-Coulomb operator. Over the decades from the 1930-1960[s] a very limited amount of applications were done (no computers; a World War and depression[2]). More progress was made in modernizing and extending the formalism by the Oxford Group (Grant and Mayers) [15 and references therein] and in starting to develop a robust RIPM algorithm which would handle exchange, open sub-shells, and orthogonality. All this was limited to bound states [16, 17]. Although Mayers worked on the algorithm for some time, he was unable to deliver it publically even as late as 1969 [15, 16]. Developing such a numerical independent particle model (RIPM) code requires a lot of not immediately publishable work, as decisions must be made as to which algorithms to

[2] Significant federal funding of research began during WW II for military research.

use to evaluate the integrals, solve the differential equations, choose the numerical mesh (compact, yet accurate), to avoid collapse into the positron sea, etc. But all of these decisions, once made, can be carried over into RCI or RMBPT. To show how the relativistic treatment adds some difficulty to the calculations we can consider the example of mercury (Hg). It has six s sub-shells and eight p+ d+ f sub-shells. So in the relativistic treatment there are 44 first order integro-differential, pseudo-eigenvalue radial equations to be calculated. While non-relativistically there are only 14 second order equations for the radials. Although the second order differential equations are more difficult than the first order ones the extra number of equations makes calculations more complicated. The techniques for solving these were summarized in Hartree's book [1] and his last student's (Charlotte Froese Fischer) book [2].

Including the Breit operator, at least to first order, is necessary to account for the relativistic electromagnetic interactions between the electrons. Another approach involved expanding[3] (low Z Pauli approximation) the Hamiltonian in powers of α and Z (α = fine structure constant) ([10] p.181) so as to maintain the use of non-relativistic wave-functions [18].The expansion gave rise to 8 complicated operators [10]. The formalism (i.e. evaluation of matrix elements involving these operators) was completed by Beck for two open sub-shell electrons in his thesis work [18]. The application was to the Tl II ion in a Na I host, appearing as a substitutional impurity. The best known low-Z Pauli operators are one-electron spin-orbit, mass variation with velocity, and the Darwin effect[4]. However, for Tl II the effective Z (~15 for the 6s, 6p valence electrons) was simply too large for the expansion to be viable. Note that the low Z Pauli approximation (one particle terms) is still in use in condensed matter studies because of its relative simplicity. Extension of the low Z Pauli approach, with correlation, to three open sub-shell electrons was done by Beck and published in 1971 [20]. The formalism can only be described as nightmarishly complicated, although it was capable of explaining a long unresolved problem of the inversion of the ^{2}D fine structure levels of Na I.

[3] This expansion is formally incorrect for a point nuclear model beyond the first terms in the expansion.

[4] An early example of one electron low Z Pauli operators used with an IPM function (Hartree-Fock-Slater approximation) is given in the work of Herman and Skillman [19] of their condensed matter studies.

Because of the inaccuracy of the low Z Pauli approximation for medium to high effective Z^s and the highly complicated formalism connected to the low-Z Pauli operators Beck chose to terminate his work along these lines. Conveniently his career took a bit of a jog at this time (1970) into learning about and developing a more efficient means of dealing with correlation effects, as practiced by the Sinanoglu research group [21]. An extensive amount of coding was done to develop efficient algorithms for Configuration Interaction (CI) treatment of atoms, including the effects of non-orthogonality. Code for several properties such as oscillator strengths and hyperfine structure were written. Nicolaides, a member of this research group, developed a comprehensive method of treating resonances (with correlation) for any "non-relativistic" atom [22] in 1972.

In 1975, J. P. Desclaux published a comprehensive atomic RIPM code (in FORTRAN) [23] that addressed many of the issues that are required to develop a foundational RCI algorithm. His work was built on the work of Grant and Mayers [15]. The main deficiency was how one would provide the required structure information, as well as lesser deficiencies related to dimension limitations, ability to extrapolate to non-integer Z (for the purposes of providing good input data to the difficult to converge neutral and negative ion cases), and no estimate of quantum electro-dynamical effects (QED)

The Desclaux code (which implements a multi-configurational Dirac-Hartree-Fock [MCDHF] formalism) constructs an energy matrix to which the variational principle is applied, which leads to coupled radial equations which now additionally involve the configurational coefficients *w* of the wavefunction.

$$E_T = \sum_{\nu,\mu} w_\nu \; E_{av}^{\nu} + \sum_{n=1}^{NFGR} w_\mu \, w_\nu \; C_n^k(i,j;l,m) R_n^k(i,j;l,m) \qquad (1.3)$$

Equation 1.3 gives the total function E_T [23]. E_{av} is the average energy of each configuration in *jj* coupling, *i, j, l,* and *m* are the index of the one-electron wavefunctions, ν and μ represent two different configurations. E_{av}^{ν} depends only on the configuration, but not on the particular level which is being considered. The angular coefficients C_n^k do depend on the level and must be given as input data along with *i, j, l, m*, and *k*. They

constitute the structure to be added to E_{av}^{v}. NFGR is the total number of structure terms to be provided

The radial integral R_n^k 7 in [23], for a given n it is;

$$R^k(i,j,l,m) = \iint \left[P_i(r)\, P_j(r) + Q_i(r)\, Q_j(r) \right] \frac{r_<^k}{r_>^{k+1}} \left[P_l(s)\, P_m(s) + Q_l(s)\, Q_m(s) \right] dr ds \qquad (1.4),$$

$r_<$ = min (*r,s*) and $r_>$ = max (*r, s*) The P and Q are the major and minor components of the one electron radial function. Inclusion of the Breit operator (that accounts for magnetic interaction and retardation) adds its own structure with angular coefficients C_B^k and new radial integrals as in equations 10 and 11 of [23].

When applying the energy variational principle, all configurational coefficients *w* and all the P^s and Q^s are to be varied. Varying the w^s leads to a familiar diagonalization of the energy matrix. Varying P^s and Q^s leads to coupled first order integro-differential pseudo-eigenvalue equations. Generation of the reference radial functions starts with an estimate of all w^s, P^s and Q^s. The P^s and Q^s are solved for self-consistently in the presence of a fixed set of w^s, after which the w^s are adjusted by diagonalizing the energy matrix using the new set of P^s and Q^s. The process only ceases when the "input and output" w^s, P^s and Q^s satisfactorily agree, i.e. are adequately self-consistent.

The ground state RIPM wavefunction for the Carbon atom in terms of the *jj* coupling scheme, which is most convenient for the Dirac-Coulomb (or Dirac-Breit) Hamiltonian, would be written as

$w_1\ 1s^2\ 2s^2\ (2p_{1/2})^2 + w2\ 1s^2\ 2s^2\ (2p_{3/2})^2 + w_3\ 1s^2\ 2s^2\ 2p_{1/2}\ 2p_{3/2}$.

This is a 3 configuration problem, whereas non-relativistically, with the formation of S^2, L^2 eigenstates, it is a 1 configuration problem. With the spin-angular (spinors) functions fixed (as in the Hydrogen atom), each matrix element becomes a linear combination of radial integrals which enter the variation.

Diagonal matrix elements have the most complicated structure, but Slater [24] introduced the concept of average energy, which allowed diagonal matrix elements to be expressed in terms of the average energy (for which he gave a general formula) plus a

"few" residual two particle radial integrals (arising from the Coulomb and Breit operators). So the residual integrals R_n^k and the determination of their coefficient C_n^k in equation 1.3 (that is equation 6 in [23]) were left for the user to supply, i.e. the structure. For the rare earth atoms, there can be over 500K (the NFGR in equation 1.3) integrals to be specified. Starting in 1978, Beck began creation of the RCI code which supplied the structure for the Desclaux code. Formally, the wavefunction was divided into a few reference functions [e.g. $1s^2$ $2s^2$ $2p^2$ in the Carbon case] and correlation functions. Desclaux's program is used to create the radial functions needed in the reference functions, i.e. 1s, 2s, $2p_{1/2}$ and $2p_{3/2}$ in the Carbon case, which is then input to the RCI code.

Most of the correlation configurations generated involve one or two sub-shells not appearing in any reference function. Their radial functions are relativistic screened hydrogenic functions or RSH (equation 14.37 of [10]) with an effective charge Z*. These radials are called "virtuals" designated "*v*l", e.g. "*v*f" . Their Z* is estimated by matching their $\langle r \rangle$ to the $\langle r \rangle$ of the reference radial they are replacing. For example, in the pair excitation $3d^2$ to vf^2 we take $\langle r_{vf} \rangle = \langle r_{3d} \rangle$. Z* is then varied to minimize the energy of the root of interest in the full RCI energy matrix. This choice for the virtual is unique to the Beck group and has the following advantages- (i) it is computationally efficient, as compared to doing a full MCDF calculation, (ii) by having the major and minor components of the virtual determined by a single parameter (Z*) whose estimate is determined by the $\langle r \rangle$ match (see above), we prevent variational collapse into the "positron" sea. This conclusion is based on the thousands of calculations we have done, and careful studies done on Hg^{78+} $1s^2$ when we first introduced the concept [6].

First order perturbation theory (FOPT) tells us that single and pair excitations from the reference functions should provide the largest correlation parts [e.g. $2s^2$ to $2p^2$]. However, FOPT has no way of selecting which parts are most important. That selection is done on the basis of prior experience with *non-relativistic* calculations because the presence of relativistic effects does *not* greatly affect the role of correlation, which occurs mainly due to the Coulomb operator. This concept *may not yet be fully appreciated* by

researchers doing RCI or MCDHF calculations. It certainly was not when Beck first noted it in 1982 [25, 26].

The RCI code was completed in 1988 [27] and first applied to electron affinities (EA) of Zn [6]. Shortly thereafter a transition probability code (RFE) was constructed and applied to transitions in Tl II [7]. At that time, this was state of the art. It should be emphasized that the philosophy and strategy of the RCI and RFE code constructions (as explained above) could (and did) closely follow the philosophy and strategy used in the prior non-relativistic coding, as mentioned above.

1.2 Computing Atomic Quantities

The RCI algorithm gives the wave functions and it also calculates the Hyperfine structure and g-values for each state. The wave functions are used in the *f*-value program [28] to calculate the transition probabilities.

1.2.1 Transition Properties and coding

The RFV program includes non-orthonormality because the initial and final states will have different radials. We prefer to use the experimental transition energies, if they are available [29]. So that the computational focus is placed solely on producing accurate transition matrix elements. This program produces the length and velocity gauges of the transition matrix element. We prefer the length gauge because it emphasizes the outer, better correlated, regions of the atom, (L **α r)**. The velocity gauge require excitations from the shallow core, as suggested by Beck and Nicolaides in [30] in First Order Theory of Oscillator Strength (FOTOS), (**V α 1/r).** Although the gauge agreement is a necessary condition it is not sufficient and in our calculations ~ 5% gauge spread is typical. There are three types of transitions that can be calculated; electric dipole, electric quadrupole, and magnetic dipole.

The non-relativistic code was originated by Westhaus et al [31]. A novel feature, state of the art at that time, was the inclusion of non-orthogonality effects, using the methods of King et al [32]. This required individual evaluation of each determinantal matrix

element, e.g. $\langle D|r|D'\rangle$ where D and D' are determinants from the two states which have different (non-orthogonal) radial basis sets. The process involved diagonalizing 2 N X N (N = the number of active electrons) matrices for each pair of determinants. Since even then (1969) each wavefunction could have ~1000 determinants ,one could face up to 2 x 1000 x 1000 diagonalizations on a slow computer (e.g. an IBM 7094). CPU times of more than 30 minutes were common.

In current RCI applications wavefunctions may have as many as 1M determinants, so improved hardware and much more efficient coding was required. Among the most effective improvements were the following:

1. Maximizing the use of symmetry, e.g. for an electric dipole transition, the configurations $1s^2\ 2s^2\ 2p^2$ and $1s^2\ 2s^2\ 2p\ 5g$ do not interact, so their contribution is zero (by "inspection")
2. Realizing that core radials [e.g. for W II, this can be 1s...4f] are nearly identical in the two states which reduces N, the number of "active electrons" , which reduces the dimensions of the matrices which must be diagonalized [from N = 73 to N = 14]
3. Using the angular symmetry of the one electron functions to screen out zeros, and avoid diagonalization for a determinantal matrix element.
4. Doing all transitions in one "shot", i.e. to distribute the result for $\langle D|r|D'\rangle$ to all transitions (multiple levels are done for each parity).

Implementing all of these which are described in more detail elsewhere [33,34] made the codes at least 1000x faster. These codes also can treat magnetic dipole and electric quadrupole transition probabilities.

Development of the relativistic version of the code [28] was done using the formalism of Grant [15] for matrix elements, with the strategy and techniques of the non-relativistic work noted above. One notable variation is that it is only possible to distribute $\langle D|r|D'\rangle$ results across all the transitions for optical transitions, because it is only for such cases that the energy difference can be removed from the radial integral [15], i.e. X-ray transitions must be computed individually. Figure 1-1 shows

the computational steps in brief (These programs (except MCDF) were created by Beck and his research group).

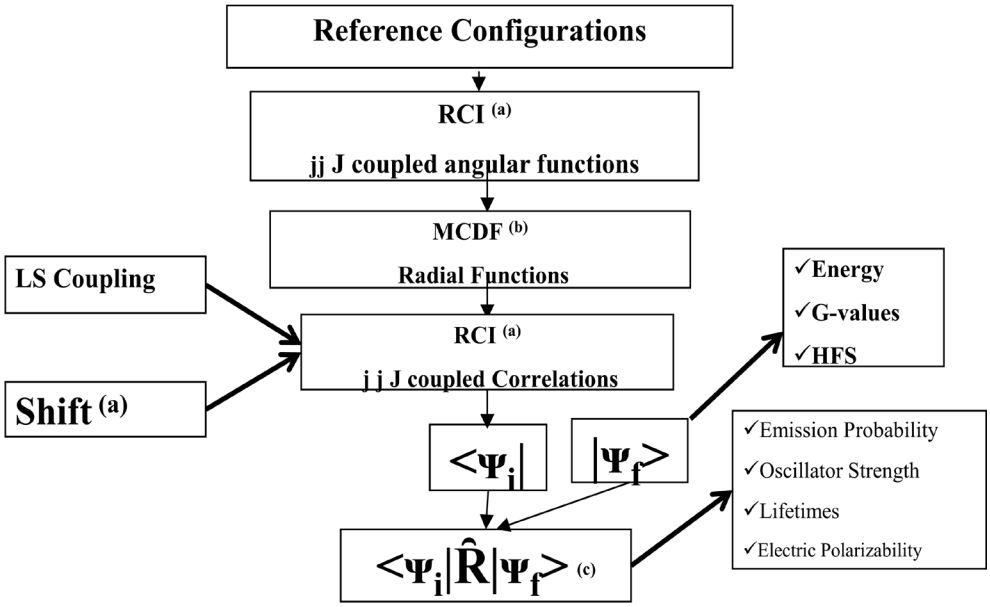

Figure 1-1: A schematic representation of the calculation steps in RCI program used by Beck and his group. Ψ_i and Ψ_f are output wave-functions generated by two separate RCI calculations.

(a) Beck RCI program unpublished

(b) Desclaux, *Comput. Phys. Comm*. **9** 31 (1975)

(c) Beck RFV program unpublished

1.2.2 Relativistic Treatment of Continuum Properties

The above codes are for bound states only. To treat continuum properties such as auto-ionization relativistically, it was essential to have a relativistic code capable of generating continuum radial functions. Very fortunately the Ph.D. work of Dr. Warren Perger [35] included the basis for developing a code which could be meshed with the existing relativistic bound state codes. Through the work of Drs. Perger and Beck and their graduate students Cai, Dinov, Tews, O'Malley and Karighattan and colleagues Halabuka and Trautmann, such a code was produced [36-38]. Initially it was applied by Cai, Beck and Perger [8] to study auto-ionization in Hg I.

1.2.2.1 Relativistic Evaluation of df/dE

In the photo-ionization calculations, instead of calculating the *f*-value (oscillator strength), *df/dE* (E is energy) is calculated. The transition operators are the same, but the bound excited one particle function is replaced by the energy normalized continuum function. Stewart and Wilkinson's non-relativistic He I work [39] provide the formalism and results, which was used as a test case during the development of the relativistic code RPI [40]. This closely follows the philosophy and structure of the relativistic bound states code RFV [28]. More details may be found in Cowan [3]. The RPI code has been extensively employed to calculate the properties of Ni II [41]. Computational issues addressed in the Ni II work include:

1. Means of extrapolating bound Rydberg state properties contributions up to the continuum threshold.
2. Means of extrapolating from the lowest energy continuum computed down to the threshold.
3. Means of extrapolating from the highest energy calculated value to infinity.
4. Means of splitting the bound calculated part into pieces with little loss of accuracy. For example, the RCI code is currently limited to 60 energy levels (fixed J and parity). Some Ni II properties required twice this number. We found

that as long as all lower radial functions were present, the lower energy N-electron bound Rydberg wavefunctions could be removed when calculating the contributions of the upper levels N-electron wavefunctions. For example, Rydberg series members; 4p-15p can be divided in two parts- 4p-8p and 9p-15p, as long as all p radials (2p-15p) are present to impose the proper orthogonality.

1.2.3 Hyperfine Structure Formalism

The hyperfine structure constants are calculated in the RCI stage. Details of the formalism do not appear in any of the published work of the Beck research group. The formulae used in this dissertation is given in appendix, section 6.2.

1.3 References

1. D. R. Hartree, The Calculation of Atomic Structures, Wiley (1957)
2. C. Froese-Fischer, T. Brage,and P .Johnsson, "*Computational Atomic Structure-An MCHF Approach*", CRC Press (1997)
3. R. D. Cowan, The Theory of Atomic Structure and Spectra, Univ. Ca. Press (1981)
4. R. L. Martin and P. J. Hay, *J.Chem.Phys*.**75**, 4539 (1981)
5. W. R. Johnson, Atomic Structure Theory: Lectures on Atomic Physics, Springer (2007)
6. D. R. Beck, *Phys. Rev. A* **37**, 1847 (1988)
7. D. R. Beck and Z. Cai, *Phys. Rev. A* **41**,301 (1990)
8. Z. Cai, D. R. Beck and W. F. Perger, *Phys. Rev. A* **43**, 4660 (1991)
9. E. R. Davidson and D. W. Silver, *Chem. Phys. Letts*. **52**, 403 (1977)
10. H. A. Bethe and E. E. Salpeter, *Quantum Mechanics of One- and Two-Electron Atoms*, ,Martino Fine Books (2014) (reprint)
11. D. R. Beck and P. L Norquist*, Phys. Rev. A* **61** , 044504 (2000)
12. D. R. Beck and P. L Norquist*, Phys. Rev. A* **61** , 044504 (2000)
13. W. R. Johnson, private communication to D. R. Beck
14. B .Swirles, *Proc.Roy.Soc.***152**, 625 (1935)
15. I. P. Grant, *Relativistic Quantum Theory of Atoms and Molecules: Theory and Computation,* Springer (2007)
16. D. F. Mayers, private communication to D. R. Beck
17. D. F. Mayers, oral public comment at 1969 Atomic Physics Conference held in Izmir, Turkey
18. D. R. Beck, *J.Chem.Phys*.**51**, 2171 (1969)
19. F. Herman and S. Skillman, *Atomic Structure Calculations*, Prentice-Hall (1963)
20. D. R. Beck and H. Odabasi, *Ann. Phys.(NY)* **67**,274 (1971)
21. I. Oksuz and O. Sinanoglu, *Phys. Rev*. **181**,42 (1969)
22. C. A. Nicolaides, *Phys. Rev. A* **6**,2078 (1972)

23. J. P. Desclaux, *Comput. Phys. Commun*. **9**, 31 (1975)
24. J. C. Slater, Quantum Theory of Atomic Structure, Volumes I and II, McGraw Hill (1960)
25. Old 23 D. R. Beck and C. A. Nicolaides, " *Phys. Rev. A* **26**,857 (1982)
26. D. R. Beck , *Relativistic Effects in Atoms, Molecules, and Solids*, G. Malli, editor, Plenum Press (1983),p. 502 (abstract)
27. D. R. Beck , RCI Program, unpublished
28. D. R. Beck, RFV program, unpublished
29. NIST atomic spectra data base http://physics.nist.gov/PhysRefData/ASD/levels_form.html
30. C. A. Nicolaides and D. R. Beck*, Chem. Phys. Lett*. **36**, 79 (1975)
31. P. Westhaus and O. Sinanoglu, *Phys. Rev*. **183**, 56 (1969)
32. H. F. King et al, *J. Chem, Phys*. **47**, 1926 (1967)
33. C. A. Nicolaides and D. R. Beck , *Excited States in Quantum Chemistry*, editor D. Reidel (1978), pps. 143-182
34. D. R. Beck*, Phys. Scr.* **71**, 447 (2005)
35. W. Perger, *Physics Ph.D. thesis*, Colorado State University (1987)
36. W. F. Perger, Z. Halabuka and D.Trautmann, *Comput. Phys. Commun,* **76**, 250 (1993)
37. M. G. Tews and W. F. Perger, *Comp.Phys.Commun*.**141**, 205(2001)
38. W. F. Perger and V. Karighattan, *Comput.Phys.Commun*.**66**, 392 (1991)
39. A. L. Stewart and W. J. Wilkinson, *Proc. Phys. Soc.* **75**, 796 (1960)
40. D. R. Beck, RPI program, unpublished
41. M. Abdalmoneam and D. R. Beck, *J. Phys. B* **47**,085003 (2014)

2 RCI Study of Dipole and Quadrupole Polarizabilities of Singly Ionized Nickel and Parameters of Effective Potential for Ni atom Rydberg States

2.1 Introduction

This is a relativistic configuration interaction study of dipole and quadrupole polarizabilities of the singly ionized Nickel, Ni II. Four quantities have been calculated [1]; the scalar dipole polarizability of the first excited state Ni II ($3d^9\ ^2D_{3/2}$), $\alpha_{D,0}(\ ^2D_{3/2})$, the non-adiabatic scalar dipole polarizability of the ground state Ni II ($3d^9\ ^2D_{5/2}$), $\beta_{D,0}(\ ^2D_{5/2})$, the quadrupole polarizability $\alpha_{Q,0}\ (\ ^2D_{5/2})$, and the off diagonal electric dipole polarizability $\alpha_{D,2}(\ ^2D_{5/2})$. These quantities also appear as parameters in an effective potential for the Nickel atom Rydberg states [2].

The Lundeen experimental group has been using the resonant excitation stark ionization spectroscopy (RESIS) method in which measurements are made on high energy Rydberg levels to determine core properties, specifically polarizabilities and moments of ions and atoms [3].

A few years ago the Lundeen experimenters group began to measure properties of Rydberg states of Ni I which has a residual ionic core Ni II with configuration of $1s^2$ …… $3d^9$ [4]. These properties are used to develop an effective potential for atoms (or ions) which then can be used to determine the effectiveness of these atoms or ions as an atomic clock or optical frequency standards [2]. The coefficients in this effective potential model are expressed in terms of matrix elements [2]. This allowed them to use measurements to fit into the effective potential model to obtain polarizabilities and moments of the ionic core [4, 5]. The derivation of this effective potential was done completely non-relativistically (which is fine because the relativistic effects in Ni are moderate, e.g. the relativistic energy difference between a 3d and a 4s electron is about 0.1 eV [6]). Ni I was chosen to test the effective potential and to demonstrate the results. Their goal was to use the same method to study more complicated atoms, e.g. U and different actinide ions [3].

On the other hand Beck's research group studied electric and magnetic characteristics of Ni I and other positive ions previously [7]. So the Beck research group was asked to provide computational results for Ni II polarizabilities and moments in order to check the accuracy of the effective potential model proposed by the experimental

group. This led to cooperation of our group with Lundeen's in calculating some of the parameters in the effective potential. These parameters represented some of the electric properties of Ni II. Our computational interest in the project was to develop the RCI techniques for treating the continuum states in order to produce more accurate results. This work led to two publications in 2012 and 2014 [8 and 1]. The first publication included calculations of an atomic hexadecapole moment, and developed some systematic methods (e.g. shifts) for treating any atomic moments [8].

In general electric and magnetic properties of Ni II, as an example of positive ions, are important in many fields, e.g. the long range interaction between atoms, van der Waals forces, in the areas where atoms interact with external fields as in the precision of optical frequency standards, and in optical clocks.

Rydberg states are the states where only one electron is excited to a high principle quantum number, n. Properties of Rydberg states can be described as hydrogenic in nature. To first order they may be described by an effective "n" which is nearly integer and/or effective charges close to 1.0 for a neutral atom [9]. Experimental studies of the electric and magnetic properties of neutral atoms have been shown to be fairly difficult. In 1933 Mayer and Mayer [10] introduced the idea of using spectroscopy of high-L Rydberg atoms where the Rydberg electron is considered as a probe to obtain the properties of the core. The dominant interaction between the ionic core and the Rydberg electron is the screened Columbic interaction. The presence of other long range interactions leads to the non-degeneracy of Rydberg electrons with the same principle quantum number "n" and produces binding energy patterns, "fine structure pattern" [9, 11]. These patterns reflect the properties of the ionic core, e.g. electric properties and permanent moments. The simplicity of the Rydberg states made them an attractive probe. The measurement of the properties of such states can yield information about the residual core more simply than direct measurements of ground or low excited states [10]. Beginning in late 1970s there was a lot of experimental work on such states and summaries may be found in the work of Connerade [9], Gallagher [12], and in Drake's handbook [6]. Also there have been many attempts at developing effective potentials [11, 14] that account for the weak long ranged interactions between the core and the Rydberg

electron. The expectation value of such a potential is approximately equal to the fine structure patterns in the energy measurements on the high L Rydberg states [5].

RCI method has been used to calculate the reduced matrix elements of four quantities; the scalar dipole polarizability $\alpha_{D,0}(\ ^2D_{3/2}\ )$, the non-adiabatic scalar dipole polarizability $\beta_{D,0}(\ ^2D_{5/2})$, the quadrupole polarizability $\alpha_{Q,0}(\ ^2D_{5/2})$, the off diagonal electric dipole polarizability $\alpha_{D,2}(\ ^2D_{5/2})$ of Ni II. Both of the bound and continuum contributions are included in the calculations. These quantities have not been computed previously. These results gain their importance form two facts; first they are pure ab-initio calculations without any experimental fit. Second, they are directly done on Ni II which is the ionic core of Ni I.

2.2 Theory

The four quantities which are considered in this study can be expressed mathematically in two ways; first the algebraic form in terms of matrix elements, which is more convenient for experimental measurements and fit. Second is the analytical form as integration or summation in terms of *f*-value. As mentioned in chapter 1 that RCI algorithm can be used to compute the electric dipole and quadrupole transition probabilities with good accuracy. This section shows a presentation of the two expressions and the derivations that were implemented in our calculations.

Dipole and quadruple polarizabilities represent the strongest factors for the deviation of the energy of the ion core- Rydberg electron system, from its hydrogenic values. The scalar dipole polarizability, Dalgarno's formula [15] in au

$$\alpha_{D,0}(i) = \sum_k \frac{f_{ik}}{(E_i - E_k)^2} + \int_{I_1}^{\infty} \frac{(df/dE)}{(E_i - E)^2}\, dE \qquad (2.1).$$

The first term represents the discrete (bound state) contributions of oscillator strengths f_{ik} and energy differences .The energies are taken from experiment when available [16]. The second term represents the continuum contributions, where E is the change of the kinetic energy of the continuum electron.

Scalar quadrupole polarizability, $\alpha_{Q,0}$, could be calculated from equation 34 in [2],

$$\alpha_{Q,0} = \frac{2}{5}\frac{1}{2J_c+1}\sum_{\lambda`,J_c}\frac{\langle \zeta J_c \| M^{(2)} \| \lambda` J_c` \rangle^2}{\Delta E(\lambda` J_c`)} \quad (2.2).$$

the angular momentum of the ionic core is J_c and $M^{(2)}$ is the quadrupole moment operator that acts on the core ion wave function. $|\zeta J_c\rangle$ and $|\lambda` J_c`\rangle$ represent the ground state and an excited state for wave functions that are eigenfunction of *J* and parity, ζ and λ stand for any extra quantum numbers required to define the wave function, and ΔE is the difference of the two states energies. For computational wavefunctions we convert this expression that uses the reduced matrix element into another that uses *f*-value or d*f* /dE table 10.6 of Martin and Wiese's article [17] can be used to get

$$\alpha_{Q,0}(i) = \frac{2}{5\, g_i * 1.1199^{18}}\sum_k \frac{g_k \lambda^5 A_{ki}}{E_k - E_i} \quad (2.3)$$

, g_i and g_k are statistical weights of the states *i* and *k*. This was used to calculate $\alpha_{Q,0}$ for the bound states, and A_{ki} is the transition probability.

For the continuum states the integral was used

$$\alpha_{Q,0}(i) = 2.253818 * 10^5 \int_{I_1}^{\infty} \frac{(df/dE)\, dE}{(E_k - E_i)^4} \quad (2.4)$$

, as derived using [18]. $\alpha_{Q,0}$ in equations (2.3) and (2.4) is in a.u.

A third parameter is the non-adiabatic scalar dipole polarizability $\beta_{D,0}$ that was first introduced to account for the dynamic effects of the Rydberg electrons. Earlier models considered a stationary electron and assumed that the core adjusts adiabatically to the motion of the Rydberg electron. It can be calculated using eq. 36 in [2], which is

$$\beta_{D,0}(i) = \frac{1}{3(2J_i+1)}\sum_k \frac{\langle \zeta_i J_i \| M^{(1)} \| \zeta_k J_k \rangle^2}{(E_i - E_k)^2} \quad (2.5).$$

$M^{(1)}$ is the dipole moment operator, $|\zeta J\rangle$ are wave functions that are eigenfunctions of angular momentum, parity, and the Hamiltonian. The sum is done over all the possible branches of transitions in the bound state calculations and it was replaced by an integral for the continuum calculations. Equation 6.81 in Johnson [6] can be used to compute the dipole matrix element in equation (2.5).

$$A_{ab} = \frac{2.02613 \times 10^{18}}{\lambda^3} \frac{S_{E1}}{[l_a]} \, s^{-1} \tag{2.6}$$

A_{ab} is the coefficient of spontaneous emission in sec^{-1} , it is computed by RCI, S_{E1} is the line strength, that is defined as $S_{E1} = \ |< a||r||b >|^2$, λ is the wavelength in Angstrom, $[l_a] = 2l_a + 1$.

The off-diagonal tensor dipole polarizability is another quantity that appears in the effective potential, equation 77 in [2].

$$\alpha_{D,2}(J_c^{`})$$
$$= 2\sqrt{\frac{10}{3}} \begin{pmatrix} J_c & 2 & J_c \\ -J_c & 0 & J_c \end{pmatrix} (-1)^{J_c^{`} - J_c^{`}}$$
$$* \sum_{\lambda'', J_c''} (-1)^{2J_c''} \begin{Bmatrix} J_c'' & 1 & J_c \\ 2 & J_c' & 1 \end{Bmatrix} \frac{\langle \zeta \, J_c \| M^{(1)} \| \, \lambda'' \, J_c'' \rangle \, \langle \, \lambda_c'' \, J_c'' \, \| M^{(1)} \| \zeta \, J_c' \rangle}{\Delta E(\lambda'' \, J_c'')} \tag{2.7}$$

This equation includes mixing the dipole transitions from the ground state $|\,\zeta \, J_c\rangle$ and the first excited state, $|\,\zeta \, J_c^{`}\rangle$ to common excited states $|\lambda_c'' \, J_c''\rangle$, $\{\}$ is the 6j symbol. Contrary to the previous 3 quantities where the sums are positive definite, calculations of $\alpha_{D,2}$ require knowing the relative phases of each of reduced matrix element, since the dipole operator acts differently on the ground state and the excited state. The Johnson expression provides the magnitude only. Applying the Wigner-Eckart theorem (eq. 1.89 in [6]) on a matrix element gives its sign, as shown in equation (2.8),

$$\langle J_1, m_1 | T_q^k | J, m_2 \rangle = \ (-1)^{j_1 - m_1} \begin{pmatrix} J_1 & k & J_2 \\ -m_1 & q & m_2 \end{pmatrix} \langle J_1 \| T^k \| J_2 \rangle \tag{2.8}$$

It produces a reduced matrix element, of the tensor operator T^k that does not depend on the magnetic quantum numbers m_1, m_2, and q. In our case T^k stands for the dipole moment operator M^l. ( ) is the 3 j symbol that is relabeled to Clebesch-Gordon coefficients. As mentioned in [1] the relative overall phase of $\psi(\zeta \, J_{c)*} \, \psi(\zeta \, J'_c)$ determines the sign of $\alpha_{D,2}$.

2.3 Method and procedure

Dipole and quadrupole polarizabilities of singly ionized nickel (Ni II) can be studied through two different approaches. The first is considering nickel atom (Ni I) in a

Rydberg state, where the core of the atom is the positive ion, Ni II, and one electron is excited to high principle quantum number. This approach is used experimentally [2, 12], where measurements are done on the Rydberg electron that is used as a probe for finding out about the core. The second approach is a direct study of Ni II, which is what we did using the RCI method. Computing each atomic property of Ni II is done in three steps; (i) bound state calculations on Ni II where we start with Ni II in its ground state and consider excitations of electrons to higher states below the ionization energies, (ii) excitations above ionization are considered, here the Ni II changes into a Ni III core and a continuum electron, (iii) step is to combine these two calculations and to reach a final value. RCI computations can be summarized in these steps:

- Bound state calculations:
  - Obtaining the wavefunctions of each J and parity of Ni II,
  - Calculating the probability of transition (dipole or quadrupole).
- Continuum state calculations:
  - Obtaining the wavefunctions of each J and parity of Ni III,
  - Obtaining the wavefunction of each (Ni III + ε) for each J and parity,
  - Calculating the probability of transition (dipole or quadrupole).
- Dipole and Quadrupole Polarizabilities calculations:
  - Adding the continuum and bound state transition probabilities for each J,
  - Interpolating between the highest bound and lowest continuum RCI results and extrapolation to infinity.
  - Calculating $\alpha^{\underline{s}}/\beta$ (equation in section 2.2) for each J,
  - Adding $\alpha^{\underline{s}}/\beta$ for all $J^{\underline{s}}$.

Dirac-Coulomb Hamiltonian was used to generate the radial wavefunctions from the program of Desclaux [19]. The Rydberg functions are also generated by Desclaux program. The Breit effect is added during the RCI calculations. The reference configurations were Ni II $1s^2$ ….$3d^9$ $^2D_{5/2}$ or $^2D_{3/2}$; these are the ground and first excited states of Ni II. Correlation was added to the Rydberg states via shifts (see appendix section 6.3).

Excited states from 3d to higher Rydberg levels, which give $3d^8$ (J_{core}) nl_j were calculated using Desclaux program. The nl_j is the Rydberg electron, that is np and nf for dipole transitions and to ns, nd, and ng for quadrupole transitions, "n" is principle quantum number and "j" is the angular momentum of the electron. Also, a few excitations from the shallow core were examined; the most important ones were 3p to 3d, dipole, and 3s to 3d, quadrupole. Excitations from the inner core were not included because the parameters being considered in this study depend on high inverse powers of energy difference, i.e. $1/dE^m$, $m \geq 2$. The excitation energy, dE, from the core is much larger than that from the valence shells. For example $E(3p_{3/2}) - E(3d_{3/2}) \sim 6$ au, $E(2p_{3/2}) - E(3d_{3/2}) \sim 65$ au, $E(3s_{1/2}) - E(3d_{3/2}) \sim 8$ au, $E(2s_{1/2}) - E(3d_{3/2}) \sim 68$ au, and $E(1s_{1/2}) - E(3d_{3/2}) \sim 377$ au.

In the bound states a significant number of Rydberg levels (n = 13) were included for each symmetry (e.g. p or f for a dipole excitation or s, d, or g for quadrupole transitions) [1]. Adding these Rydberg levels helped to reduce the interpolation range, as explained in section 2.3.5. The RCI program being used is limited to maximum of 60 excited levels in one run, but we may need as twice as many. So the calculations for each symmetry (for a given total J, e.g. $3d^8$ np J_{total} =5/2) were split into two parts; n = 4 - 8 and n = 9 – 13. The full set of np (n = 4 -13) radials were kept in each section to avoid the collapse of the higher levels (n = 9-13). To see the effect of the split of the Rydberg series on the final results a test run with 8p wavefunction in the second piece (so the highest n in the first piece was n =7) was found to give the same total contribution. It was noticed that for the high n Rydberg levels the radial wavefunctions did not always behave smoothly. Sometimes wavefunctions of Rydberg electron with the same n and l, e.g. $nf_{5/2}$ and $nf_{7/2}$, have very different $\langle r \rangle$, which reflected that one of the two functions dominated the total wavefunctions and the other was acting as a correlation effect. This led us to have different calculations for each type of valence electron, e.g. separate runs for $nf_{5/2}$ and other runs for $nf_{7/2}$ [1]. The final step in the RCI calculations of the bound states wavefunctions included shifts to the energy diagonal matrix elements. For more details on the shift please see appendix section 6.3 and references [7-8].

The transition probabilities between bound states (dipole or quadrupole) were calculated using the RFVIS code [20] which makes maximal use of symmetry and

includes the effects on non-orthonormality of the radials [1]. At this step we use the experimental energy values [16] (if they are available) because they are more accurate than the calculated energies. The transition matrix elements are ab-initio calculations with one of the inputs, energy levels, taken from experiment. The transition probabilities are calculated using the velocity and length gauges. Only the results of the length gauge results were used for further calculations, because the velocity operator emphasizes the mid-range values of *r* (distance from the origin) and it requires correlations due to the core excitations (those were not directly included). The length gauge emphasizes the long range of "*r*", which emphasizes the Rydberg electron.

The continuum calculations account for those transitions that include a Ni III core and a continuum electron. The wavefunctions of the core were generated by the program of Desclaux [19] and RCI program [21]. Then the continuum radials were generated by the program of Tews and Perger [22]. The continuum states are highly excited, Ni III $3d^8$ $\varepsilon_{l,}$ so the small energy contribution due to the interaction between the core, Ni III $3d^8$ and the continuum electron, ε_l, was neglected. Wave functions for each channel, e.g. $3d^8$ $((^{2S+1}L_J)_{core})$ εl_j , ε is the continuum electron, were calculated separately. So the total energy was considered as E ($3d^8$) + E (ε_l), where E ($3d^8$) were the experimentally measured values [16]. The transition probabilities were obtained by the RPI program [23]. The methodology used in this program is similar to that in the RFV1S, mentioned above. The main difference is that it calculates df/dE; the change of the oscillator strength with the change of the energy of the continuum electron. More details on the procedure of the continuum calculations are given below.

2.3.1 Dipole Polarizability of Ni II $3d^9\ ^2D_{3/2}$, $\alpha_{D,0}$ ($^2D_{3/2}$)

Ni II $3d^9\ ^2D_{3/2}$ is a meta-stable state of Ni II with a life time of 18.1 s [1]. We are studying it for two reasons; first its long life time may allow it to be important in different physical phenomena. Second, the value $^2D_{3/2}$ wavefunctions are required for calculating $\alpha_{D,2}$ of the ground state, equation (2.1).

The transition considered here is:

$$\text{NiII } 3d^9\ {}^2D_{3/2} + \text{photon (Energy)} \xrightarrow{Electric\ Dipole\ Transition} \text{Ni III } 3d^8(p+f)\ J_{final} = 1/2,\ 3/2,\ 5/2$$

When initial state, Ni II $3d^9$ $2D3_{/2}$, is supplied with energy that exceeds the ionization limit an electron ejects from the outer most shell. The result is Ni III $3d^8$ core and a p or f continuum electron, while the fields of the ion and the electron are affecting each other. The free electron can take any energy (it is not restricted to discrete energies as in the bound states) and this is the reason for calling this part of calculations continuum calculations. The produced core, Ni III $3d^8$, and the free electron together have J_{final} =1/2, 3/2, and 5/2 with an odd parity. So the dipole polarizability is calculated through the combination of J^{π} as in table 2-1.

Table 2-1: Combinations of single (continuum) electron (ε_j) with a Ni III core (J_{core}) to give Ni II in continuum state (J_{final}).

ε_j	J_{core}	J_{final}
$p_{1/2}$	0	½
$p_{3/2}$	1, 2	½
$f_{5/2}$	2,3	½
$f_{7/2}$	3,4	½
$p_{1/2}$	1, 2	3/2
$p_{3/2}$	0, 1, 2, 3	3/2
$f_{5/2}$	1, 2, 3, 4	3/2
$f_{7/2}$	2, 3, 4	3/2
$p_{1/2}$	2, 3	5/2
$p_{3/2}$	1, 2, 3, 4	5/2
$f_{5/2}$	0, 1, 2, 3, 4	5/2
$f_{7/2}$	1, 2, 3, 4	5/2

Labels and energies of Ni III $3d^8$ levels of interest are shown in figure 2-1. This produced 63 excited state channels. A complete list of channels is given in table 2-3. To explain the

labels of the channels consider this example: 3P0.p1.J1. Here 3P0 refers to the Ni III $3d^8$ $^3P_0$ coupling of the core, p1 stands for a p electron with j=1/2, and J1 for a final J=1/2. This method for labeling the channels was followed throughout all the tables.

Calculating the integration term in Dalgarno's expression, equation (2.1), was done by the trapezoidal rule for $(df/dE)/ (E_0-E)^2$.

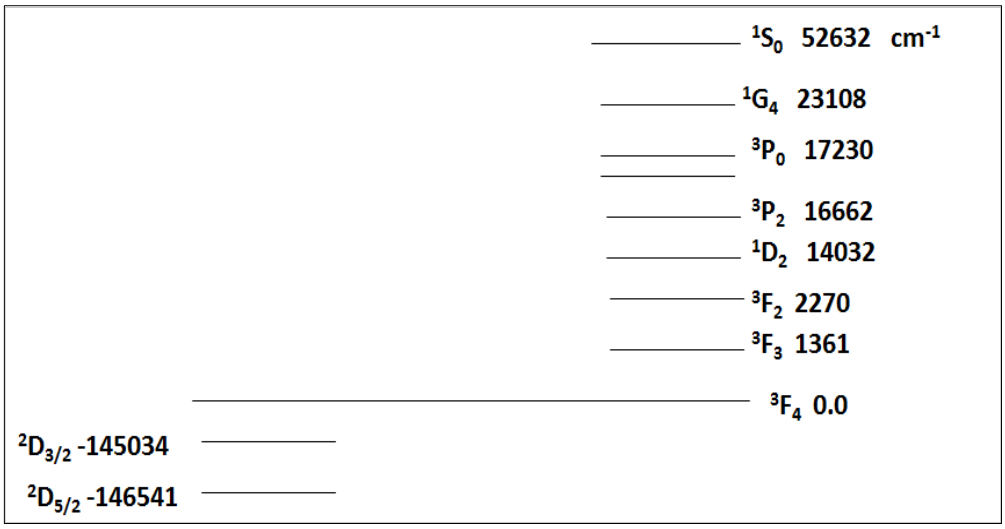

Figure 2-1: A schematic representation to Ni III levels [15] included in this study, energy in cm^{-1}.

2.3.2 Off diagonal electric dipole polarizability of Ni II $3d^9$ $^2D_{5/2}$, $\alpha_{D,2}(^2D_{5/2})$

Referring to equation (2.7) we see that calculating $\alpha_{D,2}(^2D_{5/2})$ requires computing matrix elements of the dipole transitions of both Ni II $3d^9$ $^2D_{5/2}$ and $^2D_{3/2}$ with a common state (J_c''). This is why here we considered the transitions of $^2D_{5/2}$ and $^2D_{3/2}$ to J=3/2 and 5/2, only.

Contrary to the scalar dipole polarizability in which only the magnitude of the matrix element was required $\alpha_{D,2}(^2D_{5/2})$ does include the phase of the matrix elements transitions. These were huge cancelations between some terms which consequently required extra accuracy in the calculations. Determining the phases was done by using

Wigner Eckart Theorem on each single transition, as mentioned in theory section 2.2, during the bound state calculations. Then the same phases were valid for the continuum channels. The transitions here are

$$\text{Ni II } 3d^9\ {}^2D_{5/2} \xrightarrow{Electric\ Dipole\ Transition} \text{Ni III } 3d^8\ (p + f)\quad J=3/2,\ 5/2$$

, and

$$\text{Ni II } 3d^9\ {}^2D_{3/2} \xrightarrow{Electric\ Dipole\ Transition} \text{Ni III } 3d^8\ (p + f)\quad J=3/2\ ,\ 5/2$$

There were old calculations for the continuum wave functions of Ni II $3d^9$ ($^2D_{5/2}$) done by Dr. Lin Pan [7]. The transition probabilities (df/dE verses E) between Ni II $3d^9$ ($^2D_{5/2}$) and the continuum states Ni III $3d^8$ (p + f) J = 3/2 and 5/2 were also available, as those were used to calculate some parameters for Ni II as in [7]. The transition probabilities for those old calculations were done at a different energy mesh (less dense). The transition probabilities between Ni II $3d^9$ ($^2D_{3/2}$) and the continuum states Ni III $3d^8$ (p + f) J = 3/2 and 5/2 were prepared at much denser mesh. In order calculate $\alpha_{D,2}$ the transition probabilities from ($^2D_{5/2}$) and ($^2D_{3/2}$) had to be on calculated on the same mesh. This was done by two methods;

The first method was to interpolate df/dE of $^2D_{3/2}$ (that was produced by a denser energy mesh) to the energy mesh that was used by Dr. Pan. Then the trapezoidal rule was used to integrate df/dE (of both $^2D_{5/2}$ and $^2D_{3/2}$) versus the energy. We also had two ranges of extrapolations; one from the highest calculated point to infinity and another one from the lowest calculated continuum point to the highest calculated discrete levels, those were 6p and 8f.

The second method was reproducing df/dE of $^2D_{5/2}$ using the same energy mesh that was used for $^2D_{3/2}$. Then the integration was done using Simpson Rule. Performing integration with Simpson rule requires equal energy spacing which we did not have. In order to overcome this barrier the three contiguous points were fit by a parabola and the middle point interpolated from the fit. Simultaneously more Rydberg states were added to the discrete part. We extrapolated the product of the two matrix elements from the lowest E (~ 0.0008 eV above the threshold) to the threshold using a power function, and another extrapolation was done to infinity.

The results of the two methods looked different, $\alpha_{D,2}$ = 0.963 au using the first method and 5.592 x 10^{-2} au using the second method. Since this calculation included large cancelation due to the phase difference between 46 different channels, very slight change in the result of each individual channel could cause a big difference in the final value. It was important to analyze the calculations carefully to find the reason behind this big difference of (0.907 au) in final value. If the reason for this difference was the change of the mesh of the transition probability this would imply very poor continuum wavefunctions and instable calculations. By looking at the details of the calculations of each channel more closely we found that the difference was due to the change in the range of the interpolation between the continuum and discrete states. We saw that using Trapezoidal verses Simpson's rules for integrations did not make a noticeable difference. Also, changing the mesh in the transition probability calculations was not the reason. So we conclude that including more Rydberg states was necessary for this calculation. Calculating $\alpha_{D,2}$ for the continuum range was pretty stable regardless of the method of integration. Computing $\alpha_{D,2}$ included 46 channels of transitions, which are in table 2-5.

2.3.3 Non-Adiabatic scalar dipole polarizability of Ni II $3d^9\ ^2D_{5/2}$, $\beta_{D,0}(^2D_{5/2})$

The *f*-value for the discrete part was calculated using method-B, in section 2.3.5. Also, here the effects of the shallow core 3p to 3d excitation on $\beta_{D,0}$ was significant, see table 2-6. The continuum calculation included a transition of

$$\text{Ni II } 3d^9\ 2D5_{/2} \xrightarrow{Electric\ Dipole\ Transition} \text{Ni III } 3d^8\ (p + f) \qquad J=3/2,\ 5/2, \text{ and } J=7/2.$$

Calculating $\beta_{D,0}$ as in equation s (2.5) and (2.6) included integrating $(df/dE)/(E-E_0)^3$ which was done using the trapezoidal rule with two ranges of extrapolation were added, one to infinity and one to the threshold. There were 72 continuum transition channels included in this calculation, see table 2-7.

2.3.4 Quadrupole polarizability of Ni II $3d^9\ ^2D_{5/2}$, $\alpha_{Q,0}$ ($^2D_{5/2}$)

The $\alpha_{Q,0}$ ($^2D_{5/2}$) was calculated from the following transitions of the ground state through the quadrupole operator;

$$\text{Ni II } 3d^9\ ^2D_{5/2} \xrightarrow{Electric\ quadrupole\ Transition} \text{Ni III } 3d^8\ (s + d + g) \quad J_{final} = 1/2, 3/2, 5/2, 7/2, \text{ and } 9/2.$$

Both the initial and final states have even parity.

The *f*-value for the bound states was calculated using method-B in section 2.3.5. Here the excitations of the shallow core 3s to 3d were found important. All the excitations of 3d to s + d + g were studied.

The continuum part included 133 transition channels. The list of channels is in table 2-9 in the results section. Calculating $\alpha_{Q,0}$ as in equations (2.3) and (2.4) included integration of $df/dE / (E-E_0)^4$ that was done using the trapezoidal rule.

2.3.5 Interpolating the bound and the continuum states

In order to have accurate calculation of the dipole and quadrupole polarizabilities we need to include all the range of energies starting from the ground state to the ionization level (bound or discrete states) and from the ionization limit to infinity (continuum states). Each of these two parts are infinite sums so some approximation is needed. Since we were seeking the most accurate results possible we compared two methods for the calculations, methods A and B below.

Method-A

The bound state calculations included Rydberg states up to 8p and 7f. The continuum spectrum started at about 0.01 eV and ended at about 200 eV. An interpolation was done from the top calculated bound state up to the first calculated continuum level and an extrapolation from the end of the calculated continuum to infinity using an inverse power law, $(df/dE) / (E_0 - E)^2 = A/E^n$. This method was used only for calculating the scalar dipole polarizability of Ni II $^2D_{3/2}$, because that did not have a cancelation effect due to phase changes

Method-B

The bound state calculations included Rydberg states up to 13p and 12f, which meant there were about 100-120 Rydberg levels of each type (e.g. $3d^8$ np J). The continuum spectrum started at about 0.0001 eV with a denser mesh than that used in method A, and extended to 500 eV. There were two ranges of interpolation; from the top of the bound state to the threshold, and from the threshold to the bottom of the continuum, and there was n extrapolation from the highest continuum energy to infinity. All these integrations were done using Simpson rule.

2.4 Results and Discussion

2.4.1 Scalar Dipole Polarizability of Ni II $3d^9\ ^2D_{3/2}$, $\alpha_{D,0}$ ($^2D_{3/2}$)

We computed $\alpha_{D,0}$ ($^2D_{3/2}$) to be 7.6859 au. The meta-stability of this excited state should make the dipole polarizability capable of measurement. This value is small comparing to the static polarizability of Ni I $^3F_4$, 46 au as in [24] and it is close to Ni II $^2D_{5/2}$ 7.7367 au as in [7] as expected.

Table 2-2 gives the contributions of the bound state part. Table 2-3 gives the continuum part; it gives a list of the channels of the dipole transition and the contribution of each channel. As we see in table 2-2 the bound excitations of 3d to p are dominant. Table 2-3 shows that the excitations of 3d to f are dominant in the continuum part. The contribution of 3d to f increases with J. The contribution due $f_{7/2}$ is bigger than that of $f_{5/2}$ for J = 1/2and 5/2 and they have almost equal contributions for J = 3/2.

As we see in the table 2-3 3P1.p1.J1, 3P1.p1.J3 and 3F3.p1.J5 channels give zeros. That's because the dipole matrix element is zero. We can write the transition as, $\langle \text{Ni II } 3d^9\ ^2D_{3/2} |\Omega| \text{Ni III } 3d^8\ ^3P_{1/2}p_{1/2} \rangle$, this reduces to the matrix element $\langle 3d_{5/2}|\Omega|p_{1/2}\rangle$ which is zero because "Ω" is a tensor of rank-1, etc.

2.4.2 Off diagonal electric dipole polarizability of Ni II $3d^9\ ^2D_{5/2}$, $\alpha_{D,2}(^2D_{5/2})$

This included calculations of matrix elements of Ni II $3d^9$ states; $^2D_{5/2}$ and $^2D_{3/2}$. In equation (2.7), J_c=5/2, $J_c^{`}$ = 3/2, and $J_c^{``}$ = 3/2 and 5/2 and the energy difference is the energy of the final states, where $3d^9\ ^2D_{5/2}$ is taken to be the reference. Tables 2-4 and 2-5 give the bound and continuum contributions to $\alpha_{D,2}(^2D_{5/2})$. The phase differences of the different channels resulted in huge cancellations, for a loss of two significant figures. Our result is -0.2204 au (this is the sum of -0.0559 au due to continuum and -0.1645 due to bound states). The estimated value of Woods et al is -0.04 au [5]. This estimation was based on bound state calculations done by us, as cited in [5]. As we see the two results agree on the phase (both are negative) but disagree on the magnitude.

Regarding the continuum part, the channels that included p continuum electron had the maximum df/dE very close to the threshold energy, while those that had f electron had the maximum quite far from the threshold (roughly at about 20-30 eV above threshold). These three channels; 3P1.p1.J1, 3P1.p1.J3 and 3F3.p1.J5 included forbidden transitions so their contributions were zero and they are not included in table 2-5.

2.4.3 Non-Adiabatic scalar dipole polarizability of Ni II $3d^9\ ^2D_{5/2}$, $\beta_{D,0}(^2D_{5/2})$

We calculated $\beta_{D,0}$ ($^2D_{5/2}$) to be 9.2345 au (this is the sum of 8.08944 au due to bound states and 1.1535 due to the continuum) which is in good agreement with estimated value of Wood et al, 8.9 (1.2) au [5]. Table 2-6 gives the contributions due to the different symmetries and it shows that 3d to p were stronger than 3d to f transitions in the bound state, and that some of the shallow core excitations were of significant effect. Table 2-7 gives the channels and their contributions to the continuum part.

2.4.4 Quadrupole polarizability of Ni II $3d^9\ ^2D_{5/2}$, $\alpha_{Q,0}$ ($^2D_{5/2}$)

Our value is 62.940 au (this is the sum of 54.917 au due to bound states and 8.02362 au) which agrees with the value of Wood's at 55(8) a.u. [5]. Table 2-8 gives the contributions of the different symmetries in the bound state part. The contributions of 3d to s are the most significant and 3d to g are the smallest.

Table 2-9 gives the contributions due to each continuum channel for transitions in $\alpha_{Q,0}$ ($^2D_{5/2}$). It also gives the total contribution due to all the channels for a fixed one electron type for a given J. From the table we see that $\alpha_{Q,0}$ due to transitions that includes a s electron were all small, about 10^{-3}-10^{-4} for all J^s. The contributions due to $d_{3/2}$ and $d_{5/2}$ were of order 10^{-1} for all J^s. The biggest contributions are those of g, these are of order 10^1. Although $g_{9/2}$ contributed through fewer channels –due to the selection rule as will be explained below- its contribution was almost equal or greater than that of $g_{7/2}$.

The df/dE of the channels that included d and g had very good gauge agreement, that velocity and length gauges came up at the same order of magnitude and their results were close for most of the cases. Most of df/dE verses E curves of the d channels had very smooth curves with peaks very close to the threshold. A few of them, e.g. 3F3.d5.J3, 3F4.d5.J5, 1D2.d5.J5 and 3F3.d3.J5 had the peaks about 40-60 eV above the threshold, which is not too high as the mesh extended to 500 eV. All the df/dE that included g electrons had the peaks at very high energies, about 200 eV above threshold. For the transitions that included s electrons df/dE by velocity gauge was about 1 order of magnitude off from the calculations using the length gauge for all J^s. The curves of df/dE verses E seemed to have two peaks a smaller one very close to threshold and a higher one at very high energy, about 400 eV above the threshold.

Due to the selection Rules some of the channels produced zero df/dE. We saw that in 3F3.g9J3, 3F3.g9J5, 3P1.g9J7, 3F3.g9J7, 3P1.g9J9, 3F3.g9J9. These have the matrix element $\langle \text{Ni II } 3d^9\ ^2D_{5/2} \left|\Omega.\Omega\right| \text{Ni III } 3d8\ ^3P_1\ g_{9/2}\rangle$, which reduces to $\langle 3d_{3/2} \left|\Omega.\Omega\right| g_{9/2}\rangle$ which is zero.

2.4.5 Discussion

We computed four quantities for the first time. Two of our results agree well with the values of Wood et al [5] which they deduced from measurements. For $\alpha_{D,2}$ the calculations included summations of very small quantities and many cancellations due to the phase differences, that made reaching accurate results was not so easy.

One more important quantity is $\alpha_{Q,0} - 6\beta_{D,0}$ because it was determined by a combination of measurements and fitting [5]. Then the value of $\beta_{D,0}$ was extracted from this sum [5]. Although our calculations for the $\alpha_{Q,0}$ and $\beta_{D,0}$ quantities agree well with the values given in [10] we get $\alpha_{Q,0} - 6\beta_{D,0} = 7.48$ au while Wood et al get 1.4(2.8) [10]. Adding more Rydberg states in the discrete part did not bring our result closer to Wood's. A few comments here; i) Wood's et al in [5] is not clear enough about which quantities (other than energies) were being directly measured and which were obtained by fitting, ii) their error bar for this quantity is 200%, iii) a small change in the calculations of $\beta_{D,0}$ will lead to a big effect in this quantity because $\beta_{D,0}$ is multiplied by 6.

From all the tables we see that although the continuum contributions are smaller than those of the bound state but they are significant enough and cannot be ignored.

Table 2-2: Bound state contribution to Ni II $3d^9\ ^2D_{3/2}$, $\alpha\ (^2D_{3/2})$ in au [1].

Transition	J_{final} (J')	Bound
$\boldsymbol{3d \rightarrow p}$	5/2	1.9108
$\boldsymbol{3d \rightarrow p}$	3/2	2.0644
$\boldsymbol{3d \rightarrow p}$	1/2	0.7482
$\boldsymbol{3d \rightarrow f}$	5/2	0.1679
$\boldsymbol{3d \rightarrow f}$	3/2	0.1026
$\boldsymbol{3d \rightarrow f}$	1/2	0.0406
Total		5.0345

Table 2-3: Contributions due to each continuum channel to the scalar dipole polarizability of Ni II $3d^9\ ^2D_{3/2}$, $\alpha_{D,0}\ (^2D_{3/2})$ in au.

channel#	Channel	$\alpha_{D,0}\ (^2D_{3/2})$
1	3P0.p1.J1	5.6862E-03
2	1S0.p1.J1	3.8759E-03
Sum	p1.J1	9.5621E-03
3	3P1.p3.J1	1.4368E-02
4	3F2.p3.J1	3.6673E-05
5	1D2.p3.J1	3.0977E-03
6	3P2.p3.J1	1.2216E-02
Sum	p3.J1	2.9720E-02
Sum	p(1+3).J3	3.9282E-02
7	3F2.f5.J1	4.6271E-02
8	1D2.f5.J1	9.0145E-03
9	3P2.f5.J1	7.6853E-04
10	3F3.f5.J1	1.0094E-02
Sum	f5.J1	6.6148E-02
11	3F3.f7.J1	4.6814E-02
12	3F4.f7.J1	4.5835E-02
13	1G4.f7.J1	1.8682E-01

sum	f7.J1	2.7948E-01
sum	f(5+7).J1	3.4562E-01
sum	(p+f).J1	3.8490E-01
14	3P1.p1.J3	0.0000E+00
15	3F2.p1.J3	2.8124E-02
16	1D2.p1.J3	1.0112E-02
17	3P2.p1.J3	5.7909E-03
sum	p1.J1	4.4028E-02
18	3P0.p3.J3	1.1261E-03
19	1S0.p3.J3	7.7393E-04
20	3P1.p3.J3	4.5998E-03
21	3F2.p3.J3	7.9687E-03
22	1D2.p3.J3	4.1584E-04
23	3P2.p3.J3	1.0254E-02
24	3F3.p3.J3	3.0916E-02
sum	p3.J3	5.6055E-02
sum	p(1+3).J3	1.0008E-01
25	3P1.f5.J3	9.0479E-03
26	3F2.f5.J3	2.0953E-01
27	1D2.f5.J3	5.9517E-02
28	3P2.f5.J3	1.8581E-02
29	3F3.f5.J3	4.9829E-05
30	3F4.f5.J3	2.6184E-03
31	1G4.f5.J3	1.0830E-02
sum	f5.J3	3.1017E-01
32	3F2.f7.J3	2.4579E-02
33	1D2.f7.J3	4.1619E-03
34	3P2.f7.J3	5.3277E-02
35	3F3.f7.J3	2.2004E-01
36	3F4.f7.J3	8.8031E-08

37	1G4.f7.J3	3.9153E-07
sum	f7.J3	3.0206E-01
sum	f(5+7).J3	6.1224E-01
sum	(p+ f).J3	7.1232E-01
38	3F2.p1.J5	6.4493E-03
39	1D2.p1.J5	2.4763E-03
40	3P2.p1.J5	1.4323E-03
41	3F3.p1.J5	0.0000E+00
Sum	p1.J5	1.0358E-02
42	3P1.p3.J5	1.7548E-04
43	3F2.p3.J5	7.9121E-03
44	1D2.p3.J5	6.4583E-04
45	3P2.p3.J5	1.9832E-04
46	3F3.p3.J5	1.6704E-02
47	3F4.p3.J5	1.1443E-02
48	1G4.p3.J5	4.5179E-02
Sum	p3.J5	8.2259E-02
Sum	p(1+3).J5	9.2616E-02
49	3P0.f5.J5	8.2360E-02
50	1S0.f5.J5	5.7953E-02
51	3P1.f5.J5	1.7053E-03
52	3F2.f5.J5	2.1466E-01
53	1D2.f5.J5	1.1531E-01
54	3P2.f5.J5	9.6756E-02
55	3F3.f5.J5	1.5943E-02
56	3F4.f5.J5	3.5052E-03
57	1G4.f5.J5	1.4518E-02
Sum	f5.J5	6.0272E-01
58	3P1.f7.J5	2.1121E-01
59	3F2.f7.J5	8.2806E-02

60	1D2.f7.J5	1.3962E-02
61	3P2.f7.J5	1.7861E-01
62	3F3.f7.J5	2.4932E-01
63	3F4.f7.J5	2.3080E-02
64	1G4.f7.J5	9.9876E-02
Sum	f7.J7	8.5886E-01
Sum	f(5+7).J7	1.4616E+00
Sum	(p+ f).J7	1.5542E+00
Total		2.6514E+00

Table 2-4: Bound state contributions to $\alpha_{D,2}$ ($^2D_{5/2}$) in au [1].

Transition	J_{final} (J``)	Bound
$\boldsymbol{3d \rightarrow p}$	5/2	+ 0.6553 - 0.3973 = + 0.2581
$\boldsymbol{3d \rightarrow p}$	3/2	+ 0.3967 - 0.8011 = - 0.4044
$\boldsymbol{3d \rightarrow f}$	5/2	+ 0.0320 - 0.0663 = - 0.0343
$\boldsymbol{3d \rightarrow f}$	3/2	+ 0.0255 - 0.0357 = - 0.01022
$\boldsymbol{3p \rightarrow 3d}$	3/2	+ 0.02636
Total		+ 0.2844 - 0.4490 = - 0.1645

Table 2-5: Continuum contributions to $\alpha_{D,2}$ ($^2D_{5/2}$)in au

Channel #	Channel	$\alpha_{D,0}$ ($^2D_{5/2}$)
1	1D2.p1.J3	2.9273E-03
2	3F2.p1.J3	-1.3669E-01
3	3P2.p1.J3	6.4701E-02
4	3P0.p3.J3	-8.3062E-03
5	1S0.p3.J3	7.0647E-03
6	3P1.p3.J3	-3.1824E-03
7	1D2.p3.J3	-2.9273E-03
8	3F2.p3.J3	-1.4836E-02
9	3P2.p3.J3	1.5346E-01
10	3F3.p3.J3	-1.3537E-01
11	3P1.f5.J3	-7.0147E-03
12	1D2.f5.J3	-4.8808E-01
13	3F2.f5.J3	1.5344E+00
14	3P2.f5.J3	-5.8747E-02
15	3F3.f5.J3	-3.1888E-03
16	3F4.f5.J3	-1.4539E-02
17	1G4.f5.J3	-2.4871E+00

18	1D2.f7.J3	2.5393E-02
19	3F2.f7.J3	2.2035E-02
20	3P2.f7.J3	-5.5777E-02
21	3F4.f7.J3	-8.7985E+00
22	1G4.f7.J3	7.8268E+00
23	1D2.p1.J5	9.6991E-04
24	3F2.p1.J5	-3.9677E-02
25	3P2.p1.J5	2.1586E-02
26	3P1.p3.J5	7.0236E-04
27	1D2.p3.J5	2.0746E-02
28	3F2.p3.J5	-6.8104E-02
29	3P2.p3.J5	1.7751E-04
30	3F3.p3.J5	3.7854E-04
31	3F4.p3.J5	1.3032E+00
32	1G4.p3.J5	-1.5819E-01
33	3P0.f5.J5	2.5067E-01
34	1S0.f5.J5	-2.2036E-01
35	3P1.f5.J5	3.7143E-02
36	1D2.f5.J5	-2.4858E+00
37	3F2.f5.J5	8.7950E+00
38	3P2.f5.J5	-4.2117E+00
39	3F3.f5.J5	3.0733E+00
40	3F4.f5.J5	-1.9879E-01
41	1G4.f5.J5	-2.5095E+00
42	1D2.f7.J5	1.5634E+00
43	3F2.f7.J5	1.3727E+00
44	3P2.f7.J5	-3.4282E+00
45	3F4.f7.J5	-9.9150E+00
46	1G4.f7.J5	9.3169E+00
Total		-5.59196E-02

Table 2-6: Discrete contribution to $\beta_{D,0}$ ($^2D_{5/2}$) in au [1].

Transition	J of the final state (J')	Bound
$\boldsymbol{3d \rightarrow p}$	7/2	1.9258
$\boldsymbol{3d \rightarrow p}$	5/2	3.5763
$\boldsymbol{3d \rightarrow p}$	3/2	2.2230
$\boldsymbol{3d \rightarrow f}$	7/2	0.1288
$\boldsymbol{3d \rightarrow f}$	5/2	0.1229
$\boldsymbol{3d \rightarrow f}$	3/2	0.0924
$\boldsymbol{3p \rightarrow 3d}$	3/2	0.0203
Total		8.0894

Table 2-7: Continuum contribution to $\beta_{D,0}$ ($^2D_{5/2}$)in au.

Channel #	Channel	$\beta_{D,0}$ ($^2D_{5/2}$)
1	3P1.p1.J3	4.9002E-03
2	3F2.p1.J3	1.3400E-03
3	1D2.p1.J3	6.9979E-05
4	3P2.p1.J3	2.5786E-03
5	3P0.p3.J3	1.6888E-03
6	1S0.p3.J3	1.2398E-03
7	3P1.p3.J3	1.5833E-04
8	3F2.p3.J3	5.1599E-04
9	1D2.p3.J3	8.3086E-03
10	3P2.p3.J3	3.4411E-03
11	3F3.p3.J3	1.1584E-03
Sum	p.J3	2.5400E-02
12	3P1.f5.J3	2.4545E-04
13	3F2.f5.J3	2.6810E-03
14	1D2.f5.J3	2.7032E-03
15	3P2.f5.J3	1.0128E-03
16	3F3.f5.J3	2.3080E-02
17	3F4.f5.J3	2.0158E-03
18	1G4.f5.J3	7.2142E-02

19	3F2.f7.J3	3.2568E-04
20	1D2.f7.J3	2.0019E-03
21	3P2.f7.J3	3.3603E-04
22	3F4.f7.J3	6.4239E-02
23	1G4.f7.J3	1.1458E-02
Sum	f.J3	1.8224E-01
Sum	(p+ f).J3	2.0764E-01
24	3F2.p1.J5	1.4114E-03
25	1D2.p1.J5	7.8677E-05
26	3P2.p1.J5	2.8919E-03
27	3F3.p1.J5	1.0061E-02
28	3P1.p3.J5	7.6142E-04
29	3F2.p3.J5	1.9712E-01
30	1D2.p3.J5	6.4339E-03
31	3P2.p3.J5	1.7049E-04
32	3F3.p3.J5	4.9749E-06
33	3F4.p3.J5	2.5364E-02
34	1G4.p3.J5	7.0397E-04
Sum	p.J5	4.9853E-02
35	3P0.f5.J5	8.0792E-04
36	1S0.f5.J5	6.2082E-04
37	3P1.f5.J5	5.7801E-03
38	3F2.f5.J5	1.2479E-02
39	1D2.f5.J5	5.8922E-03
40	3P2.f5.J5	1.1597E-02
41	3F3.f5.J5	5.8210E-02
42	3F4.f5.J5	1.7185E-02
43	1G4.f5.J5	4.5039E-02
44	3F2.f7.J5	5.0123E-03
45	1D2.f7.J5	3.0659E-02
46	3P2.f7.J5	5.1413E-03
47	3F4.f7.J5	1.3266E-01

48	1G4.f7.J5	2.4387E-02
Sum	f.J5	3.5547E-01
Sum	(p+ f).J5	4.0533E-01
49	3F3.p1.J7	3.0260E-03
50	3F4.p1.J7	2.8679E-03
51	1G4.p1.J7	1.1380E-02
52	3F2.p3.J7	4.4174E-04
53	1D2.p3.J7	5.4777E-04
54	3P2.p3.J7	9.4077E-05
56	3F3.p3.J7	1.4850E-03
57	3F4.p3.J7	1.0948E-02
Sum	p.J7	3.0791E-02
58	3P1.f5.J7	4.7871E-02
59	3F2.f5.J7	1.5862E-02
60	1D2.f5.J7	1.2568E-04
61	3P2.f5.J7	5.0566E-02
62	3F3.f5.J7	6.0930E-02
63	3F4.f5.J7	2.9782E-02
64	1G4.f5.J7	1.1802E-02
65	3P0.f7.J7	1.6236E-02
66	1S0.f7.J7	1.5344E-02
67	3F2.f7.J7	1.7525E-02
68	1D2.f7.J7	1.0523E-01
70	3P2.f7.J7	1.8189E-02
71	3F4.f7.J7	1.0192E-01
72	1G4.f7.J7	1.8415E-02
Sum	f.J7	5.0979E-01
Sum	(p+ f).J7	5.4058E-01
Total		1.5355E+00

Table 2-8: Discrete contributions to $\alpha_{Q,0}$ ($^2D_{5/2}$) in au [1].

Transition	J of the final state (J')	Bound
$\boldsymbol{3d \rightarrow s}$	1/2	1.4280
$\boldsymbol{3d \rightarrow s}$	3/2	5.2230
$\boldsymbol{3d \rightarrow s}$	5/2	6.6580
$\boldsymbol{3d \rightarrow s}$	7/2	24.5520
$\boldsymbol{3d \rightarrow s}$	9/2	4.4860
$\boldsymbol{3d \rightarrow d}$	1/2	0.2670
$\boldsymbol{3d \rightarrow d}$	3/2	0.8370
$\boldsymbol{3d \rightarrow d}$	5/2	1.0610
$\boldsymbol{3d \rightarrow d}$	7/2	0.9360
$\boldsymbol{3d \rightarrow d}$	9/2	1.4780
$\boldsymbol{3d \rightarrow g}$	1/2	0.0027
$\boldsymbol{3d \rightarrow g}$	3/2	0.0075
$\boldsymbol{3d \rightarrow g}$	5/2	0.0140
$\boldsymbol{3d \rightarrow g}$	7/2	0.0210
$\boldsymbol{3d \rightarrow g}$	9/2	0.0482
$3d^9\ ^2D_{5/2} \rightarrow\ ^2D_{3/2}$		6.8420
$\boldsymbol{3s \rightarrow 3d}$		0.0053
Total		54.9170

Table 2-9: Continuum contributions to $\alpha_{Q,0}$ ($^2D_{5/2}$) in au.

Channel #	Channel	$\alpha_{Q,0}$ ($^2D_{5/2}$)
1	1S0.s1.J1	5.6517E-05
2	3P0.s1.J1	6.6128E-05
3	3P1.s1.J1	5.3537E-05
Sum	s1.J1	1.7618E-04
4	3P1.d3.J1	3.2059E-03
5	3F2.d3.J1	1.6143E-02
6	1D2.d3.J1	2.0243E-02
7	3P2.d3.J1	4.7831E-03
Sum	d3.J1	4.4375E-02
8	3F2.d5.J1	9.7051E-04
9	1D2.d5.J1	1.5049E-02
10	3P2.d5.J1	9.5770E-03

11	3F3.d5.J1	1.0743E-02
Sum	d5.J1	3.6339E-02
Sum	d.J1	8.0714E-02
12	3F3.g7.J1	1.2066E-02
13	3F4.g7.J1	1.5257E-05
14	1G4.g7.J1	2.0345E-01
Sum	g7.J1	2.1553E-01
15	3F4.g9.J1	3.9878E-02
16	1G4.g9.J1	8.0060E-03
Sum	g9.J1	4.7884E-02
Sum	g.J1	2.6341E-01
Sum	(s+ d+ g).J1	3.4431E-01
17	3P1.s1.J3	7.8332E-05
18	3F2.s1.J3	5.8306E-06
19	1D2.s1.J3	2.4301E-04
20	3P2.s1.J3	2.5635E-04
Sum	s1.J3	5.8352E-04
21	3P0.d3.J3	5.3316E-03
22	1S0.d3.J3	3.6454E-03
23	3P1.d3.J3	1.9176E-02
24	3F2.d3.J3	5.7222E-03
25	1D2.d3.J3	6.1706E-06
26	3P2.d3.J3	9.9963E-03
27	3F3.d3.J3	2.2664E-02
Sum	d3.J3	6.6542E-02
28	3P1.d5.J3	1.6681E-03
29	3F2.d5.J3	1.8817E-03
30	1D2.d5.J3	3.8140E-02
31	3P2.d5.J3	3.0885E-02
32	3F3.d5.J3	1.6182E-02

33	3F4.d5.J3	1.0723E-01
34	1G4.d5.J3	2.4870E-03
Sum	d5.J3	1.9847E-01
Sum	d.J3	2.6502E-01
35	3F2.g7.J3	6.1640E-03
36	1D2.g7.J3	9.8603E-03
37	3P2.g7.J3	7.8439E-04
38	3F3.g7.J3	8.2672E-02
39	3F4.g7.J3	7.8298E-03
40	1G4.g7.J3	2.8889E-01
sum	g7.J3	3.9620E-01
41	3F3.g9.J3	0.0000E+00
42	3F4.g9.J3	2.5004E-01
43	1G4.g9.J3	5.0280E-02
Sum	g9.J3	3.0032E-01
Sum	g.J3	6.9652E-01
Sum	(s+ d+ g).J3	9.6212E-01
44	3F2.s1.J5	1.4351E-04
45	1D2.s1.J5	2.9391E-04
46	3P2.s1.J5	9.5701E-06
47	3F3.s1.J5	7.1213E-05
Sum	s1.J5	5.1820E-04
48	3P1.d3.J5	4.4216E-02
49	3F2.d3.J5	3.5199E-03
50	1D2.d3.J5	1.7160E-02
51	3P2.d3.J5	3.2571E-03
52	3F3.d3.J5	5.0535E-02
53	3F4.d3.J5	1.1526E-02
54	1G4.d3.J5	4.5177E-02
Sum	d3.J5	1.7539E-01

55	3P0.d5.J5	2.5695E-02
56	1S0.d5.J5	2.4455E-02
57	3P1.d5.J5	5.9777E-03
58	3F2.d5.J5	1.0149E-03
59	1D2.d5.J5	2.1977E-03
60	3P2.d5.J5	1.5345E-02
61	3F3.d5.J5	1.5571E-03
62	3F4.d5.J5	1.3895E-01
63	1G4.d5.J5	1.6699E-04
Sum	d5.J5	2.1536E-01
Sum	d.J5	3.9075E-01
64	3P1.g7.J5	4.8998E-03
65	3F2.g7.J5	3.6054E-02
66	1D2.g7.J5	4.2396E-02
67	3P2.g7.J5	1.2758E-02
68	3F3.g7.J5	2.0889E-01
69	3F4.g7.J5	5.4998E-02
70	1G4.g7.J5	2.3072E-01
sum	g7.J5	5.9072E-01
71	3F2.g9.J5	5.5944E-03
72	1D2.g9.J5	3.6836E-02
73	3P2.g9.J5	1.0206E-02
74	3F3.g9.J5	0.0000E+00
75	3F4.g9.J5	5.4134E-01
76	1G4.g9.J5	1.0894E-01
Sum	g9.J5	7.0292E-01
Sum	g.J5	1.2936E+00
Sum	(s+ d+ g).J5	1.6849E+00
77	3F3.s1.J7	2.9812E-04
78	3F4.s1.J7	9.4064E-04

79	1G4.s1.J7	6.4225E-05
Sum	s1.J7	1.3030E-03
80	3F2.d3.J7	7.4426E-03
81	1D2.d3.J7	1.2221E-03
82	3P2.d3.J7	4.7648E-02
83	3F3.d3.J7	1.4510E-02
84	3F4.d3.J7	2.9041E-03
85	1G4.d3.J7	6.9366E-02
Sum	d3.J7	1.4309E-01
86	3P1.d5.J7	1.4294E-02
87	3F2.d5.J7	1.7428E-02
89	1D2.d5.J7	7.2199E-02
90	3P2.d5.J7	8.0520E-03
91	3F3.d5.J7	4.1709E-03
92	3F4.d5.J7	4.6609E-03
93	1G4.d5.J7	1.9300E-02
Sum	d5.J7	1.4011E-01
Sum	d.J7	2.8320E-01
94	3P0.g7.J7	8.0188E-03
95	1S0.g7.J7	8.8755E-03
96	3P1.g7.J7	5.1993E-02
97	3F2.g7.J7	7.7008E-02
98	1D2.g7.J7	4.0552E-02
99	3P2.g7.J7	8.7492E-02
100	3F3.g7.J7	3.0207E-01
101	3F4.g7.J7	1.3559E-01
102	1G4.g7.J7	1.0766E-01
Sum	g7.J7	8.1926E-01
103	3P1.g9.J7	0.0000E+00
104	3F2.g9.J7	3.6491E-02

105	1D2.g9.J7	2.4032E-01
106	3P2.g9.J7	6.6586E-02
107	3F3.g9.J7	0.0000E+00
108	3F4.g9.J7	6.1730E-01
109	1G4.g9.J7	1.2409E-01
Sum	g9.J7	1.0848E+00
Sum	g.J7	1.9041E+00
Sum	(s+ d+ g).J7	2.1885E+00
110	3F4.s1.J9	1.2925E-05
111	1G4.s1.J9	5.5348E-04
Sum	s1.J9	5.6641E-04
112	3F3.d3.J9	4.4893E-02
113	3F4.d3.J9	9.2857E-02
114	1G4.d3.J9	4.0331E-02
Sum	d3.J9	1.7808E-01
115	3F2.d5.J9	1.0702E-02
116	1D2.d5.J9	1.6646E-02
117	3P2.d5.J9	1.4329E-03
118	3F3.d5.J9	2.6889E-02
119	3F4.d5.J9	1.1941E-01
120	1G4.d5.J9	8.2437E-02
Sum	d5.J9	2.5752E-01
Sum	d.J9	4.3560E-01
121	3P1.g7.J9	2.8507E-01
122	3F2.g7.J9	6.2949E-02
123	1D2.g7.J9	7.3676E-04
124	3P2.g7.J9	2.9263E-01
125	3F3.g7.J9	2.3605E-01
126	3F4.g7.J9	1.4000E-01
127	1G4.g7.J9	2.1424E-02

Sum	g7.J9	1.0389E+00
128	3P0.g9.J9	1.0026E-01
129	1S0.g9.J9	1.1095E-01
130	3P1.g9.J9	0.0000E+00
131	3F2.g9.J9	7.9875E-02
132	1D2.g9.J9	5.2645E-01
133	3P2.g9.J9	1.4589E-01
134	3F3.g9.J9	0.0000E+00
135	3F4.g9.J9	3.3757E-01
136	1G4.g9.J9	6.7724E-02
Sum	g9.J9	1.3687E+00
Sum	g.J9	2.4076E+00
Sum	(s+ d+ g).J9	2.8437E+00
Total		8.0236E+00

2.5 References

1. M. H. Abdalmoneam and D. R. Beck, *J. Phys. B* **47** 085003 (2014)
2. S. L. Woods and S R Lundeen, *Phys. Rev. A* **85** 042505 (2012)
3. http://www.physics.colostate.edu/our-people/stephen-lundeen/
4. M. E. Hanni, J. A. Keele, S. R. Lundeen, and W. G. Sturrus, *phys. Rev. A* **78** 062510 (2008)
5. S. L. Woods , C. Smith, J. A. Keele and S. R. Lundeen *Phys. Rev*. **187** 022511 (2013)
6. W. R. Johnson, *Atomic Structure Theory*, Springer Verlag (2007)
7. D. R. Beck and L. Pan, *J. Phys. B* **43** 074009 (2010)
8. D. R. Beck, *J. Phys. B* **45** 225002 (2012)
9. Jean-Patrick Connerade, *Highly excited atoms*. No. 9. Cambridge University Press, (1998)
10. J. E. Mayer and M G Mayer , *Phys. Rev.* **43** 605 (1933)
11. R. J. Drachmann, *Phys. Rev A* 47, 694 (1993)
12. T. F. Gallagher, *Rydberg atoms*. Vol. 3. Cambridge University Press, (2005).
13. G. W. F. Drake, editor, *Springer Handbook of Atomic, Molecular, and Optical Physics*. Springer 2nd edition, (2005).
14. R. J. Drachman *, Phys. Rev. A* **26** 1228 (1982)
15. A. Dalgarno, *Adv. Phys.* **11** 281 (1962)
16. A. Kramida, Y. Ralchenko, and J. Reader, NIST Atomic Spectra Database , http://physics.nist.gov/asd
17. W. C. Martin and W. L. Wiese, *Atomic, Molecular and Optical Physics Handbook*, G. W. F. Drake, editor, AIP Press, p.149 (1996)
18. Wiese, W. L., M. W. Smith, and B. M. Glennon. *Atomic Transition Probabilities Hydrogen through Neon, NSRD2-NBS 4* **Volume 1** *Hydrogen Through Neon*. National Bureau of Standards Washington DC INST For Basic Standards, (1966)
19. J. P. Desclaux, *Comput. Phys. Commun*. **9** 31 (1975)
20. D. R. Beck, computer code RFV1S (unpublished)
21. D. R. Beck, computer code RCI (unpublished)

22. M. G. Tews and W. F. Perger, *Comput. Phys. Commun.* **141** 205 (2001)
23. D. R. Beck, computer program RPI, unpublished
24. P. Schwerdtfeger, "Table of experimental and calculated static dipole polarizabilities for electronic ground states of the neutral elements", http://ctcp.massey.ac.nz/dipole-polarizabilities , (2014)

3 RCI study of Hyperfine Structure Constants of V II $3d^4$, $3d^3$ 4s, and $3d^2$ $4s^2$ J = 1-5 even states

3.1 Introduction

This is a study of the hyperfine structure (HFS) constants of singly ionized vanadium, V II. The two HFS constant; Magnetic dipole interaction constant , A, and the electric quadrupole interaction constant, B, have been calculated for the $3d^4$, $3d^3$ 4s, and $3d^2$ $4s^2$ J=1 to 5 even parity states in V II [1]. Lande g-values and the vector composition percentages for all the wavefunctions of those configurations have also been calculated [1].

The importance of studying HFS of V II comes from three reasons; the astrophysical importance of the iron group, the scientific need for accurate atomic data for these elements and their positive ions, and the lack of HFS data of V II and other important elements in the literature with similar configurations, i.e. d^4, d^3 4s, d^2 s^2 .

Iron group elements, $20 > Z > 30$, have been observed in many stars. Vanadium in the sun is predominately, > 99 %, V II [2, 3]. Many of the lower sequence stars, $T_e \leq$ 7000 K (T_e = effective temperature) have composition similar to the solar composition [4]. Iron-group elements have been also observed in many of the chemically peculiar (CP) stars, the group of stars in the upper main sequence with $7000 > T_e > 30{,}000$ K [4]. For example the spectrum of V II was measured in a study of the 3 Cen A star spectrum [5]. Another example is the spectrum of the Eta Carina (η Car) massive star which was found to be rich in singly ionized iron group elements [6]. Also, the abundance ratios of the iron-group elements indicate the history of nucleo-synthesis of some stellar objects in the early universe, for example the ratio of (V, Co, Zn)/ Fe in comparison to (Cr, Mn)/ Fe can provide information about the range of temperature of supernovae explosion [7 and references therein].

Many researchers have reported the importance of the availability of accurate atomic data, e.g. oscillator strength, lifetime, Lande g-value, HFS constants, etc, for the iron-group elements and their positive ions. According to Biemont et al (1989) studying the solar abundance of Vanadium through separate direct measurements on V I and V II helps to reduce the uncertainty which is introduced in the ratio (V II/ V I) dependent model. It also helps to test and constrain the model. In a study of the solar abundance of V they found that spectra of V I and V II were blended and that the HFS of V lines

complicated analysis. They used semi-empirical g*f*-values of Kurucz (1987) to estimate the relative contribution of possible V II blends to some lines. Values of empirically estimated HFS were used for the calculations of the lines that showed broad Fourier Transform Spectroscopic profiles. They concluded that although V II was the best abundance indicator of V though only very few lines are suitable to conduct an accurate study. This in my opinion stresses the need for more accurate studies on V II atomic data including its HFS. In a study of scandium and vanadium abundance in the solar photosphere Youssef and Amer stated that Sc and V in the solar photosphere are predominantly singly ionized and that accurate transition probabilities of singly ionized elements of the iron group are the key solution for understanding the abundance of these elements [3 and references therein]. Since most of the observed lines are heavily blended there must be criteria for choosing the suitable lines to be studied. One of the criteria that Youssef and Amer considered was the availability of HFS data. Also, they used earlier HFS measurements on Sc II to derive wavelength and log gf-values to calculate the abundance of Sc [3].

Almost all the elements (except thorium) in the sun have isotopes with hyperfine splitting. The spectrum received from the sun is very blended. Computer programs for analyzing spectra including the hyperfine and isotopic splitting already exist [8], e.g. ATLAS12 by Kurucz. Atomic data are required to use these programs efficiently. The required atomic data include for example energy levels, wavelength, Lande g-value, hyperfine and isotopic splitting, etc. Many elements of the iron group have isotopes with hyperfine splitting that had not been considered properly in earlier studies. Ignoring isotopic or hyperfine splitting introduces many systematic errors in the analysis of the spectral lines, e.g. abundances determined from equivalent widths are systematically too large, and the Doppler width and Voigt profile differ significantly from isotope to isotope [see Kurucz 1993 for more details]. Understanding the solar spectrum fully and analyzing it requires the availability of accurate data for the isotopic and hyperfine splitting of each energy level of every isotope of every atom and ion [8].

In studying the abundance analysis of the Homunculus (the nebula that surrounds η Car massive star) Nielsen and Gull, 2009 reported that accurate spectral analysis was highly dependent on the availability of accurate atomic data. Using old atomic data for V

II transitions (from $3d^4\ ^5D$ and $3d^3\ 4s\ ^5F$) produced ambiguous results for the blue-shift. They observed that Vanadium was ^{51}V, nuclear spin =7/2, magnetic moment (μ) 5.51 μ_N (μ_N: nuclear magneton) and was subject to hyperfine splitting. Using the results given by Arvidsson 2003 [who studied hyperfine constants and wavelengths in V II derived by Fourier transform spectrometry] for the V II spectrum removed the ambiguity in their results [6].

Until recently there were very few V II HFS constants available in the literature. In 2003 Arvidsson [9] measured 26 new values for HFS A, as cited in Cowley et al 2006 [5]. In 2011 Armstrong et al. published results of measurements of HFS A of 24 even levels and 31 odd levels. In 2015 Abdalmoneam and Beck published RCI results of 69 values of HFS constants A and B [1].

Our group had successfully used RCI method to compute HFS of different transition metals (TM), e.g. Sc II, Y II [10], Fe V [11], Ta II [12], and many others (see [13] for a complete list). Computing HFS of transition metals where d^m, d^{m-1} s, and $d^{m-2}\ s^2$ levels are interleaved can be still challenging. For example there was a clear discrepancy between theoretical and experimental results of HFS for Ti I $3d^2\ 4s^2\ ^3P$ and V I $3d^3\ 4s^2\ ^4P$ in [14].

Our long term goal of such studies has been gaining and providing a predictive understanding of the many body effects that govern HFS. In our previous studies we presented ab initio RCI calculations of HFS where many body effects, such as valence pair correlation, shallow-core-valence correlation and core polarization, were evaluated. The same ab initio methodology has been used for V II HFS calculations. Predicting the exact position of some levels was quite difficult. In this work we have improved the RCI method by additionally shifting some energy diagonal matrix elements. Shifting the diagonal matrix elements is an empirical approach that's done through comparing the calculated and experimental energy levels (see appendix, section 6.3). The effects of core-valence pair correlations, triple excitations, and other computationally expensive correlation configurations are substituted by shifts of reference diagonal matrix elements. This shifting is properly effective as long as no correction is needed for the off-diagonal matrix elements of LS degenerate states.

This study provides atomic data for the most stable vanadium isotope ^{51}V, I=7/2 . We present RCI results of hyperfine structure constants and Lande g-value of 69 V II even parity levels. The text gives a comparison of the new results with the available data found in the literature and discusses thoroughly the agreements and disagreements with the available experimental data. This study provides 43 new values for HFS A and 69 new values of HFS B. The results are ab initio and corrected through shifting the energy diagonal matrix elements. Justification of the values of shifts is in section 5.3. Also a semi empirical method for predicting HFS A for some levels is introduced. The odd parity configurations, $3d^3$ 4p and $3d^2$ 4s 4p ,of V II have been ignored in this study because of the following reasons; the LS degenerate levels are not close in energy so they do not serve our goal, and they can be studied as Rydberg states of a V III core and a Rydberg p electron.

3.2 Theory and Method

3.2.1 Hyperfine structure operators

The fine structure in atomic spectra refers to the deviation of the atomic spectra from that of the non-relativistic Schrodinger picture. It results from the relativistic momentum due to electrons together with their magnetic moment and due to the relative motion of the charge of the static nucleus.

The effect of the hyperfine structure was first observed in the yellow spectrum of Sodium, where under high resolution the spectral lines of $^2P_{3/2}$ and the singlet $^2P_{1/2}$ were split (with a slight shift) into finer lines. The same thing was observed in many other metals but a few metals did not show this behavior, e.g. ^{114}Cd $5s\ 5p\ ^1P_1 - 5s5d\ ^1D_2$ line, [15]. Later this hyperfine structure was explained to be due to the interaction between the nucleus dipole moment and the magnetic moment of the electrons. This produces a new quantum number that characterizes the system. So for a nucleus with an intrinsic spin I the total angular momentum of the nucleus and the electrons become

$$F=I+J \tag{3.1}$$

, J is the total angular momentum of the electrons.

Computationally the hyperfine structure is one of the properties that emphasize the region of space near the nucleus. Accurate calculations should include core polarization from all closed "s" sub-shells. The following equations are the non-relativistic [16]. The relativistic equations are given in the appendix, section 6.2. The hyperfine energy, that includes only the magnetic dipole and electric quadrupole contributions, is given [16 and references therein] by

$$E_{HFS} = \frac{1}{2}AK + BK(K+1) \tag{3.2}$$

Where

$$K = F(F+1) - I(I+1) - J(J+1) \tag{3.3}$$

, equations 3 and 4 are correct for both relativistic and non-relativistic treatments.

Non-relativistically the dipole magnetic interaction constant A can be considered as a result of the interaction of three operators, in this proportionality relation;

$$A \propto (\eta_s + \eta_l + \eta_d) \tag{3.4}$$

, the three operators are the contact spin-spin (Fermi-contact term), α_s, operator that's due to the nucleus- electron's field interaction at r = 0, it is strongly determined by the transitions from an s sub-shell to another s sub-shell, and open "s" sub-shells already in the reference functions, the orbital-spin operator, α_l, that's due to the orbital motion of the electrons around the nucleus and it is strongly determined by the excitations from a p sub-shell to another p sub-shell, and the spin dipolar operator, α_d ,that's due to the interaction between the electron spin and nuclear spin at r ≠ 0 and it is strongly determined by the transitions form s sub-shells to d sub-shells. The largest effect comes from the contact spin-spin operator and it contributes significantly only the presence of an open s sub-shell.

For LS coupling A can be expressed in terms of the angular factors (λ) and the reduced matrix elements (α) as follows;

$$A = 95.409\ (\mu/I)(\lambda_s\alpha_s + \lambda_l\alpha_l + \lambda_d\alpha_d) \tag{3.5}$$

, A is in MHz, α in atomic units (au), μ in nuclear magneton.

The reduced matrix elements are given by [16]

$$\alpha_s = \langle LS \left\| \sum_i^N \tfrac{8}{3}\pi\delta(r_i)s_i \right\| LS\rangle \tag{3.6a}$$

$$\alpha_l = \langle LS \left\| \sum_i^N {l_i}/{(r_i)^3} \right\| LS \rangle \tag{3.6b}$$

$$\alpha_d = \langle LS \left\| \sum_i^N \left[\left(3s_i \frac{r_i}{(r_i)^5} \right) r_i - s_i/(r_i)^3 \right] \right\| LS \rangle \tag{3.6c}$$

The sum is done over the number of electrons. The ket and bra represent the electronic wavefunction of the atomic states.

The angular factors are given by [16]; here

$$\lambda_s = -(-1)^{S+L+J} \left(\tfrac{2J+1}{J(J+1)} \right)^{1/2} \begin{Bmatrix} J & J & 1 \\ S & S & L \end{Bmatrix} \tag{3.7a}$$

$$\lambda_l = -(-1)^{S+L+J} \left(\frac{2J+1}{J(J+1)} \right)^{1/2} \begin{Bmatrix} J & J & 1 \\ L & L & S \end{Bmatrix} \tag{3.7b}$$

$$\lambda_d = \left(\frac{3(2J+1)}{J(J+1)} \right)^{1/2} \begin{Bmatrix} L & L & 2 \\ S & S & 1 \\ J & J & 1 \end{Bmatrix} \tag{3.7c}$$

The { } in equations (3.7a) and (3.7b) are the 3-j symbols, in equation (3.7c) they are the 9-j symbol. Knowledge of the non-relativistic HFS operators helps us understand what correlation is needed relativistically. I.E. once again correlation is mainly non-relativistic.

The interaction between the nuclear electric quadrupole moment and the electric field gradient within the atom produces E_Q [15]. Consider the electrostatic potential of an arbitrary charge distribution ϕ (r), r > R (R: radius of charge distribution) which can be expanded as

$$\phi(r) = k \left[\frac{q}{r} + \frac{p.r}{r^3} + \frac{r.Q.r}{2\ r^5} + \ \ldots\ldots \right] \tag{3.8}$$

Where q is the monopole moment, p is the dipole moment (zero for an eigenstate of parity) and Q is the quadrupole tensor. Q is a diagonal tensor with a vanishing trace (Q_{11} + Q_{22} = -Q_{33}).The electric quadrupole constant B is given by [16]

$$B = \frac{3}{2I\ (2I-1)} \times 234.9649\ Q\ \lambda_Q\ \alpha_Q \tag{3.9}$$

, B in MHz and Q in barns.

$$\lambda_Q = -\frac{1}{4} (-1)^{S+l+J} \left(\frac{2J+1}{J(J+1)(2J-1)(2J+3)} \right)^{1/2} \begin{Bmatrix} J & J & 2 \\ L & L & S \end{Bmatrix} \tag{3.10}$$

$$\alpha_Q = \langle LS \left\| 2 \sum_i^N C_I^{(2)} / r_i^3 \right\| LS \rangle \tag{3.11}$$

, for $l = 2$ and $m_l = 0$, $C_0^{(2)}$ is given as

$$C^{(2)} = \sqrt{\frac{4\pi}{5}}\ Y_{2,0}\ (\theta, \varphi) \tag{3.12}$$

3.2.2 Dirac-Fock functions of the reference configurations

The reference wavefunctions (configurations) are eigenstates of J^2, J_z, and parity with fixed one electron angular functions (spinors). The radial functions are numerical solutions of the Dirac-Fock Hamiltonian obtained using the Desclaux code [17]. The reference functions are $3d^4$, $3d^3$ 4s, and $3d^2$ $4s^2$. The radials of 1s , 2s, 3s, 3p, and were prepared separately for each of the reference functions $3d^4$ and $3d^3$ 4s . Then the 1s …3d radials of $3d^4$ were added to the 4s radial from $3d^3$ 4s to make the reference radial functions. The reason of this choice was the observation that this arrangement leads to the minimal corrections needed for each of reference functions. For example with this arrangement it was observed that the energy contribution from the correlation configurations to $3d^4$ was small and to $3d^3$ 4s was a little bigger but still small enough. The choice of taking 1s to 3d radials from the $3d^3$ 4s Dirac-Fock functions led to large corrections to the $3d^4$ references (~ 1 eV). This strategy was used for all V II calculations. It satisfies the requirement for having orthonormal radial RCI basis set [18].

3.2.3 Relativistic configuration Interaction Calculations

In the RCI calculations there were five main steps; LS coupling of the reference functions, diagonalizing the matrices of LS degenerate states, correlation, addition of Breit effect, and shift.

All the reference functions have been re-coupled to be eignenstates of L and S. For example a function like $3d^4$ J = 2 even with jj J coupling only it looks as made up of 8 eigen vectors with 5 eigenvalues which are automatically produced by the RCI program [18], but the LS coupling of these states (vectors) cannot be distinguished . Then

the LS coupled terms are prepared, see section 3.2.3.1. So that terms like $^3F_2$, $^3P_2$, $^5D_2$, etc will be created explicitly in the calculations. As for $3d^3$ 4s (or $3d^2$ $4s^2$) more detailed LS coupled terms for the sub-groups are created. For example we have $3d^3$ (^{2}D) 4s $^1D_2$, where L and S are specified and all possible j^s get included for each sub-group. Having the LS coupled vectors shown explicitly is very helpful for recognizing the contribution of each of them and for more accurate calculations that will be needed later (e.g. choosing the shift for each vector, recording the percentage contribution of each LS coupling, and comparing the calculated g-value to the expected g-value due to the sharing LS coupled terms).

The Breit effect is added to take two particle relativistic corrections due to electromagnetic interaction into account. It adds the energy due to the magnetic interactions and the retardation effects, that's about 1 – 200 cm^{-1}.

3.2.3.1 Treating the LS degenerate states

LS degenerate states (vectors) cannot be distinguished in regular RCI runs. Many of the levels in V II are composed of LS degenerate vectors. For example Thorne 2013 shows the composition of the level at 25191 cm^{-1} as 37 % $3d^4$ $^1D_2$, 32% $3d^4$ $^1D_2$, and 17% $3d^3$ (^{2}D) 4s ^{1}D and the level at 50951 cm^{-1} is composed of 48% $3d^4$ $^1D_2$, 30 % $3d^2$ $4s^2$ $^1D_2$, and 12% $3d^4$ $^1D_2$. So the two degenerate $3d^4$ ^{1}D vectors are distributed between two energy levels (or more). A regular RCI run (with LS coupling) will show a similar distribution to the degenerate vectors.

In order to be able to distinguish the degenerate vectors separate RCI runs were made. Each run contains only one pair of degenerate vectors which produces a 2 x 2 energy matrix for them. From this run the two vectors are orthogonalized and new mixing coefficients are produced. Later using these new coefficients to rotate the two states produced by the LS diagonalizer results in having only one vector occupying one energy level entirely, and the two vectors are no longer mixed. For example table 3-7 shows 25191 cm^{-1} has 54 % $3d^4$ ^{1}D and 50952cm^{-1} has 72% of another $3d^4$ ^{1}D (These are two different $3d^4$ ^{1}D, they are degenerate though). So the degenerate vectors are no longer

mixed in one level. This allows us to obtain individual shifts for the LS diagonal states. This approach is new to this work.

3.2.3.2 Correlations

In the RCI calculations the filled and partially filled energy sub-shells are the numerical solutions of Dirac-Fock-Breit Hamiltonian. The empty sub-shells are relativistic screened hydrogenic (RSH) functions with adjustable effective charge (Z*). Z* is determined by applying the energy variational principle. The initial value of Z* is calculated as in equation (3.14);

$$Z_i^* = m(m + 1.5)/\langle r\rangle_{nlj} \quad (3.13)$$

, m is the principle quantum number of the RSH sub-shell. Usually $m = l+1$, l is orbital quantum number. $\langle r\rangle_{nlj}$ is the average radius of the sub-shell which is being replaced. A usual choice will be taking $\langle r\rangle_{nlj}$ of the outer most sub-shell, e.g. $3d_{5/2}$, for the first radial set of the RSH functions, then $\langle r\rangle_{nlj}$ of the 2nd one, e.g. $3d_{3/2}$ for the 2nd radials of the RSH, and so on. Special cases for calculating$\langle r\rangle_{nlj}$are mentioned below. The RSH included l = 0 -5, sub-shells s, p, d, f, g, and h. They are referred to as *v*l, e.g. *v*s, *v*p, etc. These calculations included five different radials for *v*s, 2-3 radials for *v*p-*v*g, and one radial for *v*h.

The quality of the results of the HFS calculations is strongly dependent on the quality of the wave function. A very well correlated wave function will include single, double, triple, and quadrupole excitations from the valence, the shallow core and the core sub-shells. All these excitations must be done equivalently for the three reference configurations. There are many limitations for including the correlation effects this way. The first limitation is the 20K allowed vectors by the RCI code. For J = 2 one correlation like $3p^2$ to *v*h^2 includes 3888 vectors. Another correlation like 3p 3d to *v*f *v*h includes 6357 vectors. For J=5 a triple excitation from 3d to *v*p *v*f *v*h includes 9784 vectors. Even a super computer with 10^6 x 10^6 energy matrices will never be sufficient to include all double, triple and quadruple excitations, e.g. $3p^2\ 3d^2$ to *v*$f^2\ vh^2$. Another limitation is the extended effect of some correlation configurations, e.g. $3p^5\ 3d^4$ *v*f, on the rest of matrix. This effect will be discussed in section 3.2.3.3. According to these limitations the

correlation configurations are divided into three groups; correlations that must be present in the wave function, correlations which are computed separately and only their energy effects are added later as shifts, and computationally expensive correlations with very small effects that are not calculated at all.

Single and double excitations from valence and shallow core sub-shells give most of the corrections to the calculated properties. The energy contributions due to correlations are calculated through intermediate normalization $\langle\varphi|\psi\rangle = 1$, φ is the reference function and ψ is the total wavefunction [1].

Single excitations from ns to *v*s are essential for accurate HFS calculations because they represent the effect of the Fermi-contact term. Excitations are done from ns, n = 1, 2, 3, and 4 to all the included five *v*s radials. Obtaining Z* for each of these *v*s was done in a separate run, where $\langle r\rangle$ of one ns sub-shell was used to calculate the initial value of Z* then after it was optimized the final value was added in the RCI file of the whole matrix. Z* range from 1 to 25. One way to evaluate quality of the selected set of Z* was to see their effect on the sum of small HFS A^s, < 100 MHz. This effect can be seen by considering $C\ \langle ns^2|T|ns\ vs\rangle$, where T is the hyperfine structure operator and C are the RCI coefficients. A good set of Z* will maximize the product. Other important single excitations to HFS were 3s to 3d and 3p to *v*p when the sub-group $3p^5$ *v*p coupled to J = 1 or 2 (i.e. ($3p^5$ *v*p) J=1 or 2 for any J_{total}= 1 -5)).

The single excitations of 3d to *v*d were crucial for two reasons; first the *v*d RSH substituted for 4d (and higher nd) sub-shells. It was difficult to include the 4d radial in the Dirac-Fock calculations because Desclaux code does not treat two partially filled sub-shells having the same symmetry accurately. So there was a great emphasis on including many radials for *v*d. The second *v*d RSH corrected the 3d sub-shell radial especially for the $3d^3$ 4s and $3d^2$ $4s^2$ references and their correlation configurations. Only 2-3 different radials for *v*d were included. To justify this choice, it is known that$\langle r_{4d}\rangle \gg \langle r_{3d}\rangle$. Also, $= c_1 4d + c_2 5d + c_3\, 6d + \cdots$, $c < 1$ in a converging series, where c approaches zero for the higher nd Rydberg orbitals. The most effective part of this series is only the part near 3d and only 2 *vd* radials are sufficient to represent it.

Single and double excitations, e.g. 3s to 3d, 3s to 4s, $3p^2$ to $3d^2$, .. etc., that involve the exclusion effect were quite important. The exclusion effect means that only some (not all) LS couplings of the reference functions will be affected by the excitation and the other LS couplings will not, due to Pauli Exclusion Principle. For example; if the reference configuration is $3p^6\ 3d^8$ then a $3p^2$ excitation to $3d^2$ will produce $3p^4\ 3d^{10}$. The reference configuration has five LS coupling terms; ^1S, ^3P, ^1D, ^3F, and ^1G. The produced configuration has only three LS coupling terms; ^1S, ^3P, and ^1D. So that only the first three LS terms in the reference configurations will have their energies and other properties affected by the transition of two p electrons to d- sub-shell while the other LS coupling terms will not be affected. (This is an illustrative example. It is given because it is easier than the actual ones included in the calculations that have so many LS coupling terms)

The complete wavefunction included the correlations due to all single excitations from core, shallow core, and valence sub-shells to RSH sub-shells. It also included excitations from the shallow core to valence sub-shells and many pair excitation correlations. One kind of single excitation was replaced by a shift, that is 3p to *vf* and 3p to *vp* for the cases where the sub-group $3p^5$ *vp* has J = 0.

3.2.3.3 Shifting the diagonal matrix elements

Shifting the energy diagonal matrix element is done by manually adding a specific amount of energy to a specific diagonal matrix element of the reference configurations. It could be shifting up by adding positive energy or shifting down. Part of the shift is accurately prepared through ab initio RCI calculations. This is done to replace specific configurations. Another part of the shift is obtained when comparing the calculated energy to the experimental values. This part substitutes for the effects of the triple and quadruple excitations, as well as missing core-core and core-valence correlation energies, that hadn't been calculated.

Most of the correlations that have big energy effects and negligible contribution to HFS were replaced by shifts. These correlations included 3p to *v*p (J = 0) and to *v*f, 3s 3p to *v*d *v*p and to *v*d *v*f. The values of each of these shifts were prepared from RCI runs that included one vector of a reference configuration, e.g. $3d^2\ 4s^2\ ^3F$, and the correlation

configuration (e.g. $3p^5$ *v*f $3d^2$ $4s^2$) then optimizing Z*. For some bi-virtual correlations, e.g. 3s 3p to *v*d *v*f, the angular momentum sections had to be prepared by the BCB method because their determinants generated more than 1000 vectors.

The shift that comes from comparison to experiment is two parts; the first is a "global shift" which is applied to all the LS coupling (vectors) of one of the reference configurations, the second is an "individual shift" applied to each vector. The global shift is obtained by comparing RCI and experimental energies of pure levels, e.g. $3d^4$ ^5D and $3d^3$ 4s ^5F for J=1, 2, 3, and 4 and $3d^4$ ^3H and $3d^3$ 4s ^5F for J=5. This shift is done to the vectors of one reference relative to the other one (not to both references at the same time).

An RCI file with a full matrix of 20K vectors takes about 25 min to run [at a 2.0 GHz 8 CPU pc]. Each RCI run of a single correlation configuration takes 3 - 40 min. This is besides the time needed for preparing the input files, e.g. the angular momentum sections of $3s^1$ $3p^5$ *v*d *v*f $3d^3$ 4s , J=5, produces 32 angular momentum sections, 191 eigen-values and 6001 eigen-vectors. So it had to be prepared through 7 smaller runs. In each of these runs the configuration is split into two groups, for example (of $3s^1$ $3p^5$) and (*v*d *v*f $3d^3$ 4s), where a specific range of angular momentum is specified for each group, see figure 3-1. This process is repeated until the whole range of allowed angular momentums is covered. So getting accurate values for the shift was quite time consuming.

BCB= (3s^1 3p^5) (3d^3 4s^1 *vd vf*)

V_1= 3s1 3p5

J_1= 4, 0

V_2= 3d3 4s1 vd vf

J_2= 8, 0

Figure 3-1: Splitting a configuration into sub-groups and specifying a range of angular momentum for each sub-group, BCB method.

3.2.4 Approximate conservation rule

Through observation of the RCI results and experimental results of HFS A it was found that; " the sum of HFS A of two or more levels of the same LSJ (either degenerate or different configurations) and small energy gap between them is almost constant at different energy shifts".

This rule is applicable for the cases of pure LS and when the two levels have a mix of two configurations with the same LS, e.g. one level is pure $3d^4$ and the other is pure $3d^3$ 4s or each of the two levels is a mixture of $3d^4$ and $3d^3$ 4s all with the same LSJ. Shift of the diagonal matrix elements has two effects; one it changes the energy of one or more levels and it also changes the percentage of the vector composition of energy levels. The importance of this rule is the confidence that even in presence of small differences of energies between the experimental values and RCI calculations of individual levels the HFS sum for those levels will be conserved. Only a few levels have their experimental HFS measured. So the RCI sum of HFS can be used to predict of the HFS A of some levels in a semi-empirical method. Examples of levels where this rule is applicable are; the two levels at 18270 and 20687 cm^{-1} which are a mix of $3d^4$ and $3d^3$ 4s $^3D_1$. The energy difference is 2417 cm^{-1} and only one of them has an experimental A, the two levels at 19166 and 20090 cm^{-1} which are a mix of 3d3 (^{2}P) 4s and $3d^3$ (^{4}P) 4s ^{3}P. A semi-empirical value can be extracted from RCI sum by subtracting off the measured value [1].

3.3 Results

3.3.1 General Remarks

Hyperfine structure constants (HFS) A, and B/Q, energy levels, Lande g-value, and vector composition of V II $3d^4$, $3d^3$ 4s, and $3d^2$ $4s^2$ J=1-5 even states have been calculated using RCI method. For these calculations a nuclear dipole moment μ=5.149 and nuclear spin I=7/2 were used. RCI calculations give the value of B/Q, Q is the electric quadrupole moment in Barn, which can be used to determine B once Q is measured, or to obtain Q semi-empirically. In regards to units A and B are in MHz, energy in cm $^{-1}$, and the g-value is unit less.

In order to see the sequence of computational steps that was followed for obtaining the final HFS A values table 3-1 is provided. It gives the values of A that were computed using only one reference function, the results when using the three reference functions together, the contributions of single excitations, and finally the full RCI results which included double excitations and shifts. Comparing the values of one reference configuration and those of three references shows that for those pure or semi-pure levels, leading percentage $\geq$ 75 % A^s have similar values in the two cases, e.g. $3d^4$ ^{5}D and $3d^3(^4F)$ 4s ^{5}F. Mixing the three reference functions had a stronger effect on the highly mixed levels, e.g. $3d^4$ ^{3}G and $3d^3$ $4s$ ^{3}G. As for the contributions of single excitations the data do not show a relation between the purity of the levels and the effect of single excitations. So for the four 100% pure levels the single excitations contribute 9 to 186 MHz (absolute values). Also, although the correlation configurations were applied equivalently to the three references they did not have equivalent effects on them, for example the single excitations add only 1 MHz $3d^4$ ^{3}G while it adds 115 MHz to $3d^3$ 4s ^{3}G. Considering the energy impact of the single excitation the calculations showed that the strongest impact came from 3s to 3d, 3d to *v*d and from 3p to *v*p and *v*f. The first type included exclusion effect and those had bigger impact on $3d^3$ 4s and $3d^2$ $4s^2$ because they were correcting the 3d radials and exclusion effect was small in these two references. The other two types of excitations had bigger impact on $3d^4$ because they are correlating one (or two) more 3d electrons (Notice the valence electrons in this case are either 3d or 4s.

correlations have stronger effect on 3d because it has more electrons). The last column in table 3-1 gives the final values of A, where double excitations and shifts have been included. It shows that the single excitations have the greatest effect (comparing to double excitations and shifts) on improving the computed A^s. This table illustrates the conservation rule in section 3.2.4. The sum of A^s of $3d^4\ ^3F$ and $3d^3\ 4s\ ^3F$ in the 1-configuration computation is 468 MHz, for the 3 references is 474, and for the full RCI is 476 MHz. This is a pretty stable value. The experiment gives A of $3d^4\ ^3F$ only as 250.91 so a semi-empirical prediction of A of $3d^3\ (^4F)\ 4s\ ^3F$ to be ~ 476 – 251 = 225 MHz.

An analysis of the impact of single excitation on the HFS of $3d^4\ ^5D_3$ is given in table 3-2. The largest contributions are due to the ns to *v*s excitations, n = 2 and 3. That emphasizes the effect of the Fermi-Contact term on A. The smallest contribution is due to 3d to *v*g, this is expected because $l \rightarrow l+2$ is not large near r = 0. Similar effects were observed for all the other calculated levels.

The energy contributions due to individual correlations, which includes single and double excitations, to 15 energy levels of J = 3 even are given in table 3-3. The biggest contributions are due to 3d to *v*d excitations and due to $3p^2$ to $3d^2$. And their contributions were even bigger for $3d^3$ 4s reference. To explain this we can label the 3d in $3d^4$ as $3d_a$ and 3d in $3d^3$ 4s as $3d_b$, where $3d_b = 3d_a + \Delta$. Since $3d_a$ was the one used for the whole calculations then the contribution of *v*d was bigger for $3d^3$ 4s because it was giving the missed Δ. In this table the *v*d represents 3 different RSH d functions. And the present results are the sum of the contributions due to three configurations.

Tables 3-1, 3-2, and 3-3 are examples of detailed analysis for some intermediate steps during the calculations. In the following sections the focus is only on the final results.

3.3.2 RCI results of V II J = 1

There are 12 energy levels for V II J = 1 even parity that had been included in this study. Table 3-4 gives the configurations and their equivalent RCI labels, e.g. $V_1\ 3d^4\ ^3D$. The V_n is just a simple label that refers to the actual configurations. The LS degenerate

configurations have labels as $V_{n, n+1}$. Table 3-5 gives experimental data and RCI results. It gives the configurations and their energies as recorded in NIST [19]. The RCI arrangements of the configurations do agree with those in NIST. The RCI energies differ very slightly from those in NIST. Energy of the bottom level was selected to match the experimental value [19]. The difference between the RCI energy and the experimental, $E_{RCI} - E_{exp}$, ranges from 10 to 160 cm^{-1}. This meets our goal of accuracy for $E_{RCI} - E_{exp} <$ 1000 cm^{-1}, for each level. Notice that for many of the levels these absolute energies (i.e. the difference between the energy of a specific level and the ground state) are not the important factors because they will not give the strongest impact on the calculated properties. A very important factor is the energy difference between two nearby interacting levels. In general for two interacting levels "i" and "j" the accuracy goal is to have $dE_{ij\text{-}exp} - dE_{ij\text{-}RCI} < 250$ cm^{-1}. For hyperfine structure calculations this energy difference is required to be even less than this value. The reason is that sometimes the energy difference dE_{ij} effects the vector composition of the levels which has a strong impact on HFS.

There are four LS degenerate ^3P levels, three ^3D levels and the other levels are non-degenerate. The vector components of each level are given in the last column in table 3-5. There is a good agreement between the RCI vector composition and the data in Kurucz data base [20] as recorded in [21] except for two levels, 18270 and 20090 cm^{-1}, there are slight differences, where the former contains 12% $(^2P)4s\ ^3P$ and the later has 80% of $(^4P)\ 4s\ ^3P$ [21]. During the calculations these vector compositions could be relatively changed by energy shift (i.e. % of a given component increase in one level and results in a decrease in other one but usually it does not disappear completely. So the residual effect must be associated with off diagonal matrix elements shift because the shift does not have absolute control on the vector components). The most interesting levels are the two ^3P levels at 19166 and 20090 cm^{-1}, they are LS degenerate with a small dE (924 cm^{-1}). The other ^3P levels are distant. This gives a good illustration of the conservation rule (Sec. 3.2.4). The sum of A^s is 813.3 MHz. A slight shift of -100 cm^{-1} to the first and +100 cm^{-1} to the second change their individual A^s dramatically, -199 MHz and 1020 MHz, while the produced sum after the shift is 821 MHz. The other two interesting levels are the ^3D LS degenerate at 18270 and 20522 cm^{-1}, dE =2250 cm^{-1}.

Each of these levels is mix of $3d^4\ ^3D$ and $3d^3\ 4s\ ^3D$. Although they are not neighboring levels, the vector components percentage of each of them was sensitive and linked to the other. This happened because the other levels that surround them have different LS. Since the third ^3D level is about 24,000 cm^{-1} below them these two levels are another example of the conservation rule. Shifting (^2D) 4s by -300 gives A= -91 and +162, respectively. This gives a sum of 71 MHz while A^s in table 3-5 have a sum of 85.4 MHz. The experimental value of A of $3d^4\ ^3D$ is -38.51. So a semi-empirical prediction of A of (^2D) 4s is ~ 85.5 – 38.5 = 47 MHz.

As for the Lande g-values there is a good agreement between RCI calculations and six experimental values given by NIST [19], with the differences ≤ 0.03. For three other levels the difference are ≥ 0.07, which is big. The level at 13503 cm^{-1} is a pure ^5P level. Using equation 7.65 in [22] give g-value = 2.50 which agrees with the RCI calculations. Bouazza et al, 2014 [23] calculated g-value of 19166 and 20090 cm^{-1} to be 1.484 and 1.438 which agree with the RCI calculations. Also, RCI g-values of the 12 levels are in good agreement with the results of Bouazza et al [23].

Table 3-5 gives 12 values for HFS A (10 of them are new) 12 new values of HFS B, and Lande g-values of the 12 levels. Armestrong et al, 2011 [7] give two experimental values of A for the levels at 18270 and 32299 cm^{-1}. HFS A of 18270 was also measured by Arvidsson, 2003 to be 279 MHz [as given in 7]. RCI results are in good agreement with the 2011 experimental values in [7] .The percentage errors ($|A_{exp} - A_{RCI}| / A_{RCI} * 100$) for these two levels are 28.8 and14.9 % with an average of 21.9 %.

3.3.3 RCI results of V II J = 2

There are 21 levels of V II J = 2 included in this study. Most of these levels are highly mixed and for many of them it was required to define more than the largest three vector components. The presence of interleaving vectors in many levels made the study of J = 2 levels a little complicated. For the pure and nearly pure levels the RCI vector composition is in good agreement with NIST [19] and Kurucz [20]. For the six levels between 18294 and 25191 cm^{-1} the RCI main vector components agree with those given in [19] and [20] but there are some differences in the percentages of those vectors. RCI

results show that the two ^{3}F levels at 30267 and 30673 cm^{-1} have their main components as $3d^4$ and $3d^3$ (^{2}F) 4s, respectively. This is the opposite of the experimental data given in [19] and the semi-empirical fit in [20] but it agrees with the calculation of Bouazza et al [23]. In general The RCI energies differ very slightly from those in NIST [19] except the two levels at 25191 and 50952 cm-1 where $E_{RCI} - E_{exp}$ = 600 and 1560 cm^{-1}, respectively.

Table 3-7 gives 14 new values for HFS, 21 new values for HFS B and Lande g-value for the 21 levels. For HFS A there is a good agreement between the RCI results and the measured values of 7 levels of Armstrong [7] the first two were also measured by Arvidsson [as given in 7] and they are already close to those Armstrong's. The error percentages of A^s are 7.9, 1.8, 16.8, 11.2, 5.8, 0.3, and 4.1 with an average of 7.30 % (without the 32041 cm^{-1} level). The good agreement of measured and calculated A^s of the two ^{3}F levels at 30267 and 30673 cm^{-1} supports their RCI calculated vector composition.

As for the g-values there are 15 available experimental values [19]. The RCI results agree well with 8 of them, where the difference is ≤ 0.03, and for the other 7 the difference between the calculated and measured values ranges between 0.04 and 0.12. Although many of these levels are composed of many vectors, more than 90% of the composition have the same L and S. Since g-value is a function on J, L, and S only then g-value of these levels should be almost equal to that of pure levels. Using equation 7.65 in [22] give g-values of ^{5}D, ^{5}F, ^{3}F, ^{5}P, ^{3}P, ^{3}D, and ^{1}D to be 1.5, 1.0, 0.67, 1.83, 1.5, 1.17, and 1.0. These values agree very well with the RCI results. Also, there is a good agreement with Bouazza et al [23] results of g-values for 19 levels. They are different at levels 20343 cm-1 where they give 1.439 while RCI gives 1.37 which is very close to the experimental value, for level at 20981 where they give 1.027 which is close to experiment and 0.07 different with RCI. Especially for this level sum of the top three vector components is 75, all are ^{1}D, and so it cannot be concluded that RCI g-value of this level is right.

3.3.4 RCI results of V II J = 3

There are 15 levels of V II J = 3 included in this study. Calculated energies are close to the experimental measurements [19], with $E_{RCI} - E_{exp} < 300$ cm^{-1} for most of the levels. Only three levels have $E_{RCI} - E_{exp}$ between 450 and 700 cm^{-1}.

Three LS degenerate pairs have their results stand out. The first one is ^{3}G at14462 and 16341 cm^{-1}, dE_{ij} = 1880cm^{-1}. RCI dE_{ij} = 2570 cm^{-1} so the difference between the experimental and RCI dE_{ij} = is 700 cm^{-1} which exceeds our limits for accuracy. This suggests a problem with off-diagonal matrix elements. At the same time these two levels have their RCI calculated g-values agree with the measurements [19] and the RCI vector components also agree with both [19] and [21]. So the energy difference did not affect the vector components of the two levels which is the main impact on the accuracy of HFS. RCI A is 36 MHz above the experimental [7]. The second pair is the 3D at 18354 and 20623 cm^{-1}. There is a third ^{3}D level but it is very high so it is not expected that it has strong influence on these two. The experimental dE_{ij} is 2270 and the calculated is 3100 cm^{-1}, with 830 cm^{-1} difference. RCI g-value of the first is close to experiment [19], 0.03 differences, but the second is not, 0.07, and both agree with [23]. The vector components agree with both [19 and 21]. RCI A is 35 HMz below experiment [7] but it lies within the estimated experimental uncertainty, 45 MHz. The third pair is the ^{3}F at 30306 and 30642 cm^{-1}. The calculated energies are close to experiment but the main components are flipped so RCI give the first as $3d^4$ and the second as $3d^3$ 4s. This is opposite to measurements [19] and to the calculations of Kurucz [20] but it agrees with [23]. RCI g-values are close to measurements [19]. RCI A of the first level is close to experiment, 11 MHz difference, but the second is 46 MHz far from experiment. Even with the energy discrepancies I do predict that the conservation rule of the sum of A^s will still hold to a good extent. So using the sum of RCI As of the 3G pair and the single experimental measured value A of 3d3 4s is predicted to be ~ 370 – 139 = 231 MHz, and for $3d^3$ 4s ^{3}G it will be ~ 1121- 503 = 609 MHz. For the 3F three levels will be included the pair mentioned above and the $3d^2$ $4s^2$ at 38193 cm-1 because it is not too far. For this level predicted A ~ 1163 – 747= 416 MHz.

RCI g-values agree with the 8 experimental values and have big differences (> 0.04) with another 5 values. All RCI g-values agree with [23] and for the pure levels they agree with the theoretical predictions, equation 7.65 in [22]. In general the vector components percentages agree with Kurucz as given in [21] except for the two flipped levels. Table 3-9 gives 6 new values for HFS A and 15 values for HFS B. Comparing the calculated and measured [7] A^s gives these percentage errors: 2.0, 4.1, 21.0, 7.5, 7.1, 2.7, 12.1, and 1.4 %, with an average error of 7.23 %.

3.3.5 RCI results of V II J = 4

There are 15 levels of V II J = 4 included in this study. The calculated energies are close to the experimental [19], $E_{RCI} - E_{exp} < 250$ cm^{-1} for most of the levels. Only three levels have $E_{RCI} - E_{exp}$ between 450 and 700 cm^{-1}. The calculated g-values are in good agreement with most of the experimental available values [19] and they are in excellent agreement Bouazza et al [23]. RCI calculations show the ^{3}F levels at 9098 and13609 cm^{-1} have their main component inverted compared to experimental measurement [19] and to Kurcuz data [20]. We label the first as 3d^4 and the second is 3d^3 (^{2}F) 4s. The excellent agreement between the RCI and experimental values of HFS A support this result, which agrees with [23].

Table 3-11 gives 10 new values for A, 15 new values for B and it gives g-value for the 15 levels. The calculated A^s are in very good agreement with the experimental measurement [7]. The percentage errors are: 0.03, 8.0, 2.3, 2.4, and 2.6. Armstrong et al give A = 276 or -351 MHz for the 38517 cm^{-1} level. RCI results support the first value.

Sum of A^s of LS degenerate levels can be used to predict empirical values for some levels. There are five ^{3}F levels and the sum of their A^s is conserved. But looking at their energy separation the first two are close to each other and distant from the last three are close so they can make two sub groups. For the pair at 9098 and 13609 cm^{-1} sum A^s is 101 so a semi-empirical prediction of A for the other level is 101-171.4 = -70.4 MHz. The other three ^{3}F have their experimental A^s available and they are close to the RCI values. For the ^{3}G at 14556 and 16422 cm^{-1} a semi-empirical prediction of A for the first one is 397 MHz. There are four ^{1}G levels the first two have their energies close to each

other but each one of the other two is far and isolated. But none of them has any experimental A available.

3.3.6 RCI results of V II J = 5

J = 5 is a relatively simple case, it has only six energy levels four of them are pure. The most interesting levels are $^3G_5$ at 14656 and 16533 cm^{-1}, they have high mixing percentages. Studying these two levels illustrate good example for the semi-conservation of sum of HFS A with different method of calculations. Using a single reference Dirac Fock calculations HFS A are 257 and 650. Whereas double reference DF gives 289 and 574 and RCI gives 597 and 324, respectively. These give sum values of 907, 872, and 921. And the sum of the experimental values [7] is 934 MHz. Also, through different shifts it was possible to change the percentage of the vector composition of these two levels and it was observed that HFS A of each level was so sensitive to the change of the vector composition but the sum of the two levels was still semi-conserved. For example when the level at 14656 is made up of 42% $3d^4\ ^3G$ and 58 % $3d^3\ 4s\ ^3G$ and the level at 16533 is made up of 35% $3d^4$ and 65% $3d^3$ 4s (which agree with the vector components in [19]) it gives HFS A = 497 and 532, sum =1029 MHz. While the vector composition in table 3-13 (which agree with Kurucz data as given in [21]) produces HFS A = 436 and 498, sum = 934 MHz. Calculated energy for each of these two levels is in good agreement with experiment [NIST], the differences are -241 and 172 cm^{-1}. But the calculated energy difference between them is quite big comparing to experiment $(dE_{ij})_{RCI} - (dE_{ij})_{exp} = 413\ cm^{-1}$ .The other four levels are pure, and the calculated energies are in good agreement with the experiment [19]. The calculated g-values for all the levels agree well with experiment [19] except for the ground state. The ground state is ^5F using equation eq. 7.65 in [22] give g-value =1.40 which also agrees with Bouazza [23].

3.4 Conclusion

Atomic Data of the single ion of ^{51}V has been required in the scientific community due to the importance of this element in analyzing the stellar radiation and due to the lack of data in the literature. A relativistic Configuration Interaction ab initio method has been used to provide hyperfine structure constants A and B of V II J=1-5 even parity. Shifting the reference diagonal energy matrix elements has been used to improve the results. Energies of the levels, g-values and vector components have been calculated as well. These results are displayed in tables 3-5: 3-13. In general the RCI results are in good agreement with the available measurements. Cases of differences have been discussed thoroughly in the text.

We obtained 43 new values for HFS A and 69 new values of HFS B. We suggest experimental re-labeling of the some ^{3}F levels for J=2, 3, and 4 and for some g-values, details are in the text. We have established a conservation rule for the sums of HFS constants in V II.

Table 3-1:HFS of V II J=3 levels.The first three columns are experimental data from NIST [19], then the experimental A from [7]. The 4th column gives the Dirac-Fock results using only one single reference function. The fifth column gives the results using the three reference functions combined together. The seventh column gives the contributions due to the single excitations only. The last column gives RCI final results

configuration	LS	Leading percentage	A[c]	1-Con	Ref[s]	Contribution of Single excitations	Full-RCI
$3d^4$	^{5}D	100		137	136	-186	-44
$3d^3$ (^{4}F) 4*s*	^{5}F	100		513	509	26	529
$3d^3$ (^{4}F) 4*s*	^{3}F	87		180	197	22	220
$3d^4$	^{3}F	84	250.91	288	277	-26	256
$3d^3$ (^{4}P) 4*s*	^{5}P	100	840.96	816	816	-9	808
$3d^4$	^{3}G	62		378	186	-1	193
$3d^3$ 4*s*	^{3}G	63	138.96	-143	53	115	176
$3d^4$	^{3}D	67	502.93	220	458	-2	468
$3d^3$ 4*s*	^{3}D	65		943	700	-41	644
$3d^4$	^{1}F	80	301.10	318	316	0	324
3d^3 (^{2}F) 4*s*	^{3}F	47	332.24	441	375	5	379
$3d^4$	^{3}F	64	414.24	300	372	30	403
$3d^3$ (^{2}F) 4*s*	^{1}F	80	355.08	333	324	24	350
$3d^2$ (^{3}F) $4s^2$	^{3}F	75		304	304 b	70	379
$3d^3$ 4*s*	^{3}D	100		923	925	89	1013

(a) 1-Con ["Dominant" configuration], Ref[s]= $3d^4 + 3d^3\,4s + 3d^2\,4s^2$

(b) The Ref[s] and 1-configuration values appear identical because level 2 is 75% combination of $3d^2$ (^{3}F) $4s^2$ ^{3}F and 25% $3d^4$ ^{3}F. The basis functions have very similar 1-Con values and they don't interact through the HFS operators.

(c) Expt. Experimental results, Armstrong et al, 2011

Table 3-2: The largest correlation contributions to HFS A of $3d^4\ {}^5D_3$ from matrix elements of the form: $\langle Reference|HFS|Correlation\rangle$ [1]. The closed (and empty) sub-shells are not mentioned in the configurations. The virtual orbitals (v) ; the range of radials included of the same l is between brackets

Correlation configuration	Contribution to A (MHz)
$3d^3\ vd$ (v=1:2)	4.66
$3d^3\ vg$	0.076
$3s\ 3d^5$	-0.16
$3s\ 3d^4\ 4s$	-11.53
$3s\ 3d^4\ vs$ (v=1:5)	-74.42
$2s\ 3d^4\ 4s$	-4.05
$2s\ 3d^4\ vs$ (v=1:5)	-95.14
$1s\ 3d^4\ vs$ (v=1:5)	-1.76
($3p^5\ vp$) J=2, ($3d^4$) J=3 , (v=1:2)	-3.53
Total	-185.88

Table 3-3: Energy contributions (meV) due to individual correlation to each energy level for V II J=3 even. The left column gives the correlation configurations, closed and empty sub-shells are not mentioned. For vs , v= 1:5 it represents the sum of contribution due to 5 different "s" virtual orbitals. For vp , v= 1:3 , vf , v=1:3, vg, v=1. Numbers in the first row are levels numbers, with # 1 is the ground state and15 is the 14th excited state.. The energy values are negative in most of cases but we remove the '-' to save space. So that ones with '-'are positive.

Correlation Configuration	Energy Contribution (meV) to level #														
	1	2	3	4	5	6	7	8	9	10	11	12	13	14	15
$3d^3\ vd$	12	5	60	72	20	80	51	88	42	156	167	166	87	24	74
$3d^2\ 4s\ vd$	0	994	1115	191	796	286	549	229	537	105	174	417	626	47	421
$3d^2\ vd^2$	763	2	118	755	2	560	331	603	301	768	455	316	191	326	1
$3d^2\ vf^2$	461	0	62	426	0	268	161	345	176	405	263	182	106	146	1
$3d\ 4s\ vd^2$	0	255	194	30	326	125	209	126	254	82	156	274	333	5	583
$3d\ 4s\ vf^2$	0	219	192	30	316	76	130	111	230	59	104	194	242	5	468
$3p^4\ 3d^6$	856	0	127	858	0	520	307	650	324	790	505	356	195	263	1
$3p^4\ 3d^5\ 4s$	3	1162	1011	153	1256	432	725	463	931	252	436	801	987	17	1551
$3p^4\ 3d^4\ 4s^2$	1	1	2	10	0	1	1	1	1	2	249	52	2	1119	1
$3d\ 4s^2\ vd$	0	0	1	18	0	1	2	1	3	1	452	124	2	2111	0
$4s^2\ vd^2$	0	0	0	0	0	0	0	0	0	0	-1	-1	0	-12	0
$4s^2\ vf^2$	0	0	0	0	0	0	0	0	0	0	10	2	0	42	0
$3d^2\ vp^2$	35	0	71	73	0	14	52	30	61	36	38	34	103	401	28
$3d^2\ vp\ vf$	25	184	224	94	185	113	176	94	176	93	113	159	237	18	207
$3d\ 4s\ vp^2$	0	9	6	1	24	6	9	18	37	6	7	25	17	30	90
$3d\ 4s\ vp\ vf$	0	9	7	3	5	13	22	6	12	7	55	38	29	195	28
$4s^2\ vp\ vf$	0	0	0	0	0	0	0	0	0	0	1	0	0	1	0
$3d^2\ vs\ vd$	0	66	60	15	66	28	42	28	46	22	24	42	50	1	66
$3d\ 4s\ vs\ vd$	0	0	0	0	0	2	3	3	6	0	3	1	2	14	0
$4s^2\ vs\ vd$	0	0	0	0	0	0	0	0	0	0	0	0	0	0	0
$3d^3\ vs$	0	22	15	15	26	8	2	10	2	6	5	7	8	0	13
$3d^2\ 4s\ vs$	0	0	1	11	0	0	1	1	1	1	92	22	2	195	0
$3d^3\ vg$	16	1	8	44	0	41	32	43	32	86	60	26	38	24	1
$3d^2\ 4s\ vg$	0	12	9	5	28	22	29	14	18	18	25	56	64	6	55
$3d\ 4s^2\ vg$	0	0	0	0	0	0	0	0	0	0	1	2	1	10	1
$3s\ 3d^5$	42	0	10	53	0	51	29	123	60	112	35	19	27	12	0
$3s\ 3d\ 4s$	1	36	33	5	128	27	50	44	88	26	46	83	104	2	97
$3s\ 3d^3\ 4s^2$	0	17	11	2	17	6	10	5	11	3	24	4	12	22	17
$3s\ 3d^4\ vs$	1	0	0	0	0	0	0	0	0	0	0	0	0	0	0
$3s\ 3d^3\ 4s\ vs$	0	72	63	10	74	27	46	25	50	15	28	49	62	1	80
$3s\ 3d^2\ 4s^2\ vs$	0	0	0	2	0	0	0	0	0	0	49	11	0	215	0
$3p^5\ 3d^4\ vp$	1	47	22	8	51	15	27	15	24	15	17	23	25	2	48
$3p^5\ 3d^3\ 4s\ vp$	3	3	3	6	2	3	2	3	3	3	26	10	3	78	7

Table 3-4: Labels for the vector composition in V II J=1 even [1].

V_1	$3d^4$	^5D	$V_{2,3}$	$3d^4$	^3P	V_4	$3d^4$	^3D
V_5	$3d^3$ (^4F) $4s$	^5F	V_6	$3d^3$ (^4P) $4s$	^5P	V_7	$3d^3$ (^2P) $4s$	^3P
V_8	$3d^3$ (^4P) $4s$	^3P	V_9,V_{10}	$3d^3$ (^2D) $4s$	^3D	V_{11}	$3d^3$ (^2P) $4s$	^1P
V_{12}	$3d^2$ $4s^2$	^3P						

Table 3-5: Hyperfine structure constants A (MHz) and B/Q (MHz/barn) of V II $3d^4$, $3d^3$ 4s and $3d^2$ $4s^2$ J=1 even Parity [1].The vector composition % section gives the percentage of the major component then the vector number (as in table 3-4) followed by its percentage.

Label		Energy cm^{-1}		g-value		A MHz		B/Q	Vector composition %			
		NIST[a]	RCI	NIST[a]	RCI	Exp.[b]	RCI					
$3d^4$	**^5D**	36	36		1.50		-89.6	107.2	100			
$3d^3$ (^4F) $4s$	**^5F**	2605	2539		~ 0		-369.0	-38.9	100			
$3d^4$	**^3P**	11515	11497	1.48	1.50		-6.8	-0.31	88	V_8 7	V_7	4
$3d^3$ (^4P) $4s$	**^5P**	13512	13503	2.39	2.50		1426.9	23.0	100			
$3d^4$	**^3D**	18270	18074	0.49	0.51	-38.51(51)	-26.4	-29.9	55	V_9 43		
$3d^3$ (^2P) $4s$	**^3P**	19166	19007	1.40	1.49		984.9	7.0	80	V_8 17	V_4	1
$3d^3$ (^4P) $4s$	**^3P**	20090	20179	1.35	1.42		-171.8	-100.2	67	V_7 12	$V_{2,3}$	11
$3d^3$ (^2D) $4s$	**^3D**	20522	20687	0.58	0.59		111.8	11.1	51	V_4 39	V_8	5
$3d^3$ (^2P) $4s$	**^1P**	22274	22114	0.97	1.00		250.9	-73.4	96	V_9 2	V_8	2
$3d^4$	**^3P**	32299	32326	1.48	1.50	-73.33(29)	-68.1	-63.8	94	V_8 3	V_{12}	2
$3d^3$ (^2D) $4s$	**^3D**	44202	44354	0.50	0.50		-497.3	146.0	100			
$3d^2$ $4s^2$	**^3P**	48976	49007		1.50		40.5	104.2	97	V_3 2		

[a] http://physics.nist.gov/asd3

[b] Armstrong N M R, Rosner S D, and Holt R A, *Phys. Scr.* **84**, 055301(2011)

[c] Thorne A P, Pickering J C, and Semeniuk J I, *ApJ. Supp.***207**:13 (2013)

Table 3-6: Labels for the vector composition in V II J=2 even [1].

$V_{1,2}$	$3d^4$	^3F	V_3	$3d^3(^4F)\ 4s$	^3F	V_4	$3d^3\ (^2F)\ 4s$	^3F
V_5	$3d^2\ 4s^2$	^3F	$V_{6,7}$	$3d^4$	^3P	V_8	$3d^3(^2P)\ 4s$	^3P
V_9	$3d^3(^4P)\ 4s$	^3P	V_{10}	$3d^4$	^3D	$V_{11,12}$	$3d^3\ 4s$	^3D
$V_{13,14}$	$3d^4$	^1D	$V_{15,16}$	$3d^3\ 4s$	^1D	V_{17}	$3d^2\ 4s^2$	^1D
V_{18}	$3d^4$	^5D	V_{19}	$3d^3\ (^4F)\ 4s$	^5F	V_{20}	$3d^3\ 4s$	^5P
V_{21}	$3d^2\ 4s^2$	^3P						

Table 3-7: HFS constants A (MHz) and B/Q (MHz/barn) of V II $3d^4$, $3d^3$ 4s and $3d^2\ 4s^2$ J=2 even Parity [1].The vector composition % section gives the percentage of the major component then the vector number (as in table 3-6) followed by its percentage.

Label	Energy cm^{-1}		g-value		A MHz		B/Q	Vector composition %				
	NIST	RCI	NIST	RCI	Exp.[b]	RCI		RCI				
$3d^4$ ^{5}D	107	107		1.50		-69	70	100				
$3d^3\ (^4F)\ 4s$ ^{5}F	2687	2656	0.97	1.00		370	-18	100				
$3d^3(^4F)\ 4s$ ^{3}F	8640	8621	0.65	0.67		918	-104	91	V_1	9		
$3d^4$ ^{3}P	11908	11782	1.49	1.50		24.2	23	86	V_9	7	V_8	4
$3d^4$ ^{3}F	13491	13559	0.59	0.67	481.96(15)	520	-65	86	V_3	8	V_2	5
$3d^3\ (^4P)\ 4s$ ^{5}P	13595	13623	1.78	1.83	1096.69(43)	1077	-235	99				
$3d^4$ ^{3}D	18294	17946	1.13	1.18	488.08(20)	570	-66	49	V_{12}	48	V_8	2
$3d^3\ (^2P)\ 4s$ ^{3}P	19133	18895	1.38	1.48		692	47	66	V_9	28	V_{10}	3
$3d^3\ (^4P)\ 4s$ ^{3}P	20343	20363	1.36	1.37		167	4	43	V_{10}	19	V_{12}	16
$3d^3\ (^2D)\ 4s$ ^{3}D	20617	20680	1.25	1.21		736	82	21	V_{13}	19	V_{12}	16
$3d^3\ (^2D)\ 4s$ ^{1}D	20981	20895	1.02	1.10		-153	25	30	V_{13}	26	V_{12}	19
$3d^4$ ^{1}D	25191	25788	0.99	1.00		339	248	54	V_{16}	44		
$3d^4$ ^{3}F	30267	31129	0.67	0.67	-251(22)	-223	143	82	V_2	13		
$3d^3(^2F)\ 4s$ ^{3}F	30673	30591	0.67	0.67	397(26)	420	239	59	V_5	24	V_4	16
$3d^4$ ^{3}P	32041	32178	1.38	1.50	~ 0	-0.45	105	94	V_{21}	3	V_9	2
$3d^2\ 4s^2$ ^{3}F	37938	38210		0.67		534	170	69	V_2	30		
$3d^3\ (^2D)\ 4s$ ^{3}D	44160	43938	1.14	1.17		725	199	98				

$3d^2\ 4s^2$	^{1}D	44658	44506	1.00	366(86)	367	-221	68	V_{14}	29
$3d^3\ (^2$D) $4s$	^{1}D	47324	47382	1.00		379	409	95	V_{17}	3
$3d^2\ 4s^2$	^{3}P	49205	49048	1.49		396	-246	94	V_7	3
$3d^4$	^{1}D	50952	52513	1.00		339	-285	72	V_{17}	24

[a] http://physics.nist.gov/asd3

[b] Armstrong N M R, Rosner S D, and Holt R A, *Phys. Scr.* **84**, 055301(2011)

[c] Thorne A P, Pickering J C, and Semeniuk J I, *ApJ. Supp*.**207**:13 (2013)

Table 3-8: Labels for vector composition in V II J=3 even [1].

V_1	$3d^4$	^{5}D	$V_{2,3}$	$3d^4$	^{3}F	V_4	$3d^4$	^{3}G
V_5	$3d^4$	^{3}D	V_6	$3d^4$	^{1}F	V_7	$3d^3$ (^{4}F) $4s$	^{5}F
V_8	$3d^3$ (^{4}F) $4s$	^{3}F	V_9	$3d^3$ (^{2}F) $4s$	^{3}F	V_{10}	$3d^3$ (^{4}P) $4s$	^{5}P
V_{11}	$3d^3$ $4s$	^{3}G	$V_{12,13}$	$3d^3$ $4s$	^{3}D	V_{14}	$3d^3$ (^{2}F) $4s$	^{1}F
V_{15}	$3d^2$ $4s^2$	^{3}F						

Table 3-9: HFS constants A (MHz) and B/Q (MHz/barn) of V II $3d^4$, $3d^3$ 4s and $3d^2$ $4s^2$ J=3 even Parity [1]. The vector composition % section gives the percentage of the major component then the vector number (as in table 3-8) followed by its percentage.

label	Energy cm^{-1}		g-value		A MHz		B/Q	Vector composition %			
	NIST[a]	RCI	NIST	RCI	Exp.[b]	RCI					
$3d^4$ ^{5}D	209	209		1.50		-44	-65.6	100			
$3d^3$ (^{4}F) $4s$ ^{5}F	2809	2808	1.20	1.25		529	-31.4	100			
$3d^3$ (^{4}F) $4s$ ^{3}F	8842	8861	1.04	1.08		220	-98.1	87	V_2	13	
$3d^4$ ^{3}F	13543	13271	1.06	1.08	250.91(39)	256	-63.7	84	V_8	12	
$3d^3$ (^{4}P) $4s$ ^{5}P	13742	13700	1.62	1.67	840.96(48)	808	248	100			
$3d^4$ ^{3}G	14462	14456	0.74	0.75		193	-2.9	62	V_{11}	37	
$3d^3$ $4s$ ^{3}G	16341	17023	0.76	0.75	138.66(19)	176	42.1	63	V_4	37	
$3d^4$ ^{3}D	18354	17704	1.30	1.33	502.93(45)	468	-29.8	67	V_{12}	33	
$3d^3$ $4s$ ^{3}D	20623	20800	1.26	1.33		644	-106	65	V_5	33	V_{13} 2
$3d^4$ ^{1}F	26840	26965	0.97	1.00	301.10 (26)	324	337	80	V_{14}	19	
$3d^4$ ^{3}F	30306	30098	1.05	1.08	414.24(22)	403	185	64	V_3	32	V_{15} 4
$3d^3$ (^{2}F) $4s$ ^{3}F	30642	30617	1.06	1.08	332.71(26)	379	249	47	V_9	35	V_{15} 17
$3d^3$ (^{2}F) $4s$ ^{1}F	34229	34225	1.00	1.00	355.08(48)	350	201	80	V_6	20	
$3d^2$ $4s^2$ ^{3}F	38193	37743		1.08		381	198	75	V_3	23	
$3d^3$ $4s$ ^{3}D	44099	44154	1.27	1.33		1013	430	100			

[a] http://physics.nist.gov/asd3

[b] Armstrong N M R, Rosner S D, and Holt R A, *Phys. Scr.* **84**, 055301(2011)

[c] Thorne A P, Pickering J C, and Semeniuk J I, *ApJ. Supp*.**207**:13 (2013)

Table 3-10: Labels for vector composition in V II J=4 even [1].

V_1	$3d^4$	^{5}D	V_2	$3d^4$	^{3}H	$V_{3,4}$	$3d^4$	^{3}F
V_5	$3d^4$	^{3}G	$V_{6,7}$	$3d^4$	^{1}G	V_8	$3d^3$ (^{4}F) $4s$	^{5}F
V_9	$3d^3$ (^{4}F) $4s$	^{3}F	V_{10}	$3d^3$ (^{2}G) $4s$	^{3}G	V_{11}	$3d^3$ (^{2}G) $4s$	^{1}G
V_{12}	$3d^3$ (^{2}H) $4s$	^{3}H	V_{13}	$3d^3$ (^{2}F) $4s$	^{3}F	V_{14}	$3d^2$ $4s^2$	^{1}G
V_{15}	$3d^2$ $4s^2$	^{3}F						

Table 3-11:HFS constants A (MHz) and B/Q (MHz/barn) of V II $3d^4$, $3d^3$ 4s and $3d^2$ $4s^2$ J=4 even Parity [1].Vector composition % section gives the percentage of the major component then the vector number (as in table 3-10) followed by its percentage.

Label		Energy cm^{-1}		g-value		A MHz		B/Q	Vector composition %				
		NIST[a]	RCI	NIST	RCI	Exp. [b]	RCI						
$3d^4$	^{5}D	339	339		1.50		21	-290	100				
$3d^3$ (^{4}F) $4s$	^{5}F	2968	2942	1.30	1.35		613	-77.2	100				
$3d^3$ (^{4}F) $4s$	^{3}F	9098	9095	1.22	1.25		-76	-132	88	V_3	11		
$3d^4$	^{3}H	12545	12523	0.83	0.80		400	139	100				
$3d^4$	^{3}F	13609	13666	1.19	1.25	171.4(13)	177	-69	86	V_9	11	V_5	2
$3d^4$	^{3}G	14556	14732	1.00	1.05		360	-6	61	V_{10}	36	V_3	2
$3d^3$ (^{2}G) $4s$	^{3}G	16422	17128	1.03	1.05	423.32(30)	460	51	62	V_5	37		
$3d^4$	^{1}G	17911	18358	0.95	1.00		285	-45	57	V_{11}	39		
$3d^3$ (^{2}G) $4s$	^{1}G	19113	19793	0.98	0.98		329	89	52	V_6	40	V_{12}	8
$3d^3$ (^{2}H) $4s$	^{3}H	20242	20494	0.82	0.82		-29	416	90	V_{11}	6		
$3d^4$	^{3}F	30319	31249	1.23	1.25	591.70(71)	606	234	60	V_4	35	V_5	4
$3d^3$ (^{2}F) $4s$	^{3}F	30614	30602	1.25	1.25	434.52(18)	424	301	45	V_{13}	39	V_{15}	15
$3d^4$	^{1}G	36425	36567	0.96	1.00		332	136	96				
$3d^2$ $4s^2$	^{3}F	38518	38220		1.25	276.67(56)[d]	270	223	77	V_4	21		
$3d^2$ $4s^2$	^{1}G	53607	53095		1.00		412	716	97	V_7	3		

[a] http://physics.nist.gov/asd3

[b] Armstrong N M R, Rosner S D, and Holt R A, *Phys. Scr.* **84**, 055301(2011)

[c] Thorne A P, Pickering J C, and Semeniuk J I, *ApJ. Supp*.**207**:13 (2013)

[d] Armstrong 2011 gives two values for HFS A for this energy level, these are 276.67(56) and -351.28(63) [8]

Table 3-12: Labels for vector composition in V II J=5 even [1].

V_1	$3d^4$	^{3}H	V_2	$3d^4$	^{3}G	V_3	$3d^3$ (^{2}G) $4s$	^{3}G
V_4	$3d^3$ (^{4}F) $4s$	^{5}F	V_5	$3d^3$ (^{2}H) $4s$	^{3}H	V_6	$3d^3$ (^{2}H) $4s$	^{1}H

Table 3-13: HPS constants A (MHz) and B/Q (MHz/barn) of V II $3d^4$, $3d^3$ 4s and $3d^2$ $4s^2$ J=5 even Parity [1].Vector composition % section gives the percentage of the major component then the vector number (as in table 3-12) followed by its percentage.

Label		Energy cm^{-1}		g-value		A MHz		B/Q	Vector composition %		
		NIST[a]	RCI	NIST	RCI	Exp[b]	RCI				
$3d^3$ (^{4}F) $4s$	**^{5}F**	3163	3163	1.28	1.40		640	-159	100		
$3d^4$	**^{3}H**	12622	12673	1.02	1.03		271	128	100		
$3d^4$	**^{3}G**	14656	14415	1.17	1.20	436.10(42)	386	3.8	65	V_3	35
$3d^3$ (^{2}G) $4s$	**^{3}G**	16533	16705	1.16	1.20	498.41(13)	532	68	65	V_2	35
$3d^3$ (^{2}H) $4s$	**^{3}H**	20281	20283	1.01	1.03		423	438	100		
$3d^3$ (^{2}H) $4s$	**^{1}H**	23391	23423	1.04	1.00		340	474	100		

[a] http://physics.nist.gov/asd3

[b] Armstrong N M R, Rosner S D, and Holt R A, *Phys. Scr.* **84**, 055301(2011)

[c] Thorne A P, Pickering J C, and Semeniuk J I, *ApJ. Supp*.**207**:13 (2013)

3.5 Reference

1. M. H. Abdalmoneam and D. R. Beck , *J. Phys. B* **48,** 105001 (2015)
2. E. Bie`mont et al., *Astron. Astrophys*, **209**, 391 (1989)
3. N. H. Youssef and M. A. Amer, *Astron. Astrophys*. **220**, 281 (1989)
4. George Preston, *Annual Review of Astronomy and Astrophysics*, **vol 12**, p 257, 1974
5. C. R. Cowley and G. M. Wahlgren, *Astron. Astrophys*, **447**, 681 (2006)
6. K. E. Nielsen and T. R. Gull, *Phys. Scr.* **T134** , 014002 (2009)
7. N M R Armstrong, S D Rosner, and R A Holt, *Phys. Scr.* **84**, 055301 (2011).
8. Robert L. Kurucz , *Phys. Scr*. **T47**, 110 (1993)
9. K. Arvidsson , Hyperfine constants and wavelengths in V II derived by FT spectroscopy for astrophysical application, *Master's Thesis* , Lund University, (2003)
10. D. R. Beck*, Phys. Rev. A* **45**, 1399 (1992)
11. S. O'Malley, D. R. Beck, and D. P. Oros, *Phys. Rev. A* **63**, 032501 (2001)
12. P. L. Norquist and D. R. Beck, *J. Phys. B*, **34**, 2107 (2001)
13. http://www.phy.mtu.edu/~donald/pb.html
14. U. Johann, J. Dembczynski, and W. Ertmer, *J. Phys. A* **303**, 7 (1981)
15. L. J. Curtis, "*Atomic structure and Lifetimes Conceptual Approach*" Cambridge University press, (2003)
16. O. Sinanoglu and D. R. Beck, *Chem. Phys. Letters*, **20**, 211 (1973)
17. J. P. Desclaux, *Comput. Phys. Comm.* **9** 31 (1975)
18. D. R. Beck, program RCI, 1978- present, unpublished
19. Y. Ralchenko, A. E. Kramida, J. Reader and the NIST ASD team (2011), NIST Atomic Spectra Database (ver.4.1.0) (Gaithersburg, MD: National Institute of Standards and Technology) http://physics.nist.gov/asd3
20. R. Kurucz , http://kurucz.harvard.edu/atoms/2301/
21. A. P. Thorne, J. C. Pickering, and J. I. Semeniuk, *Ap J. Supp*. **207**, 13 (2013)
22. Lorenzo J. Curtis "*Atomic Structure and Lifetimes: A Conceptual Approach*", Cambridge University Press (2003)
23. S. Bouazza et al, *Journal of Modern Physics* **5**, 497 (2014)

4 Relativistic Configuration Interaction Results of Transitions and Lifetimes, Oscillator Strengths and Lande g-values in Singly Ionized Tungsten, W II

4.1 Introduction

We present relativistic configuration interaction (RCI) calculations of the lifetimes of singly ionized tungsten W II. These results are important for different fields in which atomic data of tungsten are required, such as fusion reactors, plasma temperature, solar photosphere, and abundance of tungsten in different stars. Usually the lifetime values are combined with branching ratios to obtain oscillator strength, the most important data for studying stellar spectrum. In this study we provide calculated lifetimes for 175 transitions in W II. Our results agree well with most of the published measurements of W II lifetimes. Our branching ratios did not have same good agreement with the experimental measurements; we explain the reason in section 4.3.5. This chapter presents the RCI results of W II lifetimes, comparison with the available data, and justification of the importance of our results. A more thorough calculation of branching ratios is left for a future work.

Atomic data, such as dipole transition probabilities, lifetimes, oscillator strengths, and Lande g-values, of tungsten and many other neutral and ionized atoms are required for studying the temperature structure of solar photosphere [9 and references within] and to interpret satellite-borne UV and vacuum-UV spectra [11]. In fusion devices and plasma experiments tungsten is used as a divertor and limiter which creates a demand for the data of first three spectra of tungsten (W I, W II, and W III) in order to predict plasma device efficiency and to better handle plasma impurities in fusion research [8, 11]. In high intensity discharge lamps tungsten electrodes are used. Tungsten is highly refractory (i.e. lot of energy is needed to remove an electron out of it). So tungsten data are needed to estimate the in-efficiencies in fusion reactions due to radiation absorbed by impurities. Also the data is needed in order to model the electrode erosion and for better manufacturing of these lamps [12].

The National Institute of Science and Technology [NIST] has published experimental atomic spectroscopic data for tungsten atom W I and the singly ionized tungsten, W II energy levels, configurations, and Lande g values [1]. These data are mainly taken from the compilation of atomic data of W I and W II by Karamida and Shiria, 2006 [2]. The ground state of W I is $5d^4\ 6s^2\ ^5D_0$, ionization energy = 63427 cm^{-1} =

7.864 eV. The ground state of W II is $5d^4\ 6s^1\ {}^6D_{1/2}$, ionization energy = 132000 cm^{-1} = 16.36 eV. The most recent W II energy levels were measured by Ekberg et al [3]. They identified about 2500 W II lines using Fourier transform spectroscopy (FTS) [3]. In their measurements of W II energy levels Ekberg et al used samples of natural tungsten which did not show line structure attributable to hyperfine structure or isotope shift. Tungsten has four stable isotopes (A = 182, 183, 184, and 186) with terrestrial fractional abundance of 26.3 %, 14.3 %, 30.7 %, and 28.6 % respectively, so the recorded experimental energies in [1, 2, and 3] represent the average values over all isotopes in natural tungsten [2, 10]. Only A=183 has a non-zero nuclear spin (I=1/2, μ=+0.1178). The term labels for both W I and W II in [1 and 2] do not reflect the actual nature of the states due to the strong mixing between the configurations. The percentage compositions of the W I levels were given only for the levels that were easily identified, i.e. those separated from other levels with the same J or those with pure enough LS coupling [2]. These percentage compositions were obtained by least square fitting calculations using Cowan's code for the even levels. For the odd levels they were obtained by means of ab-initio Hartree-Fock high Z (Z is the atomic number) calculations with electrostatic and configuration interaction parameters scaled by a factor of 0.8. For W II the analysis of the vector compositions of the levels were done by Ekberg et al using Cowan's code [3] and reproduced by Kramida et al [2] using the same code. Ekberg et al (2000) identified 76 even parity and 187 odd parity levels. The even levels of W II belong to strongly mixed $5d^4\ 6s$, $5d^3\ 6s^2$, and $5d^5$ configurations. The odd levels belong to strongly mixed $5d^3\ 6s\ 6p$ and $5d^4\ 6p$ configurations [2, 3]. Also, the interaction with $5d^2\ 6s^2\ 6p$ is significant but not as strong [2].

The experimental Lande g values of W II given by NIST [1] were from Laun [4] and were calculated by Ekberg et al (2000) [3]. The calculated and experimental g-values are in excellent agreement except the J=5/2 54704 cm^{-1} level where the experimental value was 0.623 and the calculated was 1.24 and it was suggested that the experimental value was wrong [2].

In W II the levels n = 1: 4 form a closed core. The 4f sub-shell is part of the closed core with a very small average radius, nearly half of the 5p radius. The filled core

of n = 1: 4 introduces screening effects in the valence part of the configuration. The open 5d sub-shells introduce intermediate coupling and configuration interaction effects [10]. Intermediate coupling is needed because neither the LS coupling nor *JJ* coupling schemes are accurate enough to describe the levels of this ion. The coupling in the zero level wavefunction (i.e. before correlation is added) is determined through the diagonalization of the energy matrix (It is simply whatever the system says it is without any prior prediction). Correlation effects are so strong that most of the levels of W II are heavily mixed. For the same J and parity each level is composed of multiple configurations and in many cases the dominant configuration occupies less than 20% of the total wavefunction. These effects apply to all singly positive ions with the same configuration where 5d is filled with 3 to 7 electrons. For these ions the transitions $5d^x$ 6s to $5d^x$ 6p are particularly strong between the levels of high J for of maximum spin multiplicity [10]. By a strong transition we mean one that has significant energy difference and large oscillator strength ($f \geq 0.5$). .

The absorption spectra of positive ions $5s^2$ $5p^6$ $5d^x$ 6s, x=3:7, in the range 2000-3000 Å has been very helpful in obtaining their astrophysical abundance. But these spectra are so complex it is difficult to determine their absolute oscillator strengths either through relative absorption/emission measurements methods or through lifetimes. To obtain oscillator strengths from lifetime data we need to have reliable branching fractions. In ions like W II there is a great deal of configuration interaction effects. The even parity ground state consists mainly of one configuration but excited even levels are highly mixed of $(5d+6s)^5$ configurations while the odd states are mixed of $(5d+6s)^4$ 6p configurations. This makes it fairly difficult to rule out the transition on criteria other than energy, parity, and angular momentum [10] (for example; usually there are cases in which some transitions are more favorable, e.g. nl to n($l \pm 1$). But since each level already has many configurations in it there is not one l and the favorable configurations for the transitions are many).

Oscillator strengths can be obtained experimentally through two approaches; the first is by emission, absorption or dispersion direct measurements. The second is through the lifetime and branching ratio measurements. The direct measurements include

comparing different atomic transitions simultaneously. They require sample equilibrium, measurement of absolute intensity and determination of absolute number density (e.g. emission measurements involve the number density of the upper level) [18]. Most of the early experiments used one of these direct approaches but the preciseness of the results was only about 50 percent. On the other hand measurements of radiative lifetimes are usually time-resolved which include comparing relative intensities from the same transitions at different times and it does not require any absolute measurements [18]. One of the factors that limit the accuracy of these measurements is the cascade repopulation of the levels of interest. This difficulty could be eliminated through selective excitations of the levels of interest, where the laser source is tuned to the frequency of the desired absorption transition. At the same time this method is limited only to atomic levels that can be accessed directly from the ground state by strong dipole transitions [18]. Add to this that measurements of branching fractions used are still pretty challenging and very few measurements are available even now. Also, lifetime and branching fractions are usually done as separate measurements. That is why computational studies of these data are highly important. They are not limited to any specific level and many data are obtained in one study.

The following paragraphs give an overview of the most recent lifetime measurements in W II. The technique of selective laser excitations and time-resolved laser-induced-florescence (TR-LIF) had been used by Kwiatkowski et al [9] for 3 measurements, by Schnabel et al [6] for 19 measurements, by Schults-Johanning et al [4] for 2 measurements and by Nilsson et al (2008) for 9 measurements. Also, Henderson et al [10] used the beam-foil method for 3 measurements. Lifetimes of some transitions were measured by different groups for comparison of techniques so for two decades. Only 28 radiative lifetime measurements of W II transitions are available from five experimentalists.

Kwiatkowski et al 1984 used selective time-resolved laser induced florescence to measure lifetimes of three transitions in W II and the ions were produced by a sputtering technique. They also used the relative transition probabilities and relative oscillator strength measurements of Obbarius and Kock [14] to calculate absolute transition probabilities and oscillator strengths. According to Kwiatkowski et al the uncertainty in

the relative sets of *f*-values were 10 - 20% but the method that was used by Obbarius and Kick to convert them to absolute values increased the uncertainty to 50%. Kwiatkowski et al used their lifetime measurements of the two J=1/2 transitions to calculate the absolute *f*-values of these two transitions and to rescale the absolute f-values of the other 25 transitions that were given by Obbarius and Kock [9].

Schnabel et al, 1998 gave radiative lifetimes of 19 W II levels that were measured using time-resolved-laser-technique with uncertainty 1-3% [6]. This was done as part of their program to obtain transition probabilities of W I, W II, and W III which were required by the scientific community, especially for plasma experiments. The goal was to combine the measurements of lifetimes with the measurements of branching ratios in order to obtain W II oscillator strengths.

Henderson et al (1999) published lifetime measurements (with ~ 10% precision) of three W II transitions which are known to be of astrophysical importance. They also used Corliss and Bozman [13] transition probability measurements and their lifetimes to estimate oscillator strengths of four W II transitions. And they used their results to discuss the abundance of W II in the Sirius star. The most important line was that due to the 54498.57 $^{o}_{11/2}$ transition to $^{6}D_{7/2}$ with lifetime 2.7(0.3) ns. This line has large oscillator strength and is only slightly affected by line blending. It was suggested as a good line for studying the abundance of W II in Sirius [10]. Notice that the absolute oscillator strengths values used in this work were quite old. So they might be not so accurate, which would effect on the accuracy of the lifetimes.

Kling at el (2000) [5] gave transition probabilities which were obtained using the branching ratios derived from FTS. To convert the measured branching ratios to absolute transition probabilities Kling et al used the lifetimes measured by Schnabel et al, 1998. The uncertainty of these values ~ 7 – 9% and could be as large as 50%. Kling also calculated the spontaneous transition probability “A” for some lines [2].

Ekberg et al (2000) besides giving measurements to W II energy levels also calculated the vector composition of all the levels by fitting parameters to observed levels using Cowan’s code. They found that very few levels, either even or odd parity, have a dominant configuration that occupies 50% or more of the wave function. Also, they used Cowan’s code to calculate lifetimes, transition probabilities, oscillator strengths, and

Lande g-value. Their calculated lifetimes are clearly bigger than the experimental values given by Schnabel et al [6]. The ratios of calculated to observed lifetimes were 0.66-0.93, see table VIII in [3]. This approach depends on comparisons with observed lifetimes to calculate scaled theoretical transition probabilities [3]. This makes difficult for us to compare our transition probabilities and/or oscillator strengths to theirs. As for the calculated g-values most of them are in good agreement with the ones measured by Laun et al (1964) [4]. For the $54704^{o}_{5/2}$ level the difference between the calculated and observed g-values is quite big (1.24 vs. 0.623). Both Ekberg et al and Wyart et al [15] doubted the experimental g-value of this level. [3].

Nilsson et al, (2008) gave radiative lifetimes measurements of nine W II levels. They used their lifetime measurements and the previously measured ones and calculated branching fractions to deduce 290 transition probabilities. Also, they calculated the oscillator strength of 290 transitions using a relativistic Hartree Fock approach modified with core-polarization effects inclusion (HFR+CP). Both the relativistic effects and some correlation single excitations were included. The correlation effects due to core valence interactions were included in two different forms; in the first an Er $4f^{14}$ ionic core surrounded by 5 valence electron was considered, HFR+CP (A) model. The second considered a Yb- $4f^{14}$ $5d^{2}$ ionic core surrounded by 3 valence electrons, HFR+CP (B) model. In the second form all the single excitations from 5d to the virtuals orbitals n*l* were taken into account, which built a core-polarization potential that 5d shell into the ionic core. So when these were used to calculate lifetimes the HFR+CP (B) results came closer to experiment. Nilsson et al mentions that the Ekberg et al (2000) calculated lifetimes are 30% lower than measurements and 15-25% lowers than their HFR+CP calculations. So that in table-1 in their paper they adjusted Ekberg's lifetimes by dividing by a 0.69 scaling factor. That made Ekberg's calculated lifetimes in good agreement with Nilsson's measured and calculated lifetimes.

Quinet et al, (2010) published a compilation of data for the radiative decay rates of W I, W II, and W III. They evaluated the available data in literature and gave the most recommended data for those transitions of interest for the plasma fusion experiments [18]. The data given included oscillator strengths and emission transition probabilities.

Although the RCI calculated branching ratios do not show excellent agreement with the experimental values, tables 4-9 : 4-14, we see that the RCI calculated lifetimes, tables 4-1 and 4-3 : 4-8, do and so they are valuable to the scientific community. Our lifetimes of W II do agree well with most of the available experimental measurements. Many of the available calculations of branching fractions use fits with old experimental transition probabilities [e.g. Henderson 1999]. The energy levels of W II are heavily mixed which means that so many transitions are allowed this makes giving accurate branching fractions so complex. The experimental available branching fractions are only for 10 transitions. So within this complexity it is not conclusive to consider RCI results as not accurate. The rest of this chapter includes theoretical background in section 4.2 and the results are presented and discussed in section 4.3. As for the tables, and throughout the discussion, due to the strong mixing between the different configurations in most of the levels we found that it is better not to give a general label for each level. So we are going to refer to the levels by their energies with the parity super-scripted and total J sub-scripted. The transitions studied have large energy differences. Based on our previous theory [20], the sum of oscillator strengths from nearly degenerate levels (i.e. levels that have same J, parity and are close in energy) to a single level is almost a constant. Thus the lifetimes are nearly insensitive to the mixing of the even levels into which the odd levels decay. On the contrary the branching ratios are sensitive to the mixing in both even and odd levels.

4.2 Theoretical background and computational details

4.2.1 Theory and general background

Interpreting the astrophysical data requires determination of wavelengths, intensity and shape of the spectral lines being received from the stars, where these spectral lines are due to radiative transitions between atomic states. The wavelengths have been measured precisely (about 1 part in 10^8) by classical spectroscopic methods. The intensity of a line could be determined through emission transition probability, A_{ki}, or through absorption oscillator strengths, f_{ik} (k > i). The shape of a line is determined though its natural width $\Gamma_k = \hbar/\tau_k, \tau_k$is the lifetime of the excited state" [17]. Accurate

measurements of some W II oscillator strengths and lifetimes became available recently and for a long time they had not been as precise. For cases where lifetimes are used to determine oscillator strength branching fractions, BF_{ji}, is also an important quantity that can be either measured or calculated. Measurements of branching fractions had been quite challenging and some have become available very recently.

For a homogeneous light source of length *l* and for the optically thin case the total line intensity (SI unit radiance) is

$$I_{line} = \int_0^\infty I(\lambda) d\lambda = \frac{hc\, A_{ki}\, N_k\, l}{4\,\pi\ \lambda_0} \tag{4.1}$$

, $I(\lambda)$ is the intensity at wavelength λ and λ_0 is the wavelength at the center of the line. N_k is the number per unit volume of excited atoms in state "k". [18]

In the case of absorption, the reduced line intensity (W_{ik}) from a homogeneous and optically thin absorbing medium of length *l* is [18]

$$W_{ik} = \int_0^\infty W(\lambda)\, d\lambda = \frac{e^2}{4\epsilon_0\, m_e\, c^2}\, \lambda_0^2\, N_i\, f_{ik}\, l \tag{4.2}$$

The atomic transition probability A_{ki} is the spontaneous emission probability per unit time for an atom in any one of the g_k degenerate states of the energy level *k* to make a transition to any of the g_i degenerate states of the level *i* [18]. (in general $g_{k/i}$ accounts for the m_j degeneracy).

For electric dipole transition, E1, (J → J, J±1, and parity change) A_{ki} and f_{ik} are related as follows;

$$A_{ki} = \frac{2\pi\, e^2}{m_e\, c\, \epsilon_0\, \lambda^2}\ \frac{g_i}{g_k}\, f_{ik} \tag{4.3}$$

Equation 3 is in SI units. In customary units (that's more commonly used with atomic units)

$$A_{ki} = \frac{6.6702\ \times\ 10^{15}}{\lambda^2}\, \frac{g_i}{g_k}\, f_{ik} \tag{4.4}$$

, A in s^{-1}, λ in Å, and *f* is dimensionless. g_i and g_k are statistical weights $g_{i(k)} = 2J_{i(k)} + 1$. f_{ik} is the oscillator strength, also called *f*-value.

The radiative lifetime is the time required for a state "*i*" to decay into any one of the lower states k. It is equal to the inverse of the total transition rates summed over all decay channels.

$$t_k = \left(\sum_i A_{ki}\right)^{-1} \tag{4.5}$$

The branching fraction is the ratio of atoms that decay from an upper level "*i*" to a specific lower level, to the total number of atoms that decay from the same upper level to any lower level [19]. So the branching fraction for the j^{th} channel of decay from level "*i*" is defined [17] as

$$F_B = \frac{A_{ji}}{\sum_k A_{ki}} = \tau_k A_{ji} \tag{4.6}$$

Measurements of branching fractions include measuring the relative intensity of the spectral line between two specific levels and comparing it to the total intensity of the emission from that upper level.

The branching ratio between two decay channels [17] is

$$R_B = \frac{A_{ji}}{A_{ki}} \tag{4.7}$$

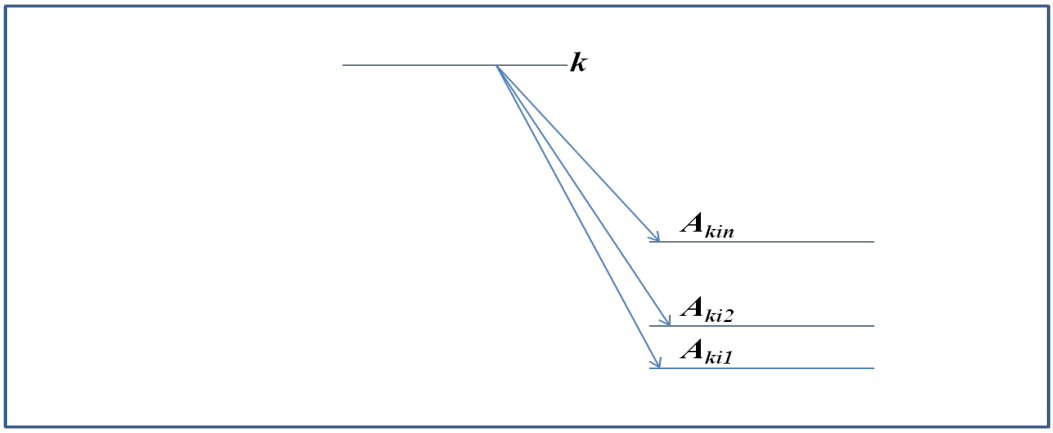

Figure 4-1: Illustration of a level "k" decays into lower levels "i".

4.2.1.1 Relative and absolute transition probabilities

If 1, 3 are high levels and 2 and 4 are low levels then relative oscillator strength is measuring f_{12}/f_{32} and uses it with other data to obtain f_{34} which is absolute.

4.2.1.2 Conservation of the Sums of f-values

The logic of Nicolaides and Beck [20] which dealt with the dipole transition from a single lower energy state i to two upper states k_1, k_2 is extended in this thesis. For f-values, it was assumed the condition that condition of having |dE (k, i)| >> |dE (k_1, k_2)| was met. If so this implies [20] that the sum of the oscillator strengths $f_{i,k1} + f_{i,k2}$ is nearly constant. Equivalently, it means the sum of the squares of the dipole transition matrix elements is constant.

Here, we extend this to include an arbitrary number of lower levels (even parity) i, and any number of closely spaced odd parity upper levels k. The conditions and energy differences are, for all i, k combinations (with moderate to large $f_{i,k}$) |dE(k, i)| >> |dE(k, k')|, |dE(i, i')| for all (k, k') and (i, i') combinations. Since the lifetime for level k, t_k is inversely proportional to $\sum_i A_{ki}$ which is in turn proportional to $\sum_i f_{ik}$, the extended conservation rule is $\sum_k \frac{1}{t_k}$ is nearly constant where k is a member of a group of closely spaced odd parity levels. This can be summarized as in equations (4-8): (4-10)

$$\sum_k \sum_i f_{ik} \cong C_1 \tag{4.8}$$

Since

$$f_{ik} \, \alpha \, A_{ki} \;\; then \;\; \sum_k \sum_i A_{ki} \cong C_2 \tag{4.9}$$

And since

$$t_k = \frac{1}{\sum_i A_{ki}} \;\; then \;\; \sum_k \frac{1}{t_k} = C_3 \tag{4.10}$$

Where C_1, C_2, C_3 are arbitrary constants.

For very many cases in the W II levels studied here, this is proven to be valid. Qualitatively it is saying that while the mixing coefficients for closely spaced levels may be harder to get accurately, whatever is "lost" by one these levels is redistributed over the other levels in the "k" set.

In this thesis, an equivalent conservation rule is confirmed for hyperfine structure and Lande g-values, without involving energy differences which are not present for these operators. These "rules" have also been confirmed for a large number of cases. Finally, in all instances the rules may be used to make a semi-empirical estimate of the property for a "missing" member of the "k group", providing the other members have been measured.

4.2.2 RCI calculations

Relativistic configuration interaction calculations included all W II odd parity states with angular momentum J = 1/2 up to J = 11/2 and all even states from J = 1/2 up to J=13/2. Which are almost all the experimentally measured enerty levels given in [1-2] . The goal of these calculations was to obtain the lifetimes due to the electric dipole transitions between these states. Also, three other quantities were obtained; emission probabilities, oscillator strength, branching fractions, and Lande g-values.

The reference configurations are $5d^4$ 6s and $5d^3$ $6s^2$ for the even states and $5d^3$ 6s 6p and $5d^4$ 6p for the odd states. The radial functions of the reference configurations were obtained as numerical solutions of the Multi-Configurational-Dirac-Fock equations using Desclaux code [19]. The experimental energy differences are used to calculate the transition probabilities and oscillator strengths.

The correlation effects were taken into account by using relativistic screened hydrogenic functions, RSH functions, (or virtual orbitals). For W II two sets of l =0 to 4 were included. And all single and double excitations from the valence shells (n = 5-6) were considered. The effective charge, Z*, of the RSH functions is determined by applying the energy variational procedure to valance electrons in the RCI matrix.

Some of the configurations have a large number of matrix elements and also large energy contributions, e.g. 5p to *v*f contributes ~ 1.3 eV. It is better to exclude these configurations from energy matrix because it is limited only to 20, 000 vectors and a few of them can use up all the allowed space. The second reason for excluding them is the disturbance they produce to other configurations. For example; when the reference configurations are $5s^2$ $5p^6$ $5d^4$ 6p and $5s^2$ $5p^6$ $5d^3$ 6s 6p, introducing a 5p to *v*f excitation must be done to the two references. While it gives the right effect to fix one of the references it will disturb the other one. In these cases our solution is to perform separate calculations that include only one reference and one correlation configuration, for example $5s^2$ $5p^6$ $5d^4$ 6p and $5s^2$ $5p^5$ $5d^4$ 6p *v*f are included in the matrix. Then another matrix that includes $5s^2$ $5p^6$ $5d^3$ 5s 6p and $5s^2$ $5p^5$ $5d^3$ 5s 6p *v*f. In each of these runs the Z* of *v*f was recalculated. Then compare the energy contribution due to the correlation configuration on the two references. Finally only the relative energy difference is taken as

shift of the diagonal energy matrix element of one of the references with respect to the other. This idea of shift is also discussed in [22]. Calculating the relative energy shift this way was done to all single and double excitations that had big matrix size and big energy contributions, examples are 5p to *v*p, 5p to *v*f, 5s 5p to *v*d *v*f, and 5p 6d to *v*p *v*d.

The electric dipole transitions between J odd to J, J$\pm$1 even states were calculated by the *f*-value code [21]. This code deals with the non-orthonormal states which are required because the initial (even levels with lower energies) and final states (odd levels with higher energies) have different radials. In this stage of calculations we used the experimentally measured energies, not the RCI calculated, because they are more accurate. It produces the emission probabilities and oscillator strength by two different calculations, the length gauge and the velocity gauge. The results of length gauge are proportional to radial operator while the results of the velocity gauge are proportional to the inverse of the radial operator [23]. In cases where excitations are done from both the core and the valence sub-shells usually the gauge spread [|velocity- length|/ (velocity + length)] is about 10% or less. In the case of W II only the excitations from the valence shells were done so only the results on the length gauge were used.

4.3 Results and Discussion

In this section we present RCI results in comparison with recent experimental data and some of the previous calculations. First there are three tables for RCI results, lifetime, oscillator strength, and Lande g-value, for the odd parity levels that have experimental measurements only. So that the comparisons between RCI and experimental results are clear. Then we present tables of RCI results, lifetime and g-values, for all the published odd parity levels. We also give oscillator strength, emission probabilities and branching for the lowest 10 levels for each odd J. The RCI results are compared with some available data in the literature. A conservation of the sum of the inverse lifetimes of two (or more) neighboring levels that have same J and parity was observed.

4.3.1 Lifetime of W II transitions; comparing RCI results to experimental values

We are comparing RCI lifetime calculations to the most recent reliable measurements and calculations; Nilsson's et al 2008 and Ekberg's et al 2000. Nilsson's calculations had shown to be in good agreement with experimental values. Ekberg gave the most recent most accepted energy level measurements and LS vector composition calculations. It is expected that the same parameters which they used to derive the LS vector composition will yield good lifetime values. In table 4-1 we compare RCI calculations to recent measured values and to the calculated values by Nilsson's [7] two methods and to Ekberg's [3] calculations. The values for Ekberg's results in table 4-1 are those given in table 4-8 in [3] multiplied by 0.69 as a scaling factor. This was the same scaling factor used by Nilsson's et al in [7]. For reasons of choosing this value see [7] and [3].The percentage errors are calculated as $(|\tau_{RCI} - \tau_{exp}|/ \tau_{exp}) * 100$.

In general the short lifetimes have big percentage errors although most of calculated short lifetimes are of order of 10^{-2} ns difference from the experimental values. In total the average error percentage between RCI calculated lifetimes and the 28 experimental values is 15.9 % (or 14.3 % if the smaller errors are considered, for those levels that have multiple measured values)

A conservation of the sum of the inverse of lifetimes of neighboring levels with the same J, and parity is observed in some cases. Since the conservation of sum of the inverse also implies conservation of the sum we are going to give the examples of these conservation cases in terms of sum of lifetimes directly. This conservation rule can be applied on levels that have same radials, i.e. either $5d^4$ 6p or $5d^3$ 6s 6p. But the levels of W II are highly mixed of different configurations for the two different radials (see columns 1 and 2 in table 4-1). Also, the given percentages of the configurations in the different levels show that it is not possible to follow a given configuration to see how it is distributed on the different levels. Because of these two reasons we decided that the sum of the *f*-values (or sum of lifetimes) can be applied approximately and collectively on all levels that have small energy differences, same J and same parity and they don't have to

have same radials. The best case of applying this rule was J=3/2 because many levels in a raw have available lifetime measurements. Other J^s have a fewer measurements available with many levels in between are not measured.

In regards to Nilsson's two methods of calculations; they stated that the second method ((HFR+CP (B), Yb-like ionic core and 3 valence electrons) gave values that were closer to the experimental ones. But studying table 4-1 and table 1 in [7] shows that in some cases the first method ((HFR+CP(A) , Er-like core and 5 valence electrons) gave better results. This reflects the complexity of W II electronic states and the difficulty to specify an exact model for it.

4.3.1.1 Comparing RCI lifetimes to experimental values for W II J=1/2

$36165.36^{o}_{1/2}$ Level; RCI is in excellent agreement with both experimental values but it is closer to the Kwiatkowski's. RCI is better than the Nilsson's calculations and as good as Ekberg's.

$38576.31\,^{o}_{1/2}$; RCI is in good agreement with both experimental values but it is closer to the Kwiatkowski's. RCI is closer to experiments than the Nilsson's calculations.

$44455.21\,^{o}_{1/2}$; RCI is in excellent agreement with experimental value. RCI is also close to the Nilsson's second calculations and both are better than Ekberg's

These are the lowest three levels for J=1/2 the sum of lifetime from RCI is 26.84 ns and the experimental is 27.97 ns. So the error in the sum of the three levels is 4%.

Lifetimes of $36165.35^{o}/_{2}$ and $38576.32^{o}/_{2}$ were also measured by Shultz et al, 1998 [11] as part of testing their experimental technique of using Linear Paul trap with TRLF for lifetime measurements. They gave the same results as those given by Schnabel et al 1998 [Shultz and Schnabel belong to the same experimental group]. Schnabel's and Kwiatkowski's measurements of the lifetimes of $36165^{o}/_{2}$ and $38576^{o}/_{2}$ are close to each other.

4.3.1.2 Comparing RCI lifetimes to experimental values for W II J=3/2

$39129.46^{o}_{3/2}$; RCI is 28% off the experimental value. Both of Nilsson's second calculation and Ekberg's are better than RCI.

$42298.22^{o}_{3/2}$; RCI is in excellent agreement with the experimental value. RCI is better than the 3 previous calculations.

$44911.66^{o}_{3/2}$; The difference between RCI calculated lifetime and the measured one is 0.56 ns. Since this is a relatively short lifetime the error percentage is quite big, 12.87%. RCI is slightly better than Nilsson's two calculations. Ekberg's is better than the other calculations.

$45553.65^{o}_{3/2}$; This is an average lifetime. But RCI is giving a relatively long lifetime. RCI is 23.73 off experiment. All previous calculations are closer to experiment than RCI. And this is one of the biggest error percentages for RCI.

$47179.94^{o}_{3/2}$; The two experimental values are quite close, almost the same. RCI is in excellent agreement with both of them and slightly closer to Schnabel's than to Nilsson's. RCI is as good as Nilsson's first calculation and clearly better than the other two calculations.

The sum of lifetimes of the three levels, $44911.66^{o}_{3/2}$, $45553.65^{o}_{3/2}$ and $47179.94^{o}_{3/2}$ is 18.75 ns for RCI calculation, and 17.94 for the experimental values (measured by Shnabel) with a 0.81% error.

$47588.65^{o}_{3/2}$; RCI is in good agreement (9.71 % error) with the experimental value and it is as good as Nilsson's second calculation and Ekberg's.

$48982.94^{o}_{3/2}$; RCI has 19.60 % error. Both of Nilsson's measurements look as good as RCI with one of them less than experiment and the other is higher. Ekberg's value is good, as well.

$50431.00^{o}_{3/2}$; This is a short lifetime, 6.6 ns. RCI is 17.58% off experiment. It is a little better than Nilsson's first calculations and almost as good as their second calculations.

$51254.43^{o}_{3/2}$; RCI is 13.33% off experiment. It is close to Nilsson's first calculation.

These are three levels in sequence so the sum of their lifetimes should be conserved, $(\tau)_{RCI}$ is 13.6 ns and $sum\ (\tau)_{exp}$ is 13.7 ns with an error of 0.72%, which is an excellent application for the conservation of the sum.

4.3.1.3 Comparing RCI lifetimes to experimental values for W II J=5/2

$42049.48^{o}_{5/2}$; RCI is in excellent agreement with experiment and it is better than the three previous calculations.

$44354.78^{o}_{5/2}$; RCI is in excellent agreement with experiment. It is better than the Nilsson's previous calculations and as good as Ekberg's.

$48284.50^{o}_{5/2}$; RCI is 18.81% off the experimental value. Both of Nilsson's calculations are bigger than RCI with the first value closer to experiment.

$49242.04^{o}_{5/2}$; RCI 12.91% off experiment and it is better than the three previous calculations.

$50292.35^{o}_{5/2}$; RCI is 28.40 % of experiment. RCI is very close to Nilsson's second calculation and to Ekberg's. Nilsson's first calculation is the closest to experiment.

$51438.06\,^{o}_{5/2}$; RCI is in very good agreement with experiment. Nilsson's two calculations are slightly better than RCI.

These four levels for J=5/2 are in sequence and they illustrate a good example of the conservation of the sum of lifetimes. $sum\ (\tau)_{RCI}$ of $48284.50^{o}_{5/2}$ and $49242.04^{o}_{5/2}$ is 8.55 ns, $sum\ (\tau)_{exp}$ is 9.23 ns with 7.4% error. Adding to them the lifetime of $50292.35^{o}_{5/2}$ gives $sum\ (\tau)_{RCI}$ 15.15 ns and $sum\ (\tau)_{exp}$ is 14.37 ns with 5% error. Then adding to them lifetime of $51438.06\,^{o}_{5/2}$ gives $sum\ (\tau)_{RCI}$ 20.13 ns and $sum\ (\tau)_{exp}$ is 18.97 ns with 6% error.

4.3.1.4 Comparing RCI lifetimes to experimental values for W II J=7/2

$42390.29^{o}_{7/2}$; The difference between RCI and experiment is 2 ns. Since it is a long lifetime the error percentage is just 2.71 %. RCI is in excellent agreement with Schnable's measurement and disagrees with Kwiatkowski's. It's better than the three

other measurements. For this level the value given by Kwiatkowski's measurement is much smaller than that given by Schnabel's measurement and Ekberg's and Nilsson's calculations and also RCI calculations. So we agree with Nilsson that this value should be rejected. Schnable et al explain this disagreement to be due to misidentification of the wave length of the measured lifetime by the Kwiatkowski group [8].

$44877.21^{o}_{7/2}$; RCI is in excellent agreement with experiment and it is better than Nilsson's calculations and slightly better than Ekberg's. Although the energy difference between this level and the one above is quite big 2500 cm^{-1}. The $sum\ (\tau)_{RCI}$ is 84.49 ns and $sum\ (\tau)_{exp}$ is 82.68 ns with an error of 2.18 %

$51045.29^{o}_{7/2}$; This is one of the short lifetimes. RCI is bigger than experimental value. The two Nilsson's calculations look closer to experiment than RCI. The error percentage of RCI (32.98 %) is less than that of the Nilsson's first calculation (41%) and bigger than the second (9.8 %).

$54498.61^{o}_{7/2}$; The two experimental values are close and show it as a fast transition. RCI is closer to Nilsson's measurement than it is to Hendersson's. Both of Nilsson's calculations are closer to Hendersson's measurement.

For the $42390^{o}_{7/2}$ and $54498^{o}_{7/2}$ there is a disagreement between TR-LIF Nilsson's et al measurements and both of their calculations which seem to be in good agreement between the HFR-CP results by Nilsson's and the measurements of Henderson's. And we see that the RCI result is in excellent agreement with Nilsson's measurement, as it falls within the range of experimental uncertainty. Between the 44877 and 51045 cm^{-1} levels there are 3 levels missing measured lifetimes, between the 51045 and 54498 there are 4 missed levels. So it is not useful to apply the conservation of the sum rule for these levels.

4.3.1.5 Comparing RCI lifetimes to experimental values for W II J=9/2

$44758.10\ ^{o}_{9/2}$; RCI is in good agreement, 13.27 % error, with this average sized lifetime and it is better than the three previous calculations.

$46493.36^{o}_{9/2}$; RCI is in good agreement with this average sized lifetime and it is better than Nilsson's calculations. Ekberg's is even better than RCI.

$49181.03^{o}_{9/2}$; Although it is not a short lifetime RCI and experiment differ by 18.60%.

$55392.45^{o}_{9/2}$; This has a short lifetime and RCI and experiment differ by 19.57%. Both of Nilsson's calculations are closer to experiment than RCI.

$44758.10\,^{o}_{9/2}$, $46493.36^{o}_{9/2}$, and $49181.03^{o}_{9/2}$ levels are in sequence, $sum\,(\tau)_{RCI}$ is 53.44 ns and $sum\,(\tau)_{exp}$ is 55.5 with a 3.7% error. There are 5 levels are missing lifetime measurements above $55392.45^{o}_{9/2}$. So the conservation of the sum cannot be applied here in order to predict individual semi-empirical lifetimes.

4.3.1.6 Comparing RCI lifetimes to experimental values for W II J=11/2

$51495.05^{o}_{11/2}$; This is the biggest RCI error percentage, 45.71 %.

$54229.08^{o}_{11/2}$; RCI is in better agreement with Hendersson's measurement than it is with Schnabel's. The three other calculations are closer to Schnabel's measurement. The energy difference between this level and the one above is 2700 cm^{-1}. $sum\,(\tau)_{RCI}$ is 7.32 ns and $sum\,(\tau)_{exp}$ is 11.2 ns (or 10.18 using Shcnabel's value) with an error of 35 % (or (28.1%). The decays of $51495^{o}_{11/2}$ and $54229^{o}_{11/2}$ levels produce astrophysically important lines [10]. The agreement of RCI calculation with the experimental values is not satisfactory for these two levels.

4.3.2 Lande g-value of W II odd levels; comparing RCI results to experimental values

Table 4-2 presents RCI calculated Lande g-value (g-factor) for W II odd levels that have their experimental values measured and published. Those are in NIST data base [1] which is taken form Kramida et al 2006 [2] and originally they are the measurements of Laun et al (1964) [4]. The Ekberg's et al (2000) [3] calculated results for these levels are also displayed.

Since g-values are already small I am considering all error < 10% excellent agreement with experiment for the individual levels. The average error over the available 71 experimental values is 8.51%.

4.3.2.1 Comparing RCI g-values to experimental values for W II J=1/2odd

For most of W II J=1/2 levels RCI calculations are in excellent agreement with experiment except for a few levels.

$44455.21\ ^{o}_{1/2}$; The difference between RCI and experiment is pretty small but the value of g-factor is small, too. This gives a big percentage error.

$52355.25\ ^{o}_{1/2}$; RCI and Ekberg agree and they are pretty different from experiment so we suggest that g-value needs to be re-measured.

$52593.77\ ^{o}_{1/2}$; RCI is quite different form experiment (error is 34.8%) and Ekberg's. Since the energy difference between this level and the one above is only 250 cm^{-1} then an effective mixing is expected to affect the results of these two levels. $sum\ (g)_{RCI}$ is 2.87 and $sum\ (g)_{exp}$ is 2.54 with an error of 13%. This illustrates the conservation of g-value sum for nearly degenerate levels.

4.3.2.2 Comparing RCI g-values to experimental values for J=3/2 odd

Most of the levels have very good to excellent agreement with the experimental values except $56084.33^{o}_{3/2}$ and $58007.69^{o}_{3/2}$ where there is about 20% error. For the $58007.69^{o}_{3/2}$ level and the $58748.04^{o}_{3/2}$ (directly above it), $sum\ (g)_{RCI}$ is 2.298 and $sum\ (g)_{exp}$ is 1.98 with an error of 16%.

4.3.2.3 Comparing RCI g-values to experimental values for J=5/2 odd

RCI calculated g-values are in excellent agreement with experiment for all the levels except the following ones;

$54704.59\ ^{o}_{5/2}$; RCI is almost double the experimental value but it is very close to Ekberg's calculations.

$55162.39\,^{o}_{5/2}$; RCI is 19.71% off experiment but it is close to Ekberg's result. We suggest re-measuring g-values of these two levels.

$56874.98\,^{o}_{5/2}$; RCI is much bigger than experiment and Ekberg's.

$57856.76\,^{o}_{5/2}$; RCI is much smaller than experiment and Ekberg's. It seems as if g-values of these two levels have been exchanged, $sum\ (g)_{RCI}$ is 2.3 and $sum\ (g)_{exp}$ is 2.17 with an error of 5.7%.

4.3.2.4 Comparing RCI g-values to experimental values for J=7/2 odd

All levels have excellent-very good agreement between RCI results and experimental values. For 48830.70 The RCI error % is less than 10% but it is pretty close to Ekberg's. A couple of levels are quite different from Ekberg's calculations 58537.63 and 58709.61, but these don't have their experimental measurements available. But the difference in the sum is only 2.2%.

4.3.2.5 Comparing RCI g-values to experimental values for J=9/2 odd

Only 8 levels have experimental g-values available. RCI of 5 levels is in excellent agreement with experiment. For the 53370.01 and 54056.59 the error percentages are 17 and 15 %, the error of the sum is only 3.3%. For the 55392.45 the three values RCI, experiment and Ekberg's are quite different from each other, the errors % of RCI is 21% and that of Ekberg's is 14%.

4.3.2.6 Comparing RCI g-values to experimental values for J=11/2 odd

RCI g-values are in excellent agreement with the experimental measurements except for one level 51495.05. In section 4.3.1 we saw that summing lifetime of this level with the 54229 cm^{-1} level reduced the error drastically. The g-value of the second level not measured so we can't compare the sum for g-values. But I think that the sum g-values for the two levels will show very small error % when new measurements are provided.

4.3.3 RCI results of W II odd levels; lifetimes and g-values

Tables 4-3 to 4-8 display the RCI results of the lifetime and Lande g-value of the lowest odd levels of W II. Calculated g-values by Ekberg et al (2000) are also given. The overall agreements between RCI and Ekberg's calculations are good. A few values show some disagreement. Ekberg et al have the most recent measurements of W II energy levels and it is expected that their g-value calculations are accurate enough and good to compare with.

4.3.4 Oscillator strength of W II odd levels; comparing RCI results to experimental values

Tables 4-9 to 4-14 present RCI results for emission probabilities A_{ki}, absorption oscillator strength (or *f*-value) f_{ik}, and branching fractions of the lowest 10 energy levels for each J odd state. The calculations included all the W II 175 odd parity levels, J=1/2 – 11/2, but we chose to display the results of only a few of them to avoid lengthy tables. Also, because the experimental measurements of Lennartsson et al [16] included lower levels only, these values are given in the tables for comparisons. The tables also gives $\log_{10}$ (g*f*) which is the most commonly used quantity in literature; g is the statistical weight of the lower level. In these tables we also give calculated log (g*f*) values that were compiled by Quinet et al (2010). Lennartsson et al measured the branching fractions associated with the most recent lifetime's measurements, Nilsson's et al 2008. From these measurements of branching fractions and lifetimes their oscillator strengths values were derived [16].

Looking at the tables we see a good agreement between RCI *f*-values and those compiled by Quient [18]. This puts the quality of RCI branching fractions and f-value calculations on equal footing with the most important previous calculations. Also, when comparing the branching fractions of the nine decays measured by Lennartsson et al [16] to the RCI calculations we see that both agree on identifying the strongest 2 or 3 branches for each decay. In many cases the calculated and experimental values of these strong

branches are similar. Other small branches have less agreement between the calculated and experimental values.

$47179.94^{o}_{3/2}$; decays into 11 even levels, table 4-1, gives10.17 % error in lifetime calculation (τ_{error}). Table 4-10, shows that both RCI and experiment give the strongest three branches of decay to be $0.0^{e}_{1/2}, 1519^{e}_{3/2}, \text{and } 8711^{e}_{3/2}$with the same order. The RCI and experiment values are different, error 30, 33, 40%.

$50431.00^{o}_{3/2}$; decays into 14 branches, τ_{error} is 17.58%, RCI branching fractions shows 51% to the ground and 16.8 % to $13173^{e}_{1/2}$, other branches are small. Experiment show 31.3% decay to $13173^{e}_{1/2}$ and 14.3 % to ground and 9.86% to $11303^{e}_{5/2}$. So RCI did identify the biggest two branches as experiment, but with a reversed order and bigger values and it missed the third branch.

$51254.43^{o}_{3/2}$; decays to 14 branches, τ_{error} is 13.33 %, both of RCI and experiment show the biggest three branches ,in order, to be $0.0^{e}_{1/2}, 3172^{e}_{5/2}, \text{and } 1519^{e}_{3/2}$, errors 43, 68, and 20.5%.

$48284.50^{o}_{5/2}$; decays to 16 branches, τ_{error} is 18.8 %, both of RCI and experiment show the biggest three branches ,in order, to be $7420^{e}_{5/2}, 3172^{e}_{5/2}, \text{and } 4716^{e}_{7/2}$, errors 13.5, 7, and 50%.

$51438.06\,^{o}_{5/2}$; decays via 24 branches, τ_{error} is 8.7 %, both of RCI and experiment show the biggest two branches, in order, to be $3172^{e}_{5/2}$ and $14634^{e}_{3/2}$, error 5 and 2 %. The third decay branches of RCI and experiment are different. This transition shows the small error in lifetime calculation is associated with small errors in branching fraction calculations.

$51045.29^{o}_{7/2}$; decays to 16 branches, τ_{error} is 32.98 %, both of RCI and experiment show the biggest three branches ,in order, to be $3172^{e}_{5/2}, 4716^{e}_{7/2}, \text{and } 6147^{e}_{9/2}$, errors 6, 26, and 75%.

$54498.61^{o}_{7/2}$; decays to 16 branches, τ_{error} is 9.05 %, both of RCI and experiment show the biggest two branches ,in order, to be $4716^{e}_{7/2}$ and $6147^{e}_{9/2}$, error 34 and 10 %. The third decay branches of RCI and experiment are different. This transition shown a small

error in lifetime calculation not associated with small error in branching fraction calculations.

$49181.03^{o}_{9/2}$; decays to 5 branches, τ_{error} is 18.6 %, both of RCI and experiment show the biggest two branches ,in order, to be $4716^{e}_{7/2}$ and $6147^{e}_{9/2}$, error 27 and 15 %. The third decay branches of RCI and experiment are different.

$55392.45^{o}_{9/2}$; decays to 21 branches, τ_{error} is 19.57 %, both of RCI and experiment show the biggest two branches ,in order, to be $4716^{e}_{7/2}$ and $6147^{e}_{9/2}$, error 25 and 72 %. The third decay branches of RCI and experiment are different

The analysis of lifetime and branching fractions of these levels does not give a clear link between the error percentages in the RCI calculations of the two quantities.

4.3.5 Conclusion

Relativistic configuration interaction calculations were performed to obtain the lifetimes due to the electric dipole transitions between W II J=1/2 to J=11/2 odd parity states and J=1/2 to J=13/2 even states. Lifetimes of 175 transitions are given in this study. In general the agreement between the RCI lifetimes and the available 28 measured lifetimes is good, average error is 15.9 %. Comparing RCI lifetime values to the 9 measurements by Nilsson et al [7] the average error is 16.53 %. Oscillator strengths, emission probabilities, and branching fractions were obtained for all the mentioned transitions. In this study we provide these quantities for the lowest 10 energy levels for each J odd value. The agreement between the measured branching fractions of 9 lifetimes (Lennartsson et al 2011) is not excellent. Qualitatively it is good because all the measured important branches of decay were also shown to be important in RCI calculations. On the other hand the agreement between RCI oscillator strengths and the previous calculations (Quinet et al 2010) is good. This puts the quality of RCI *f*-value and branching fractions on equal footing to all the previous important calculations. A conservation of sum of lifetimes of levels that have close energies, same J, and parity was observed in the RCI results. This reflects the conservation of the sum of the oscillator strengths values that was mentioned earlier by Nicolaides and Beck in [20]. Although the

individual values (either life times or oscillator strengths) may disagree with the measured values the sums are nearly the same. Also Lande g-values were calculated and they are in good agreement with measured and previously calculated values. A conservation of the sum of g-values of nearby energy levels is observed.

According to Henderson et al , 1999 [10] the transitions $5d^x$ 6s to $5d^x$ 6p are particularly strong between the levels of high J for terms of maximum spin multiplicity for all the positive ions that have ground state configuration $5d^x$ 6s, x = 3-7. Looking at the *f*-values of RCI calculations (tables 4-9: 4-14) and the available experimental results [16] and other calculations [18] I see that all J^s have almost equal average log g*f* values. There for I do not see this point given in reference [10] about the stronger transitions verified in case of W II.

Although the lifetimes result from summing up the emission probabilities over the different branches we found that RCI lifetimes have much better agreement with experimental values than the branching fractions and oscillator strength (which is closely related to emission probabilities), see also section 4.2.1.2. This can be explained as follows; first all W II levels are very impure where many configurations are mixed to make each level. In our calculations we were more concerned with the mixing percentages in the odd states, while we did not give same attention to the mixing in the even states. The lifetime values (which are the goal of this study) are sensitive to mixing in the odd states, while the branching fractions are sensitive to mixing of the odd and even states. Since each odd state decays into multiple even states, the branching fractions show even more sensitivity to the mixing and formation of the even states.

One thing to mention here is that experimentally the lifetimes and branching fractions are obtained in different sets of experiments and then they are used to calculate the oscillator strength (which is the most required quantity for spectroscopic analysis and diagnoses). In this study we calculate the emission probabilities and oscillator strength first then they were used to get the lifetime. The goal of this study was to provide lifetimes that can be used later with measured branching fractions to obtain oscillator strength. The goal of this study has been achieved by providing these lifetimes values. A future work can improve the mixing coefficients in the even states and thus the branching fractions.

Table 4-1: Comparision of RCI lifetimes to the experimental measurements. *Error % between RCI calculations and experimental values are given. Also, previous calculations are given. Previous calculations include: HFR-CP (A), HFR-CP (B) of Nilsson's et al and Ekberg's (scaled).*

Level Energy	**LS coupling [a]**			**T_{RCI} (ns)**	**T_{exp} (ns)**	**Error**	**T_{calc} (ns)**
(cm^{-1})[a]	%	Configuration	LS^O			**%**	
$\mathbf{36165.36^o_{1/2}}$	17	$5d^4(^5D)6p$	^6F	13.61	14.42 ± 0.14^c	5.62	11.11^f, 11.91^g
	10	$5d^4$ (^3P)$6p$	^4D		14.0 ± 0.7^d	2.79	13.70 [h]
$\mathbf{38576.31^o_{1/2}}$	21	$5d^4$ (^5D)$6p$	^4P	10.33	11.88 ± 0.07^c	13.05	9.11^f, 9.82^g
	17	$5d^4$ (^5D)$6p$	^6F		11.3 ± 0.6^d	8.85	11.17 [h]
$\mathbf{44455.21^o_{1/2}}$	43	$5d^4$ (^4F)$6s$(^5F)$6p$	^6F	2.90	2.67 ± 0.07^c	8.61	2.46^f, 2.87^g
	24	$5d^4$ (^5D)$6p$	^6F				3.07 [h]
$\mathbf{39129.46^o_{3/2}}$	34	$5d^4$ (^5D)$6p$	^6F	17.89	13.94 ± 0.09^c	28.34	10.97^f, 12.52^g
	12	$5d^3$ (^4F)$6s$(^5F)$6p$	^4D				12.52 [h]
$\mathbf{42298.22^o_{3/2}}$	23	$5d^4$ (^5D)$6p$	^6D	10.69	10.88 ± 0.13^c	1.75	8.30^f, 9.00^g
	17	$5d^4$ (^5D)$6p$	^4P				10.09 [h]
$\mathbf{44911.66^o_{3/2}}$	25	$5d^3$ (^4F)$6s$(^5F)$6p$	^6F	3.79	4.35 ± 0.06^c	12.87	3.25^f, 3.75^g
	17	$5d^4$ (^5D)$6p$	^4P				4.09 [h]
$\mathbf{45553.65^o_{3/2}}$	31	$5d4(^5D)6p$	^6F	9.75	7.88 ± 0.24^c	23.73	6.15^f, 6.79^g
	5	$5d^3$ (^2P)$6s$(^3P)$6p$	^4D				7.17 [h]
$\mathbf{47179.94^o_{3/2}}$	29	$5d^3$ (^4F)$6s$(^5F)$6p$	^6F	5.21	5.8 ± 0.3^b	10.17	5.91^f, 6.82^g
	13	$5d^4$ (^5D)$6p$	^4F		5.71 ± 0.08^c	8.76	7.67 [h]
$\mathbf{47588.65^o_{3/2}}$	46	$5d^4$ (^5D)$6p$	^6P	3.07	3.40 ± 0.11^c	9.71	2.88^f, 3.23^g
	9	$5d^3$ (4P)$6s$(5P)$6p$	^6P				3.67 [h]
$\mathbf{48982.94^o_{3/2}}$	35	$5d^3$ (^4F)$6s$(^5F)$6p$	^6D	4.02	5.00 ± 0.08^c	19.60	4.54^f, 5.37^g
	12	$5d^4$ (^5D)$6p$	^4P				5.83 [h]
$\mathbf{50431.00^o_{3/2}}$	14	$5d^4$ (^5D)$6p$	^4F	7.76	6.6 ± 0.4^b	17.58	4.69^f, 5.31^g
	11	$5d^4$ (^5D)$6p$	^6D				
$\mathbf{51254.43^o_{3/2}}$	17	$5d^4$ (^5D)$6p$	^6D	1.82	2.1 ± 0.2^b	13.33	1.87^f, 2.16^g
	15	$5d^3$ (4P)$6s$(5P)$6p$	^6D				
$\mathbf{42049.48^o_{5/2}}$	45	$5d^4$ (^5D)$6p$	^6F	11.97	11.07 ± 0.19^c	8.13	8.34^f, 9.04^g
	11	$5d^3$ (^4F)$6s$(^5F)$6p$	^6F				9.45 [h]
$\mathbf{44354.78^o_{5/2}}$	22	$5d^4$ (^5D)$6p$	^6D	10.18	9.90 ± 0.12^c	2.83	7.74^f, 8.61^g
	13	$5d^3$ (^4F)$6s$(^5F)$6p$	^6D				9.86 [h]
$\mathbf{48284.50^o_{5/2}}$	21	$5d^3$ (^4F)$6s$(^5F)$6p$	^6F	4.79	5.9 ± 0.3^b	18.81	6.61^f, 7.63^g
	10	$5d^4$ (^5D)$6p$	^6P				
$\mathbf{49242.04^o_{5/2}}$	30	$5d^3$ (^4F)$6s$(5F)$6p$	^6F	3.76	3.33 ± 0.11^c	12.91	2.52^f, 2.87 [g]

	27	$5d^4$ (^{5}D)6p	^{6}P				3.09 [h]
50292.35$^o_{5/2}$	32	$5d^3$ (^{4}F)6s(^{5}F)6p	^{6}D	6.60	5.14 ± 0.06[c]	28.40	5.08[f], 6.61[h]
	13	$5d^4$ (^{5}D)6p	^{4}F				6.61 [h]
51438.06$^o_{5/2}$	15	$5d^4$ (^{5}D)6p	^{4}F	5.00	4.6± 0.4[b]	8.70	4.30[f] , 4.75[h]
	14	$5d^4$ (^{5}D)6p	^{4}P				
42390.29$^o_{7/2}$	73	$5d3$(^{4}F)6s(^{5}F)6p	^{6}G	78.16	76.1 ± 0.9[c]	2.71	67.89[f] , 72.32[g]
	4	$5d^4$ (^{5}D)6p	^{6}F		3.0 ± 0.03 [d]		72.90 [h]
44877.21$^o_{7/2}$	44	$5d^4$ (^{5}D)6p	^{6}F	6.33	6.58 ± 0.15[c]	3.80	5.22[f] , 5.72[g]
	15	$5d^3$ (^{4}F)6s(^{5}F)6p	^{6}G				6.13 [h]
51045.29$^o_{7/2}$	35	$5d^3$ (^{4}F)6s(^{5}F)6p	^{6}F	6.25	4.7± 0.4[b]	32.98	3.71[f] , 4.28[g]
	19	$5d^4$ (^{5}D)6p	^{6}D				
54498.61$^o_{7/2}$	17	$5d^4$ (^{5}D)6p	^{6}D	1.91	2.1± 0.2[b]	9.05	2.59[f] , 2.94[g]
	7	$5d^4$ (^{5}D)6p	^{4}D		2.7 ± 0.3[e]	29.26	
44758.10$^o_{9/2}$	29	$5d^3$ (^{4}F)6s(^{5}F)6p	^{6}G	24.50	21.63 ± 0.22[c]	13.27	15.29[f] , 16.35[g]
	12	$5d^4$ (^{5}D)6p	^{6}F				17.09 [h]
46493.36$^o_{9/2}$	53	$5d^3$ (^{4}F)6s(^{5}F)6p	^{6}G	11.44	12.37 ± 0.10[c]	7.52	10.00[f] , 11.09[g]
	8	$5d^4$ (^{5}D)6p	^{4}F				12.46 [h]
49181.03$^o_{9/2}$	25	$5d^4$ (^{5}D)6p	^{6}F	17.50	21.5 ±1.0[b]	18.60	19.17[f] , 20.44[g]
	20	$5d^3$ (^{4}F)6s(^{5}F)6p	^{6}D				
55392.45$^o_{9/2}$	15	$5d^4$ (^{3}H)6p	^{4}H	1.85	2.3± 0.2[b]	19.57	2.12[f] , 2.45[g]
	15	$5d^3$ (^{4}F)6s(^{5}F)6p	^{6}D				
51495.05$^o_{11/2}$	44	$5d^4$ (^{5}D)6p	^{6}F	4.18	7.7 ± 0.8[e]	45.71	5.37[f] , 5.83[g]
	32	$5d^3$ (^{4}F)6s(^{5}F)6p	^{6}G				
54229.08$^o_{11/2}$	35	$5d^4$ (^{5}D)6p	^{6}F	3.14	2.48 ± 0.08[c]	26.61	2.05[f] , 2.35[g]
	17	$5d^3$(^{4}F)6s(^{5}F)6p	^{6}F		3.5 ± 0.3[e]	10.29	2.49 [h]

(a) NIST

(b) Nilsson, et al (2008) , lifetime experimental measurements [7]

(c) Schnabel et al (1998), lifetime experimental measurements [8]

(d) Kwiatkowski et al (1984), lifetime experimental measurements [9]

(e) Henderson et al (1999), lifetime experimental measurements [10]

(f) Nilsson et al (2008), HFR +CP (A) lifetime calculations [7]

(g) Nilsson et al (2008), HFR + CP (B) lifetime calculations [7]

(h) Ekberg et al (2000) [3] lifetime calculations, table VIII scaled (/0.69) as was scaled by Nilsson 2008 [7]

Table 4-2: Comparison of RCI Lande g-values to experimental values [NIST, Laun] and Ekberg et al calculations.

Level Energy (cm^{-1})[a]	g-value $_{RCI}$	g-value $_{exp}$	Error %	g-value $_{calc}$
$36165.36\,^{o}_{1/2}$	0.74	0.678	9.14	0.73
$38576.31\,^{o}_{1/2}$	1.54	1.614	4.58	1.58
$44455.21\,^{o}_{1/2}$	-0.31	-0.217	-42.86	-0.23
$45457.07\,^{o}_{1/2}$	0.56	0.519	7.90	0.43
$46625.28\,^{o}_{1/2}$	1.76	1.70	3.53	1.79
$49154.48\,^{o}_{1/2}$	2.74	2.78	1.44	2.71
$52355.25\,^{o}_{1/2}$	0.767	0.981	21.81	0.73
$52593.77\,^{o}_{1/2}$	2.103	1.56	34.81	1.75
$53440.21\,^{o}_{1/2}$	2.098	2.038	2.94	2.44
$54485.70\,^{o}_{1/2}$	1.386	1.46	5.07	1.42
$39129.46\,^{o}_{3/2}$	1.152	1.147	0.44	1.14
$42298.22^{o}_{3/2}$	1.510	1.498	0.80	1.48
$44911.66^{o}_{3/2}$	1.218	1.221	0.25	1.27
$45553.65^{o}_{3/2}$	1.028	1.033	0.48	1.04
$47179.94^{o}_{3/2}$	0.924	1.007	8.24	0.97
$47588.65^{o}_{3/2}$	2.123	2.00	6.15	1.99
$48982.94^{o}_{3/2}$	1.768	1.72	2.79	1.73
$50431.00^{o}_{3/2}$	0.856	0.93	7.96	1.01
$51254.43^{o}_{3/2}$	1.597	1.58	1.08	1.46
$53329.76^{o}_{3/2}$	1.204	1.357	11.27	1.17
$53423.05^{o}_{3/2}$	1.033	0.976	5.84	1.35
$54137.23x^{o}_{3/2}$	1.729	1.608	7.52	1.72
$56084.33^{o}_{3/2}$	1.276	1.021	24.98	1.00
$56932.35^{o}_{3/2}$	1.181	1.06	11.42	1.10
$58007.69^{o}_{3/2}$	1.496	1.20	24.67	1.26
$58748.04^{o}_{3/2}$	0.802	0.78	2.82	1.00
$39936.84\,^{o}_{5/2}$	0.889	0.889	0.00	0.89
$42049.48\,^{o}_{5/2}$	1.310	1.292	1.39	1.29
$44354.78\,^{o}_{5/2}$	1.415	1.390	1.80	1.40
$46355.40\,^{o}_{5/2}$	1.298	1.236	5.02	1.29
$47413.27\,^{o}_{5/2}$	1.018	1.111	8.37	1.22
$48284.50\,^{o}_{5/2}$	1.481	1.366	8.42	1.18
$49242.04\,^{o}_{5/2}$	1.464	1.510	3.05	1.53
$50292.35\,^{o}_{5/2}$	1.395	1.334	4.57	1.37
$51438.06\,^{o}_{5/2}$	1.221	1.301	6.15	1.28

$\mathbf{53113.53}\,^{o}_{5/2}$	1.323	1.262	4.83	1.23
$\mathbf{54375.90}\,^{o}_{5/2}$	1.520	1.51	0.66	1.44
$\mathbf{54704.59}\,^{o}_{5/2}$	1.264	0.623	102.89	1.24
$\mathbf{55162.39}\,^{o}_{5/2}$	1.246	1.00	24.60	1.27
$\mathbf{56874.98}\,^{o}_{5/2}$	1.352	0.815	65.89	0.91
$\mathbf{57856.76}\,^{o}_{5/2}$	0.956	1.36	29.71	1.27
$\mathbf{60901.02}\,^{o}_{5/2}$	0.927	0.92	0.76	0.98
$\mathbf{61566.86}\,^{o}_{5/2}$	1.103	1.07	3.08	1.05
$\mathbf{42390.29}\,^{o}_{7/2}$	1.167	1.161	0.52	1.16
$\mathbf{44877.21}\,^{o}_{7/2}$	1.303	1.277	2.04	1.28
$\mathbf{46175.40}\,^{o}_{7/2}$	1.464	1.452	0.83	1.45
$\mathbf{48830.70}\,^{o}_{7/2}$	1.109	1.008	10.02	1.15
$\mathbf{49124.51}\,^{o}_{7/2}$	1.458	1.499	2.74	1.36
$\mathbf{51863.00}\,^{o}_{7/2}$	1.006	0.937	7.36	0.96
$\mathbf{52275.29}\,^{o}_{7/2}$	1.291	1.297	0.46	1.33
$\mathbf{52901.79}\,^{o}_{7/2}$	1.256	1.374	8.59	1.36
$\mathbf{53338.08}\,^{o}_{7/2}$	0.927	0.968	4.24	0.96
$\mathbf{56612.84}\,^{o}_{7/2}$	1.136	1.22	6.89	1.21
$\mathbf{56768.60}\,^{o}_{7/2}$	1.219	1.147	6.28	1.12
$\mathbf{57729.99}\,^{o}_{7/2}$	1.147	1.184	3.12	1.22
$\mathbf{59276.85}\,^{o}_{7/2}$	1.080	1.102	2.00	1.14
$\mathbf{59869.15}\,^{o}_{7/2}$	1.059	1.125	5.87	1.10
$\mathbf{44758.10}\,^{o}_{9/2}$	1.288	1.270	1.42	1.27
$\mathbf{46493.36}\,^{o}_{9/2}$	1.336	1.311	1.91	1.30
$\mathbf{49181.03}\,^{o}_{9/2}$	1.427	1.409	1.28	1.42
$\mathbf{50863.11}\,^{o}_{9/2}$	1.217	1.194	1.93	1.19
$\mathbf{53370.01}\,^{o}_{9/2}$	1.306	1.086	20.26	1.17
$\mathbf{54056.59}\,^{o}_{9/2}$	0.977	1.123	13.00	1.08
$\mathbf{55392.45}\,^{o}_{9/2}$	1.345	1.061	26.77	1.23
$\mathbf{59399.34}\,^{o}_{9/2}$	1.187	1.179	0.68	1.19
$\mathbf{51495.05}\,^{o}_{11/2}$	1.403	1.054	33.11	1.38
$\mathbf{54958.57}\,^{o}_{11/2}$	1.136	1.141	0.44	1.11
$\mathbf{58891.74}\,^{o}_{11/2}$	1.138	1.144	0.52	1.14
$\mathbf{60219.02}\,^{o}_{11/2}$	1.172	1.130	3.72	1.15
$\mathbf{61240.81}\,^{o}_{11/2}$	1.116	1.120	0.36	1.13
$\mathbf{61589.46}\,^{o}_{11/2}$	1.128	1.149	1.83	1.14

Tables (4-3: 4-8): RCI results of W II odd levels, g-values from Ekberg calculations are also given.

Table 4-3: RCI lifetimes and g-values of J =1/2 W II odd parity levels.

Energy (cm^{-1})[a]	**τ_{RCI} (ns)**	**g-value $_{RCI}$**	**g-value [b]**
36165.36	13.61	0.742	0.73
38576.31	10.33	1.539	1.58
44455.21	2.90	-0.305	-0.23
45457.07	18.56	0.561	0.43
46625.28	13.51	1.756	1.79
49154.48	2.49	2.743	2.71
51536.62	2.80	2.461	2.48
52355.25	4.30	0.767	0.73
52593.77	10.26	2.103	1.75
53440.21	2.11	2.098	2.44
54485.70	8.91	1.386	1.42
58308.80	7.70	0.502	0.45
62131.11	10.52	1.758	0.62

a) NIST [1]
b) Ekberg et al (2000) g-value calculations [3]

Table 4-4: RCI lifetimes and g-values of J =3/2 W II odd parity levels.

Energy (cm^{-1})[a]	**τ_{RCI} (ns)**	**g-value RCI**	**g-value [b]**
37971.53	411.93	0.079	0.12
39129.46	17.89	1.152	1.14
42298.22	10.69	1.510	1.48
44911.66	3.79	1.218	1.27
45553.65	9.75	1.028	1.04
47179.94	5.21	0.924	0.97
47588.65	3.07	2.123	1.99
48982.94	4.02	1.768	1.73
50431.00	7.76	0.856	1.01
51254.43	1.82	1.597	1.46
52803.01	4.11	1.738	1.49
53329.76	2.46	1.204	1.17
53423.05	13.6	1.033	1.35
54137.23	2.11	1.729	1.72
55488.13	2.30	1.630	1.85
56084.33	4.15	1.276	1.00
56932.35	4.62	1.181	1.10
58007.69	2.68	1.496	1.26
58748.04	3.75	0.802	1.00
59370.49	3.47	0.916	0.76
59816.39	3.19	1.041	1.27
60665.36	2.42	1.303	1.22
61117.66	1.78	0.745	0/76
62454.56	7.27	1.108	1.15
62724.69	2.91	1.294	1.42
63134.77	2.99	1.066	1.02
64255.16	2.95	0.999	1.03
64804.17	2.16	0.888	1.06
65299.72	1.52	1.333	1.19
68499.49	3.55	1.064	1.08

a) NIST [1]

b) Ekberg et al (2000) g-value calculations [3]

Table 4-5: RCI lifetimes and g-values of J =5/2 W II odd parity levels.

Energy (cm^{-1})[a]	τ_{RCI} (ns)	g-value RCI	g-value [b]
39936.84	239.50	0.889	0.89
42049.48	11.97	1.310	1.29
44354.78	10.18	1.415	1.40
46355.40	7.94	1.298	1.29
47413.27	10.82	1.018	1.22
48284.50	4.79	1.481	1.18
49242.04	3.76	1.464	1.53
50292.35	6.60	1.395	1.37
51438.06	5.00	1.221	1.28
52087.11	4.53	1.225	1.21
53113.53	2.07	1.323	1.23
54026.31	6.41	1.149	1.18
54375.90	18.09	1.520	1.44
54704.59	2.33	1.264	1.24
55162.39	9.51	1.246	1.62
56544.51	2.28	1.589	1.26
56874.98	7.03	1.352	0.91
57252.14	3.68	1.126	1.09
57856.76	4.52	0.956	1.27
58337.10	2.21	1.306	1.21
59443.05	2.47	1.292	1.45
59992.38	3.21	1.162	1.13
60474.73	5.72	1.075	1.14
60656.54	3.11	1.077	1.09
60901.02	2.55	0.927	0.98
61566.86	7.29	1.103	1.05
62333.25	2.89	1.060	1.05
62989.64	3.20	1.016	1.01
63880.27	2.17	1.289	0.96
64030.51	3.05	0.994	1.29
64310.11	5.83	1.300	1.11
64990.38	1.84	1.408	1.13
65481.01	2.58	1.081	1.63
66144.50	3.15	1.156	1.09
67173.56	4.68	1.043	1.00
68443.79	2.13	1.188	1.21
69060.71	3.97	1.038	1.10
69481.71	2.13	1.187	1.01

a) NIST [1]

b) Ekberg et al (2000) g-value calculations [3]

Table 4-6: RCI lifetimes and g-values of J =7/2 W II odd parity levels.

Level Energy (cm^{-1})[a]	τ_{RCI} (ns)	g-value RCI	g-value [b]
42390.29	78.16	1.167	1.16
44877.21	6.33	1.303	1.28
46175.40	20.30	1.464	1.45
48830.70	7.33	1.109	1.15
49124.51	3.63	1.458	1.36
51045.29	6.25	1.424	1.41
51863.00	5.30	1.006	0.96
52275.29	3.50	1.291	1.33
52901.79	8.54	1.256	1.36
53338.08	12.82	0.927	0.96
54498.61	1.91	1.435	1.34
55022.93	3.50	1.284	1.29
56612.84	13.72	1.136	1.21
56768.60	4.20	1.219	1.12
57729.99	5.99	1.147	1.22
58537.63	4.34	1.102	1.37
58709.61	5.21	1.483	1.16
59276.85	5.03	1.080	1.14
59869.15	3.61	1.059	1.10
59933.69	1.77	1.249	1.17
60256.55	3.90	1.459	1.29
60424.24	3.42	1.088	1.22
61326.28	2.04	1.046	1.08
61550.65	2.98	1.145	1.12
62561.09	4.42	1.202	1.16
63266.46	4.35	0.988	0.97
63788.24	3.47	1.097	1.09
64356.75	2.03	1.146	1.17
64896.33	2.96	1.085	1.06
65455.50	4.68	0.926	0.96
65643.97	3.82	1.182	1.23
66026.80	1.92	0.987	1.03
66898.06	2.76	1.060	1.13
68362.32	3.35	1.115	1.06
68619.99	2.02	1.259	1.15
69580.33	3.78	1.083	1.13
70211.80	2.12	1.184	1.17
70674.18	2.34	1.102	1.10
72597.30	1.47	1.138	1.16
73427.54	1.79	1.071	1.14

a) NIST [1]

b) Ekberg et al (2000) g-value calculations [3]

Table 4-7: RCI lifetimes and g-values of J =9/2 W II odd parity levels.

Energy (cm^{-1})[a]	τ_{RCI} (ns)	g-value RCI	g-value [b]
44758.10	24.50	1.288	1.27
46493.36	11.44	1.336	1.30
49181.03	17.50	1.427	1.42
50863.11	6.87	1.217	1.19
52567.28	6.86	1.349	1.34
53370.01	2.58	1.306	1.17
54056.59	7.26	0.977	1.08
55392.45	1.85	1.345	1.23
56413.65	4.42	1.195	1.18
57089.48	5.76	0.987	1.07
57986.94	16.89	1.128	1.09
58687.97	8.86	1.234	1.29
59399.34	2.97	1.187	1.19
60278.73	5.48	1.073	1.10
61055.85	5.63	1.190	1.15
61360.58	2.99	1.23	1.12
62330.86	10.51	1.402	1.26
62437.09	1.88	1.220	1.08
62716.16	2.47	1.096	1.43
64207.59	4.14	1.193	1.11
64516.23	3.81	1.111	1.19
65003.29	3.64	1.033	1.04
66271.00	4.31	1.116	1.10
66816.29	2.64	1.142	1.14
67028.65	2.45	1.109	1.17
67847.27	2.34	1.035	1.04
68734.66	3.43	0.991	1.03
69105.78	2.95	1.031	1.03
70902.47	1.88	1.067	1.11
71245.03	2.89	1.122	1.05
71785.39	2.29	1.088	1.08
72401.58	1.94	1.048	1.11
72557.90	2.45	1.172	1.09
73705.97	1.29	1.103	1.06
74446.93	1.53	0.998	1.16

a) NIST [1]

b) Ekberg et al (2000) g-value calculations [3]

Table 4-8: RCI lifetimes and g-values of J =11/2 W II odd parity levels.

Energy (cm^{-1})[a]	**τ_{RCI} (ns)**	**g-value RCI**	**g-value [b]**
48332.76	88.36	1.333	1.32
51495.05	6.16	1.403	1.38
54229.08	3.85	1.361	1.36
54958.57	3.24	1.136	1.11
56376.57	10.63	1.182	1.20
58891.74	3.75	1.138	1.14
60219.02	8.70	1.172	1.15
61240.81	3.82	1.116	1.13
61589.46	3.08	1.128	1.14
62966.51	3.82	1.095	1.09
64969.17	5.52	1.169	1.13
65326.55	1.95	1.109	1.17
65684.87	4.65	1.085	1.09
66703.46	4.23	1.123	1.10
68013.63	2.16	1.113	1.11
69587.79	1.42	1.208	1.13
71164.17	1.52	1.103	1.09
72180.63	2.56	1.075	1.14
73266.32	1.68	1.139	1.07

a) NIST [1]

b) Ekberg et al (2000) g-value calculations [3]

Tables 4-9: 4-14 give RCI results of emission transition probability A_{ki} (s^{-1}) , the absorption oscillator strength f_{ik}, and the branching fractions, BF of the lowest 10 levels in J = 1/2, 3/2, 5/2, 7/2, 9/2, and 11/2 odd parity in W II. Some experimental oscillator strength, experimental and calculated BF fractions are given.

Table 4-9: RCI transition probability A_{ki} (s^{-1}) , the absorption oscillator strength f_{ik}, and the branching fractions, BF of the lowest 10 energy levels of W II J=1/2 odd.

E_k[a]	E_i[a]	$2J_i$[a]	A_{ki}	f_{ik}	Log (g*f*)	BF	log(g*f*)[O]
36165	0	1	5.33E+07	0.0611	-0.91	0.7251	-0.89[b]
	8711	3	1.18E+07	0.0117	-1.33	0.1605	-1.33[b]
	8833	1	2.89E+06	0.0058	-1.94	0.0394	
	13173	1	4.57E+06	0.013	-1.59	0.0621	-1.4[b]
	19404	1	4.74E+05	0.0025	-2.30	0.0064	
38576	0	1	6.48E+06	0.0065	-1.89	0.0669	
	1519	3	6.29E+07	0.0343	-0.86	0.6499	-0.87[b]
	8833	1	5.59E+06	0.0095	-1.72	0.0577	
	10592	3	1.35E+07	0.0129	-1.29	0.139	-1.18[b]
	13173	1	2.72E+06	0.0063	-1.90	0.0281	
	14634	3	3.85E+06	0.005	-1.70	0.0398	
	18991	3	6.63E+05	0.0013	-2.28	0.0069	
	22503	3	4.31E+05	0.0012	-2.32	0.0044	
	22536	1	2.73E+05	0.0016	-2.49	0.0028	
44455	0	1	2.77E+08	0.2104	-0.38	0.803	-0.32[b]
	1519	3	4.05E+07	0.0165	-1.18	0.1174	
	8711	3	2.90E+06	0.0017	-2.17	0.0084	
	8833	1	7.35E+06	0.0087	-1.76	0.0213	
	10592	3	1.32E+07	0.0086	-1.46	0.0383	
	14634	3	2.35E+06	0.002	-2.10	0.0068	
	22536	1	4.43E+05	0.0014	-2.55	0.0013	
45457	0	1	1.35E+07	0.0098	-1.71	0.2504	
	1519	3	5.15E+06	0.002	-2.10	0.0956	
	8711	3	3.00E+06	0.0017	-2.17	0.0557	
	8833	1	2.32E+07	0.0259	-1.29	0.4305	
	10592	3	3.48E+06	0.0021	-2.08	0.0647	
	18991	3	1.15E+06	0.0012	-2.32	0.0213	
	19404	1	2.65E+06	0.0058	-1.94	0.0491	
	22536	1	6.59E+05	0.0019	-2.42	0.0122	
46625	0	1	5.10E+07	0.0351	-1.15	0.6885	
	8711	3	1.92E+06	0.001	-2.40	0.026	

	10592	3	1.17E+07	0.0068	-1.57	0.158
	13173	1	1.31E+06	0.0018	-2.44	0.0177
	18991	3	2.55E+06	0.0025	-2.00	0.0344
	19404	1	3.08E+06	0.0062	-1.91	0.0416
	22536	1	6.81E+05	0.0018	-2.44	0.0092
49154	0	1	6.03E+07	0.0374	-1.13	0.1502
	1519	3	3.07E+08	0.1013	-0.39	0.7639
	13173	1	5.97E+06	0.0069	-1.86	0.0149
	14634	3	1.06E+07	0.0066	-1.58	0.0263
	18991	3	2.85E+06	0.0023	-2.04	0.0071
	19404	1	6.66E+06	0.0113	-1.65	0.0166
	25045	1	2.22E+06	0.0057	-1.94	0.0055
	25170	3	2.75E+06	0.0036	-1.84	0.0069
51537	0	1	6.49E+07	0.0366	-1.14	0.1819
	1519	3	2.19E+08	0.0657	-0.58	0.6142
	8711	3	1.05E+07	0.0043	-1.76	0.0294
	8833	1	5.48E+06	0.0045	-2.05	0.0154
	10592	3	3.00E+07	0.0134	-1.27	0.0842
	13173	1	1.27E+07	0.0129	-1.59	0.0355
	18991	3	4.21E+06	0.003	-1.92	0.0118
	19404	1	3.27E+06	0.0047	-2.03	0.0092
	20456	3	2.26E+06	0.0018	-2.14	0.0063
	25045	1	2.35E+06	0.005	-2.00	0.0066
52355	0	1	9.71E+06	0.0053	-1.97	0.0417
	1519	3	7.12E+06	0.0021	-2.08	0.0306
	8711	3	5.80E+07	0.0228	-1.04	0.2493
	8833	1	6.38E+07	0.0505	-1.00	0.2742
	13173	1	4.40E+07	0.043	-1.07	0.1891
	14634	3	9.06E+06	0.0048	-1.72	0.0389
	19404	1	1.06E+07	0.0146	-1.53	0.0456
	20456	3	2.96E+06	0.0022	-2.06	0.0127
	22503	3	1.62E+07	0.0136	-1.26	0.0694
	24992	3	2.08E+06	0.0021	-2.08	0.0089
	25045	1	2.66E+06	0.0053	-1.97	0.0114
	28491	3	8.51E+05	0.0011	-2.36	0.0037
	32950	3	9.03E+05	0.0018	-2.14	0.0039
52594	8711	3	2.37E+07	0.0092	-1.43	0.2433
	8833	1	3.03E+07	0.0237	-1.32	0.3109
	13173	1	2.04E+07	0.0197	-1.40	0.2093
	18991	3	3.56E+06	0.0024	-2.02	0.0365
	19404	1	1.68E+06	0.0023	-2.34	0.0172
	20456	3	4.61E+06	0.0033	-1.88	0.0473

	22503	3	1.29E+06	0.0011	-2.36	0.0132
	24992	3	2.14E+06	0.0021	-2.08	0.0219
	25045	1	3.29E+06	0.0065	-1.89	0.0338
53440	0	1	2.72E+07	0.0143	-1.54	0.0574
	1519	3	1.25E+08	0.0347	-0.86	0.2629
	8711	3	7.24E+06	0.0027	-1.97	0.0153
	8833	1	2.00E+08	0.151	-0.52	0.4227
	10592	3	1.49E+07	0.0061	-1.61	0.0315
	13173	1	1.34E+07	0.0124	-1.61	0.0283
	14634	3	5.27E+07	0.0262	-0.98	0.1112
	19404	1	7.12E+06	0.0092	-1.74	0.015
	24992	3	5.18E+06	0.0048	-1.72	0.0109
	25045	1	5.87E+05	0.0011	-2.66	0.0012
	25170	3	1.54E+07	0.0144	-1.24	0.0325
	26527	1	2.97E+06	0.0061	-1.91	0.0063

([a]) NIST [1]

([O]) Results from literature, other work (b and c)

([b]) Quinet et al , 2010 [18]

([c]) Lennertsson et al, 2011 [16]

Table 4-10: RCI transition probability A_{ki} (s^{-1}) , the absorption oscillator strength f_{ik}, and the branching fractions, BF of the lowest 10 energy levels of W II J=3/2 odd.

E_k	E_i	$2J_i$	A_{ki}	f_{ik}	log (g*f*)	BF	log(gf)[o]	BF[o]
37912	8711	3	1.75E+06	0.0031	-1.91	0.7225	-1.72[b]	
39129	0	1	1.16E+07	0.0228	-1.34	0.2081	-1.07[b]	
	1519	3	2.67E+07	0.0283	-0.95	0.4784	-0.77[b]	
	3172	5	2.98E+06	0.0023	-1.86	0.0533		
	8711	3	2.42E+06	0.0039	-1.80	0.0434		
	8833	1	4.54E+05	0.0015	-2.53	0.0081		
	11301	5	5.73E+06	0.0074	-1.35	0.1026		
	13173	1	1.89E+06	0.0084	-1.77	0.0338		
	14634	3	1.28E+06	0.0032	-1.89	0.0229		
	14968	5	8.15E+05	0.0014	-2.08	0.0146		
	20456	3	2.59E+05	0.0011	-2.35	0.0056		
	22536	1	2.07E+05	0.0023	-2.34	0.0037		
	24992	3	1.98E+05	0.0015	-2.22	0.0035		
42298	1519	3	1.95E+07	0.0176	-1.15	0.208	-1.04[b]	
	3172	5	4.41E+07	0.0288	-0.76	0.472	-0.7[b]	
	7420	5	1.93E+06	0.0016	-2.02	0.021		
	8711	3	3.22E+06	0.0043	-1.77	0.034		
	8833	1	4.45E+06	0.0119	-1.62	0.048		
	13434	5	5.68E+06	0.0068	-1.39	0.061		
	14634	3	9.41E+06	0.0184	-1.13	0.101	-1.07[b]	
	14968	5	2.71E+06	0.0036	-1.66	0.029		
	22536	1	3.00E+05	0.0023	-2.34	0.003		
44912	0	1	1.12E+08	0.1665	-0.48	0.4245	-0.46[b]	
	1519	3	9.97E+07	0.0793	-0.50	0.378	-0.56[b]	
	3172	5	1.99E+06	0.0011	-2.16	0.008		
	7420	5	7.43E+06	0.0053	-1.50	0.028		
	8711	3	1.10E+07	0.0126	-1.30	0.042		
	11301	5	4.47E+06	0.0040	-1.63	0.017		
	13173	1	1.17E+07	0.0348	-1.16	0.044		
	13434	5	6.32E+06	0.0064	-1.42	0.024		
	14968	5	2.00E+06	0.0022	-1.87	0.008		
	16235	5	3.40E+06	0.0041	-1.61	0.013		
	18991	3	8.63E+05	0.0019	-2.11	0.003		
	19276	5	7.68E+05	0.0012	-2.15	0.003		
	23450	5	5.55E+05	0.0012	-2.14	0.002		
45554	0	1	2.37E+07	0.0342	-1.16	0.231		
	1519	3	2.95E+07	0.0228	-1.04	0.287		

	3172	5	2.21E+07	0.0123	-1.13	0.215		
	7420	5	2.12E+06	0.0015	-2.06	0.021		
	8711	3	1.25E+06	0.0014	-2.26	0.012		
	8833	1	1.76E+06	0.0039	-2.11	0.017		
	10592	3	4.46E+06	0.0055	-1.66	0.043		
	11301	5	8.74E+06	0.0074	-1.35	0.085		
	13173	1	1.91E+06	0.0055	-1.96	0.019		
	14968	5	1.43E+06	0.0015	-2.04	0.014		
	19404	1	8.16E+05	0.0036	-2.15	0.008		
	20456	3	1.04E+06	0.0025	-2.01	0.0101		
	22536	1	9.56E+05	0.0054	-1.97	0.009		
	24992	3	7.11E+05	0.0025	-2.00	0.007		
47180	0	1	9.08E+07	0.1223	-0.61	0.473	-0.77 [c]	0.364 [c]
	1519	3	5.74E+07	0.0413	-0.78	0.299	-0.95 [c]	0.224 [c]
	3172	5	4.17E+06	0.0022	-1.89	0.022	…	…
	8711	3	2.06E+07	0.0209	-1.08	0.1075	-0.9 [c]	0.182 [c]
	8833	1	1.61E+06	0.0033	-2.18	0.008	-1.5 [c]	0.0451 [c]
	13173	1	7.05E+06	0.0183	-1.44	0.037	-1.45 [c]	0.04 [c]
	14634	3	4.23E+06	0.0060	-1.62	0.022	-1.34 [c]	0.0465
	16235	5	1.52E+06	0.0016	-2.02	0.008	-1.79 [c]	0.015 [c]
	18990	3	…	…	…	…	-2.11 [c]	0.0059 [c]
	19276	5	…	…	…	…	-2.25 [c]	0.0042 [c]
	22139	5	…	…	…	…	-2.06 [c]	0.0053 [c]
47589	0	1	4.77E+07	0.0632	-0.90	0.147		
	1519	3	3.24E+07	0.0229	-1.04	0.0995		
	3172	5	1.06E+08	0.0539	-0.49	0.327		
	7420	5	1.25E+08	0.0773	-0.33	0.383	-0.34 [b]	
	8833	1	1.09E+06	0.0022	-2.36	0.003		
	10592	3	2.62E+06	0.0029	-1.94	0.008		
	14634	3	6.29E+06	0.0087	-1.46	0.019		
	22536	1	4.60E+05	0.0022	-2.36	0.001		
48983	0	1	5.10E+07	0.0638	-0.89	0.205		
	1519	3	1.03E+08	0.0683	-0.56	0.413		
	3172	5	5.20E+07	0.0248	-0.83	0.209		
	7420	5	1.16E+07	0.0067	-1.39	0.047		
	8833	1	5.73E+06	0.0107	-1.67	0.023		
	10592	3	1.75E+06	0.0018	-2.15	0.007		
	11301	5	2.39E+06	0.0017	-2.00	0.01		
	13173	1	1.75E+06	0.0041	-2.09	0.007		
	13434	5	8.98E+06	0.0071	-1.37	0.036		
	14634	3	4.92E+06	0.0063	-1.60	0.0198		
	18991	3	7.30E+05	0.0012	-2.31	0.003		

	23450	5	7.54E+05	0.0012	-2.16	0.003		
50431	0	1	6.57E+07	0.0774	-0.81	0.51	-1.29 [c]	0.143 [c]
	1519	3	1.97E+06	0.0012	-2.30	0.015	…	…
	3172	5	5.94E+06	0.0027	-1.80	0.046	-1.58 [c]	0.0641 [c]
	7420	5	4.14E+06	0.0022	-1.87	0.032	-1.84[c]	0.0294[c]
	8711	3	9.40E+06	0.0081	-1.49	0.073	-1.42 [c]	0.0588 [c]
	8833	1	5.44E+06	0.0094	-1.72	0.042	-1.93 [c]	0.0226 [c]
	11301	5	4.32E+06	0.0028	-1.77	0.034	-1.23 [c]	0.0986 [c]
	13173	1	2.17E+07	0.0468	-1.03	0.168	-0.69 [c]	0.313 [c]
	14968	5	2.18E+06	0.0017	-1.98	0.017	-1.5 [c]	0.0439 [c]
	16235	5	2.42E+06	0.0021	-1.91	0.019	-1.57 [c]	0.035 [c]
	19404	1	4.83E+05	0.0015	-2.52	0.004	…	…
	19637	5	1.06E+06	0.0011	-2.17	0.008	-1.95 [c]	0.0117 [c]
	23450	5	…	…	…	…	-1.89 [c]	0.0103 [c]
	25045	1	5.49E+05	0.0026	-2.29	0.004	-1.87 [c]	0.0096[c]
51254	0	1	3.14E+08	0.3583	-0.14	0.5701	-0.6 [c]	0.233 [c]
	1519	3	4.42E+07	0.0268	-0.97	0.0803	-0.93 [c]	0.101 [c]
	3172	5	1.47E+08	0.0636	-0.42	0.267	-0.5 [c]	0.1586 [c]
	7420	5	1.25E+07	0.0065	-1.41	0.023	-0.87 [c]	0.0903 [c]
	8711	3	4.05E+06	0.0034	-1.87	0.007	-0.63 [c]	0.15 [c]
	10592	3	1.66E+06	0.0015	-2.22	0.003	…	…
	11301	5	1.90E+06	0.0012	-2.15	0.003	-1.25 [c]	0.0318 [c]
	13434	5	1.19E+07	0.0083	-1.30	0.022	-0.77 [c]	0.0841 [c]
	14634	3	4.72E+06	0.0053	-1.68	0.009	-0.98 [c]	0.0493 [c]
	18991	3	2.07E+06	0.0030	-1.92	0.004	-0.94 [c]	0.0416 [c]
	19404	1	7.80E+05	0.0023	-2.34	0.001	…	…
	19637	5	1.75E+06	0.0018	-1.98	0.003	…	…
	22139	5	…	…	…	…	-1.38 [c]	0.0124 [c]
	22503	3	6.95E+05	0.0013	-2.30	0.001	-1.09 [c]	0.0232 [c]

([a]) NIST [1]

([O]) Results from literature, other work (b and c)

([b]) Quinet et al , 2010 [18]

([c]) Lennertsson et al, 2011 [16]

Table 4-11: RCI transition probability A_{ki} (s^{-1}), the absorption oscillator strength f_{ik}, and the branching fractions, BF of the lowest 10 energy levels of W II J=5/2 odd.

E_k	E_i	$2J_i$	A_{ki}	f_{ik}	log (g *f*)	BF	log(g*f*)[o]	BF[o]
39937	8711	3	1.32E+06	0.0030	-1.92	0.316	-1.68[b]	
	10592	3	7.20E+05	0.0019	-2.12	0.172	-2.12[b]	
	11301	5	4.21E+05	0.0015	-2.05	0.101		
	14634	3	4.21E+05	0.0015	-2.23	0.101		
42049	1519	3	2.47E+07	0.0338	-0.87	0.295	-0.78[b]	
	3172	5	4.09E+07	0.0405	-0.61	0.489	-0.49[b]	
	4716	7	4.82E+06	0.0039	-1.51	0.058		
	8711	3	2.16E+06	0.0044	-1.76	0.026		
	10592	3	9.46E+05	0.0022	-2.07	0.011		
	11301	5	9.24E+05	0.0015	-2.05	0.011		
	13411	7	1.16E+06	0.0016	-1.89	0.014		
	14634	3	1.84E+06	0.0055	-1.66	0.022		
	15147	7	2.15E+06	0.0033	-1.57	0.026		
	16235	5	6.35E+05	0.0014	-2.07	0.008		
	18001	7	5.93E+05	0.0012	-2.04	0.007		
	18991	3	4.36E+05	0.0018	-2.13	0.005		
	22140	5	2.71E+05	0.0010	-2.21	0.003		
	22503	7	1.78E+05	0.0011	-2.08	0.002		
	23047	7	4.05E+05	0.0013	-2.00	0.005		
	24992	3	2.33E+05	0.0018	-2.14	0.003		
44355	1519	3	1.34E+07	0.0164	-1.18	0.136		
	3172	5	2.78E+07	0.0246	-0.83	0.283	-0.76[b]	
	4716	7	2.71E+07	0.0194	-0.81	0.276		
	7420	5	2.83E+06	0.0031	-1.73	0.029	-0.76[b]	
	10592	3	3.88E+06	0.0077	-1.51	0.039		
	11301	5	9.95E+06	0.0136	-1.09	0.101		
	13434	5	8.01E+05	0.0013	-2.12	0.008		
	14634	3	1.25E+06	0.0032	-1.90	0.013		
	14968	5	5.07E+06	0.0088	-1.28	0.052		
	16235	5	2.94E+06	0.0056	-1.48	0.03		
46355	1519	3	5.27E+07	0.0590	-0.63	0.419	-0.14[b]	
	3172	5	3.46E+07	0.0278	-0.78	0.275	-0.66[b]	
	7420	5	5.43E+06	0.0054	-1.49	0.043		
	8711	3	3.63E+06	0.0058	-1.64	0.029		
	13434	5	5.72E+06	0.0079	-1.32	0.045		
	14634	3	2.52E+06	0.0056	-1.65	0.02		
	15147	7	5.46E+06	0.0063	-1.30	0.043		

	16590	7	8.20E+06	0.0104	-1.08	0.065		
	18991	3	1.28E+06	0.0039	-1.81	0.01		
	19276	5	1.17E+06	0.0024	-1.84	0.009		
	19637	5	8.22E+05	0.0017	-1.98	0.007		
	20456	3	4.98E+05	0.0017	-2.18	0.004		
	24992	3	1.07E+06	0.0053	-1.67	0.009		
47413	4716	7	2.44E+07	0.0150	-0.92	0.264	-0.51 [b]	
	7420	5	2.28E+07	0.0213	-0.89	0.246	-0.52 [b]	
	11301	5	1.23E+07	0.0141	-1.07	0.133		
	13434	5	8.27E+05	0.0011	-2.19	0.009		
	13411	7	4.98E+06	0.0049	-1.41	0.054		
	14634	3	8.26E+06	0.0173	-1.16	0.089		
	15147	7	2.24E+06	0.0024	-1.71	0.024		
	16235	5	1.92E+06	0.0030	-1.75	0.021		
	16590	7	4.03E+06	0.0048	-1.42	0.044		
	18001	7	1.97E+06	0.0026	-1.69	0.021		
	19276	5	6.44E+05	0.0012	-2.14	0.007		
	20456	3	3.70E+06	0.0114	-1.34	0.04		
	22140	5	7.02E+05	0.0017	-2.00	0.008		
	22194	7	5.86E+05	0.0010	-2.08	0.006		
48284	1519	3	9.24E+06	0.0095	-1.42	0.044	-1.33 [c]	0.0673[c]
	3172	5	5.30E+07	0.0391	-0.63	0.254	-0.75[c]	0.237[c]
	4716	7	5.08E+07	0.0301	-0.62	0.243	-0.89[c]	0.162[c]
	7420	5	7.54E+07	0.0677	-0.39	0.361	-0.54[c]	0.318[c]
							-0.84 [b]	
	8711	3	7.27E+05	0.0010	-2.38	0.003	-1.79[c]	0.0166[c]
	11301	5	2.02E+06	0.0022	-1.88	0.01	-1.69[c]	0.0183[c]
	13411	7	3.83E+06	0.0036	-1.55	0.018	-1.47[c]	0.0269[c]
	14634	3	1.22E+06	0.0024	-2.01	0.006	…	…
	14968	5	3.51E+06	0.0047	-1.55	0.017	-1.5[c]	0.0232[c]
	16235	5	1.24E+06	0.0018	-1.96	0.006	…	…
	16590	7	1.27E+06	0.0014	-1.94	0.006	…	…
	18991	3	1.14E+06	0.0030	-1.92	0.005	-1.19 [c]	0.0365[c]
	20456	3	1.70E+06	0.0049	-1.70	0.008	-1.57 [c]	0.0177 [c]
	23046	7	…	…		…	-2.04 [c]	0.0038 [c]
	23450	5	4.20E+05	0.0010	-2.21	0.002	…	…
	26227		7.65E+05	0.0024	-2.63	0.004	…	…
49242	1519	3	1.77E+08	0.1750	-0.15	0.666	-0.05 [b]	
	3172	5	1.65E+07	0.0116	-1.16	0.062		
	4716	7	3.67E+07	0.0208	-0.78	0.138		
	7420	5	3.19E+07	0.0274	-0.78	0.12	-0.42 [b]	
	18991	3	5.31E+05	0.0013	-2.28	0.002		

	24992	3	3.01E+05	0.0012	-2.34	0.001		
50292	1519	3	7.63E+07	0.0721	-0.54	0.503		
	3172	5	1.19E+07	0.0080	-1.32	0.078		
	4716	7	4.80E+06	0.0026	-1.68	0.032		
	7420	5	3.72E+06	0.0030	-1.74	0.025		
	10592	3	1.29E+07	0.0184	-1.13	0.085		
	11301	5	6.37E+06	0.0063	-1.42	0.042		
	13434	5	3.22E+06	0.0036	-1.67	0.021		
	14634	3	1.73E+06	0.0031	-1.91	0.011		
	14968	5	1.08E+07	0.0130	-1.11	0.071		
	16235	5	6.41E+06	0.0083	-1.30	0.042		
	16590	7	1.84E+06	0.0018	-1.84	0.012		
	18001	7	3.64E+06	0.0039	-1.50	0.024		
	18991	3	6.22E+05	0.0014	-2.24	0.004		
	20456	3	1.36E+06	0.0034	-1.86	0.009		
	22194	7	1.57E+06	0.0022	-1.75	0.01		
51438	1519	3	2.32E+07	0.0209	-1.08	0.116	…	…
	3172	5	7.05E+07	0.0453	-0.57	0.352	-0.55[c]	0.334[c]
	4716	7	…	…		..	-1.67[c]	0.0237[c]
	7420	5	3.68E+06	0.0029	-1.77	0.018	-1.45[c]	0.0354[c]
	8711	3	4.13E+06	0.0051	-1.69	0.021	-1.58[c]	0.0245[c]
	10592	3	8.70E+05	0.0012	-2.33	0.004	…	…
	11301	5	1.78E+07	0.0165	-1.00	0.089	-0.98[c]	0.0888[c]
	13434	5	5.22E+06	0.0054	-1.49	0.026	-1.49[c]	0.0242[c]
	13411	7	1.08E+07	0.0084	-1.17	0.054	-0.98[c]	0.078[c]
	14634	3	3.78E+07	0.0628	-0.60	0.189	-0.62[c]	0.168[c]
	16590	7	9.98E+06	0.0092	-1.13	0.05	-0.88[c]	0.0824[c]
	18001	7	1.88E+06	0.0019	-1.82	0.009	…	…
	18991	3	2.92E+06	0.0062	-1.60	0.015	-1.25[c]	0.03[c]
	20040	7	2.56E+06	0.0029	-1.63	0.013	-1.56[c]	0.0139[c]
	20456	3	1.82E+06	0.0043	-1.77	0.009	...	…
	22502	5	…	…	..	…	-1.69[c]	0.0088[c]
	23450	5	8.98E+05	0.0017	-1.99	0.004	-1.89[c]	0.0051[c]
	24804	7	…	…	...	…	-1.75[c]	0.0064[c]
	24992	3	3.82E+05	0.0012	-2.31	0.002	…	…
	25672	5	…	…	...	…	-2.11[c]	0.0027[c]
	27274	7	6.87E+05	0.0013	-1.98	0.003	-1.85[c]	0.0043[c]
	30224	3	2.22E+05	0.0011	-2.35	0.001	…	…
	32487	3	1.70E+05	0.0011	-2.37	0.001	…	…
	32950	7	2.01E+05	0.0013	-1.98	0.001	…	…
52087	1519	3	7.02E+07	0.0617	-0.61	0.318		
	3172	5	5.58E+07	0.0350	-0.68	0.253		

4716	7	5.44E+07	0.0273	-0.66	0.247
7420	5	1.43E+06	0.0011	-2.19	0.006
10592	3	1.16E+07	0.0151	-1.22	0.053
14634	3	6.75E+06	0.0108	-1.36	0.031
14968	5	1.62E+06	0.0018	-1.98	0.007
18001	7	4.09E+06	0.0040	-1.50	0.019
18991	3	3.04E+06	0.0063	-1.60	0.014
22140	5	1.17E+06	0.0020	-1.93	0.005
23047	7	2.97E+06	0.0040	-1.50	0.013
25170	3	1.96E+06	0.0061	-1.61	0.009
25672	5	4.91E+05	0.0011	-2.20	0.002
28632	7	6.44E+05	0.0013	-1.98	0.003

([a]) NIST [1]

([O]) Results from literature, other work (b and c)

([b]) Quinet et al , 2010 [18]

([c]) Lennertsson et al, 2011 [16]

Table 4-12: RCI transition probability A_{ki} (s^{-1}) , the absorption oscillator strength f_{ik}, and the branching fractions, BF of the lowest 10 energy levels of W II J=7/2 odd.

E_k	E_i	$2J_i$	A_{ki}	f_{ik}	Log (g*f*)	BF	log (g*f*)[O]	BF [O]
42390.0	3172	5	1.98E+06	0.0026	-1.81	0.154		
	4716	7	4.48E+06	0.0047	-1.42	0.351	-1.5[b]	
	11301	5	1.60E+06	0.0033	-1.70	0.125	-1.54[b]	
	13434	5	5.24E+05	0.0013	-2.12	0.041		
	13411	7	9.62E+05	0.0017	-1.86	0.075		
	14968	5	1.48E+06	0.0039	-1.63	0.116	-1.55[b]	
44877.0	3172	5	6.03E+07	0.0693	-0.38	0.382	-0.39[b]	
	4716	7	7.61E+07	0.0708	-0.25	0.482	-0.19[b]	
	6147	9	8.08E+06	0.0065	-1.19	0.051		
	13434	5	1.76E+06	0.0036	-1.67	0.011		
	13411	7	2.00E+06	0.0030	-1.62	0.013		
	14968	5	4.73E+06	0.0106	-1.20	0.030		
	16235	5	1.62E+06	0.0040	-1.63	0.010		
	16553	9	1.44E+06	0.0022	-1.67	0.009		
	19637	5	3.57E+05	0.0011	-2.17	0.002		
	23450	5	2.58E+05	0.0011	-2.17	0.002		
46175.0	6147	9	1.58E+07	0.0118	-0.93	0.320	-0.76[b]	
	7420	5	1.11E+07	0.0148	-1.05	0.226	-0.76[b]	
	11301	5	8.18E+05	0.0013	-2.09	0.017		
	13411	7	1.16E+07	0.0163	-0.88	0.236	-0.75[b]	
	14968	5	1.79E+06	0.0037	-1.66	0.036		
	16590	7	2.65E+06	0.0046	-1.44	0.054		
	20780	9	5.39E+05	0.0010	-2.00	0.011		
	22194	7	1.08E+06	0.0028	-1.65	0.022		
	25209	9	4.13E+05	0.0011	-1.95	0.008		
	26227	5	2.62E+05	0.0013	-2.10	0.005		
48831.0	3172	5	4.95E+07	0.0475	-0.55	0.363		
	4716	7	2.61E+06	0.0020	-1.79	0.019		
	6147	9	2.90E+07	0.0191	-0.72	0.213		
	7420	5	1.90E+07	0.0221	-0.88	0.139		
	11301	5	7.26E+05	0.0010	-2.21	0.005		
	13411	7	1.23E+07	0.0148	-0.93	0.091		
	14857	9	2.63E+06	0.0027	-1.56	0.019		
	14968	5	9.09E+06	0.0158	-1.02	0.067		
	16235	5	7.71E+05	0.0015	-2.06	0.006		
	16553	9	1.21E+06	0.0014	-1.86	0.009		
	16590	7	2.96E+06	0.0043	-1.47	0.022		

	19637	5	1.39E+06	0.0033	-1.71	0.010		
	22140	5	1.49E+06	0.0042	-1.60	0.011		
	23804	7	6.53E+05	0.0016	-1.90	0.005		
49125.0	3172	5	1.83E+06	0.0017	-1.98	0.007		
	4716	7	5.00E+07	0.0380	-0.52	0.182		
	6147	9	9.71E+07	0.0630	-0.20	0.353	-0.49 [b]	
	7420	5	1.08E+08	0.1240	-0.13	0.393	-0.59 [b]	
	13434	5	4.02E+06	0.0063	-1.42	0.015		
	13411	7	2.13E+06	0.0025	-1.70	0.008		
	15147	7	9.89E+05	0.0013	-1.99	0.004		
	16235	5	3.14E+06	0.0058	-1.46	0.011		
	16553	9	1.86E+06	0.0021	-1.68	0.007		
	20780	9	9.23E+05	0.0014	-1.86	0.003		
	22140	5	8.40E+05	0.0023	-1.86	0.003		
	22194	7	9.33E+05	0.0019	-1.81	0.003		
51045	3172	5	9.71E+07	0.0847	-0.29	0.607	-0.18 [c]	0.596 [c]
							-0.02 [b]	
	4716	7	3.69E+07	0.0258	-0.69	0.231	-0.66 [c]	0.183 [c]
	6147	9	4.86E+06	0.0029	-1.54	0.030	-0.83 [c]	0.118 [c]
	7420	5	…	…	…	…	-1.39 [c]	0.0302 [c]
	13411	7	8.83E+06	0.0094	-1.13	0.055	-1.38 [c]	0.0233 [c]
	14968	5	4.28E+06	0.0066	-1.40	0.027	-1.52 [c]	0.0153 [c]
	16235	5	7.79E+05	0.0013	-2.11	0.005	…	…
	16590	7	2.01E+06	0.0025	-1.69	0.013	…	…
	20780	9	…	…	…	…	-1.91 [c]	0.0045 [c]
	22194	7	9.92E+05	0.0018	-1.84	0.006	…	…
	23450	5	…	…	…	…	-2.05 [c]	0.0026 [c]
	26227	5	3.77E+05	0.0012	-2.14	0.002	…	…
51863.0	3172	5	1.37E+08	0.1150	-0.16	0.726		
	4716	7	3.49E+06	0.0024	-1.73	0.018		
	6147	9	1.03E+07	0.0059	-1.23	0.055		
	7420	5	6.73E+06	0.0068	-1.39	0.036		
	11301	5	4.65E+06	0.0056	-1.47	0.025		
	13411	7	9.08E+06	0.0092	-1.13	0.048		
	14968	5	9.27E+05	0.0014	-2.09	0.005		
	16235	5	2.18E+06	0.0034	-1.69	0.012		
	16590	7	4.63E+06	0.0056	-1.35	0.025		
	19071	9	2.20E+06	0.0025	-1.61	0.012		
	20780	9	9.57E+05	0.0012	-1.92	0.005		
	22194	7	8.76E+05	0.0015	-1.92	0.005		
	24804	7	5.26E+05	0.0011	-2.06	0.003		
	26227	5	1.70E+06	0.0052	-1.51	0.009		

52275.0	3172	5	1.34E+08	0.1110	-0.18	0.469
	4716	7	3.14E+06	0.0021	-1.78	0.011
	6147	9	6.41E+07	0.0362	-0.44	0.225
	7420	5	6.93E+06	0.0069	-1.38	0.024
	11301	5	3.32E+06	0.0040	-1.63	0.012
	13434	5	1.35E+07	0.0178	-0.97	0.047
	13411	7	4.95E+06	0.0049	-1.40	0.017
	14968	5	5.57E+06	0.0080	-1.32	0.020
	15147	7	4.00E+06	0.0044	-1.46	0.014
	16235	5	2.32E+07	0.0356	-0.67	0.081
	16553	9	1.10E+07	0.0103	-0.99	0.039
	19071	9	1.10E+06	0.0012	-1.92	0.004
	19637	5	1.93E+06	0.0036	-1.66	0.007
	20780	9	2.00E+06	0.0024	-1.62	0.007
	22140	5	2.24E+06	0.0049	-1.53	0.008
	23804	7	6.64E+05	0.0012	-2.01	0.002
	28632	7	4.99E+05	0.0013	-1.97	0.002
52902.0	6147	9	2.50E+06	0.0014	-1.86	0.021
	11301	5	1.06E+07	0.0123	-1.13	0.091
	13434	5	3.36E+06	0.0043	-1.59	0.029
	13411	7	2.48E+06	0.0024	-1.72	0.021
	14857	9	1.53E+07	0.0127	-0.90	0.130
	14968	5	1.83E+07	0.0254	-0.82	0.156
	15147	7	1.31E+07	0.0138	-0.96	0.112
	16235	5	1.52E+06	0.0023	-1.87	0.013
	16553	9	2.61E+06	0.0024	-1.63	0.022
	16590	7	9.99E+05	0.0011	-2.04	0.009
	18001	7	1.42E+06	0.0018	-1.85	0.012
	19071	9	9.58E+06	0.0100	-1.00	0.082
	19276	5	1.67E+07	0.0295	-0.75	0.143
	19637	5	4.42E+06	0.0080	-1.32	0.038
	22140	5	5.88E+05	0.0012	-2.13	0.005
	23047	7	1.56E+06	0.0026	-1.68	0.013
	23235	5	2.25E+06	0.0031	-1.73	0.019
	23450	5	1.22E+06	0.0028	-1.77	0.010
	25209	9	1.47E+06	0.0023	-1.64	0.013
	25672	5	9.59E+05	0.0026	-1.81	0.008
	26227	5	6.82E+05	0.0019	-1.94	0.006
	27274	7	1.65E+06	0.0038	-1.52	0.014
	30618	5	3.20E+05	0.0013	-2.11	0.003
	31447	7	3.41E+05	0.0011	-2.05	0.003
53338.0	11301	5	3.04E+06	0.0034	-1.69	0.039

	14968	5	8.16E+06	0.0111	-1.18	0.105		
	15147	7	5.09E+06	0.0052	-1.38	0.065		
	16235	5	1.96E+07	0.0284	-0.77	0.251		
	16553	9	6.00E+06	0.0053	-1.27	0.077		
	16590	7	6.58E+06	0.0073	-1.23	0.084		
	19071	9	1.92E+06	0.0020	-1.71	0.025		
	19276	5	4.52E+06	0.0078	-1.33	0.058		
	20040	7	1.67E+06	0.0023	-1.74	0.021		
	22140	5	4.00E+06	0.0082	-1.31	0.051		
	22194	7	6.55E+06	0.0101	-1.09	0.084		
	23235	9	7.99E+05	0.0011	-1.97	0.010		
	23450	5	7.32E+05	0.0016	-2.01	0.009		
	23804	7	4.37E+06	0.0075	-1.22	0.056		
	25209	9	7.24E+05	0.0011	-1.96	0.009		
	30618	5	4.05E+05	0.0016	-2.03	0.005		
54499	4716	7	2.94E+08	0.1780	0.03	0.561	-0.02 [c]	0.418 [c]
	6147	9	8.18E+07	0.0419	-0.38	0.156	-0.46 [c]	0.141 [c]
	13411	7	3.01E+06	0.0027	-1.67	0.006	-1.05 [c]	0.0267 [c]
	13434	5	..	…	…	…	-0.91 [c]	0.0361 [c]
	14857	9	3.13E+06	0.0024	-1.62	0.006	…	…
	14967	5	..	..	..	..	-0.78 [c]	0.0451 [c]
	15147	7	3.28E+06	0.0032	-1.60	0.006	…	…
	16553	9	6.17E+06	0.0051	-1.29	0.012	…	…
	18001	7	1.32E+06	0.0015	-1.93	0.003	-0.72 [c]	0.0481 [c]
	20040	7	1.34E+06	0.0017	-1.87	0.003	…	…
	20780	9	1.68E+06	0.0018	-1.75	0.003	…	…
	23047	7	8.11E+05	0.0012	-2.01	0.002	…	…
	23804	7	1.46E+06	0.0023	-1.73	0.003	…	…
	24 804	7	…	…	…	…	-0.32 [c]	0.0747 [c]
	28 118	5	…	…	…	…	-1.26 [c]	0.0066 [c]
	31 538	5	…	…	…	…	-1.26 [c]	0.0063 [c]

([a]) NIST [1]

([O]) Results from literature, other work (b and c)

([b]) Quinet et al , 2010 [18]

([c]) Lennertsson et al, 2011 [16]

Table 4-13: RCI transition probability A_{ki} (s^{-1}) , the absorption oscillator strength f_{ik}, and the branching fractions, BF of the lowest 10 energy levels of W II J=9/2 odd.

E_k	E_i	$2J_i$	A_{ki}	f_{ik}	log (g*f*)	BF	log (g*f*)^{o}	BF ^{o}
44758	4716	7	8.60E+06	0.0100	-1.10	0.211	-1.00[b]	
	6147	9	1.85E+07	0.0186	-0.73	0.453	-0.59 [b]	
	14857	9	3.24E+06	0.0054	-1.27	0.079		
	15147	7	4.28E+06	0.0092	-1.14	0.105		
	16590	7	2.80E+06	0.0066	-1.28	0.069		
	18001	7	2.08E+06	0.0055	-1.36	0.051	-1.08 [b]	
	23047	7	4.99E+05	0.0020	-1.80	0.012		
46493	4716	7	2.73E+07	0.0293	-0.63	0.312	-0.62 [b]	
	6147	9	3.85E+07	0.0354	-0.45	0.44	-0.45 [b]	
	13411	7	2.45E+06	0.0042	-1.47	0.028		
	14857	9	5.37E+06	0.0080	-1.09	0.061		
	15147	7	2.59E+06	0.0049	-1.40	0.03		
	16590	7	7.32E+06	0.0153	-0.91	0.084	-1.03 [b]	
	17437	11	1.22E+06	0.0018	-1.66	0.014		
	18001	7	1.19E+06	0.0028	-1.66	0.014		
49181	4716	7	3.81E+07	0.0361	-0.54	0.667	-0.73[c]	0.526 [c]
							-0.68 [b]	
	6147	9	1.52E+07	0.0123	-0.91	0.265	-0.93 [c]	0.311[c]
	14857	9	1.51E+06	0.0019	-1.72	0.026	…	…
	16553	9	8.62E+05	0.0012	-1.92	0.015	-1.44 [c]	0.056 [c]
	16589	7	…	…	…	…	-1.75 [c]	0.027 [c]
50863	4716	7	8.48E+07	0.0746	-0.22	0.582	-0.08 [b]	
	6147	9	9.80E+06	0.0073	-1.13	0.067		
	13411	7	8.72E+06	0.0117	-1.03	0.06		
	14857	9	1.96E+07	0.0227	-0.64	0.135		
	15147	7	1.17E+07	0.0173	-0.86	0.081		
	16553	9	1.62E+06	0.0021	-1.69	0.011		
	20040	7	2.55E+06	0.0050	-1.40	0.018		
	22194	7	1.24E+06	0.0028	-1.65	0.009		
	23235	9	1.50E+06	0.0030	-1.53	0.01		
	23804	7	4.83E+05	0.0012	-2.00	0.003		
	25209	9	1.54E+06	0.0035	-1.45	0.011		
	28632	7	4.84E+05	0.0018	-1.83	0.003		
	30633	9	2.85E+05	0.0010	-1.98	0.002		
52567	4716	7	4.48E+07	0.0367	-0.53	0.308		
	6147	9	6.49E+07	0.0451	-0.35	0.445	-0.48 [b]	
	13411	7	4.62E+06	0.0057	-1.34	0.032		
	14857	9	1.93E+06	0.0020	-1.69	0.013		
	15147	7	3.04E+06	0.0041	-1.49	0.021		
	16553	9	2.47E+06	0.0029	-1.54	0.017		

	16590	7	1.60E+07	0.0232	-0.73	0.11		
	17437	11	1.68E+06	0.0017	-1.69	0.012		
	20040	7	7.99E+05	0.0014	-1.94	0.005		
	22194	7	7.45E+05	0.0015	-1.92	0.005		
	23047	7	1.49E+06	0.0032	-1.59	0.01		
	23235	9	6.59E+05	0.0012	-1.94	0.005		
	24804	7	5.12E+05	0.0012	-2.00	0.004		
	26159	9	7.28E+05	0.0016	-1.80	0.005		
53370	4716	7	3.35E+08	0.2610	0.32	0.866		
	6147	9	4.59E+06	0.0030	-1.52	0.012		
	15147	7	8.77E+05	0.0011	-2.06	0.002		
	16553	9	9.48E+06	0.0103	-0.99	0.024		
	16590	7	2.51E+07	0.0340	-0.57	0.065	-0.23[b]	
	17437	11	4.44E+06	0.0042	-1.30	0.011		
	20040	7	1.67E+06	0.0027	-1.66	0.004		
	20534	11	1.54E+06	0.0017	-1.68	0.004		
	20780	9	1.17E+06	0.0016	-1.79	0.003		
	22194	7	8.89E+05	0.0017	-1.87	0.002		
54056	6147	9	1.98E+07	0.0130	-0.89	0.144		
	13411	7	8.89E+06	0.0101	-1.09	0.064		
	14857	9	5.81E+06	0.0057	-1.25	0.042		
	15147	7	4.75E+07	0.0588	-0.33	0.345		
	16553	9	1.70E+07	0.0181	-0.74	0.123		
	16590	7	1.67E+07	0.0223	-0.75	0.121		
	17437	11	5.30E+06	0.0050	-1.23	0.038		
	19071	9	2.59E+06	0.0032	-1.50	0.019		
	20534	11	9.97E+05	0.0011	-1.88	0.007		
	20780	9	6.34E+06	0.0086	-1.07	0.046		
	24804	7	1.52E+06	0.0033	-1.58	0.011		
	26159	9	5.27E+05	0.0010	-1.99	0.004		
	27274	7	4.63E+05	0.0012	-2.01	0.003		
	30633	9	7.45E+05	0.0020	-1.69	0.005		
55392	4716	7	8.18E+07	0.0597	-0.32	0.151	-0.68[c]	0.088[c]
	6147	9	4.07E+08	0.2520	0.40	0.752	0.13[c]	0.507[c]
	13411	7	..	..	..	..	-0.98[c]	0.029[c]
	14857	9	1.15E+06	0.0011	-1.98	0.002	..	..
	15147	7	1.31E+06	0.0015	-1.92	0.002	-0.75[c]	0.044[c]
	16553	9	6.83E+06	0.0068	-1.17	0.013	-1.40[c]	0.009[c]
	16590	7	7.79E+06	0.0097	-1.11	0.014	-0.54[c]	0.067[c]
	17437	11	3.79E+06	0.0033	-1.40	0.007	-0.95[c]	0.025[c]
	18001	7	1.02E+07	0.0136	-0.96	0.019	-0.32[c]	0.010[c]
	19071	9	1.36E+06	0.0016	-1.81	0.003	..	..
	20534	11	1.42E+06	0.0015	-1.76	0.003	-1.03[c]	0.018[c]
	22194	7	6.58E+05	0.0011	-2.05	0.001	..	..
	23047	7	3.23E+06	0.0058	-1.33	0.006	..	..
	23235	9	4.82E+06	0.0070	-1.16	0.009	-0.79[c]	0.026[c]

	23804	7	3.43E+06	0.0064	-1.29	0.006	-1.12 [c]	0.012[c]
	23955	11	2.30E+06	0.0029	-1.46	0.004	-0.75 [c]	0.027[c]
	24804	7	…	…	…	…	-0.97 [c]	0.015[c]
	25209	9	7.02E+05	0.0012	-1.94	0.001	…	…
	26159	9	6.00E+05	0.0011	-1.98	0.001	-1.34 [c]	0.006[c]
	28632	7	4.58E+05	0.0012	-2.02	0.001	…	…
	30632	11	…	…	…	…	-1.26 [c]	0.005[c]
56414	4716	7	3.15E+07	0.0221	-0.75	0.139		
	6147	9	1.04E+08	0.0617	-0.21	0.459		
	13411	7	8.76E+06	0.0089	-1.15	0.039		
	14857	9	8.89E+06	0.0077	-1.11	0.039		
	15147	7	1.30E+07	0.0143	-0.94	0.057		
	16553	9	9.79E+06	0.0092	-1.03	0.043		
	16590	7	8.97E+06	0.0106	-1.07	0.04		
	18001	7	1.67E+07	0.0212	-0.77	0.074		
	23047	7	1.28E+07	0.0215	-0.76	0.056		
	23235	9	2.97E+06	0.0041	-1.39	0.013		
	23955	11	1.08E+06	0.0013	-1.81	0.005		
57089	6147	9	1.20E+07	0.0070	-1.16	0.069		
	13411	7	1.59E+07	0.0157	-0.90	0.092		
	15147	7	2.94E+07	0.0313	-0.60	0.169		
	18001	7	6.04E+07	0.0740	-0.23	0.348		
	20534	11	6.89E+06	0.0064	-1.11	0.04		
	20780	9	9.67E+06	0.0110	-0.96	0.056		
	23047	7	1.02E+07	0.0164	-0.88	0.059		
	23955	11	6.55E+06	0.0075	-1.05	0.038		

([a]) NIST [1]

([O]) Results from literature, other work (b and c)

([b]) Quinet et al , 2010 [18]

([c]) Lennertsson et al, 2011 [16]

Table 4-14: RCI transition probability A_{ki} (s^{-1}), the absorption oscillator strength f_{ik}, and the branching fractions, BF of the lowest 10 energy levels of W II J=11/2 odd.

E_k	E_i	$2J_i$	A_{ki}	f_{ik}	log(gf)	BF	log(gf) [o]
48332.8	6147	9	2.53E+06	0.0026	-1.59	0.224	
	14857	9	1.79E+06	0.0029	-1.54	0.158	
	16553	9	3.50E+06	0.0062	-1.20	0.309	-1.12[b]
	20780	9	1.49E+06	0.0035	-1.45	0.132	
	25209	9	6.69E+05	0.0023	-1.65	0.059	
	26159	9	2.86E+05	0.0011	-1.98	0.025	
51495.1	6147	9	1.60E+08	0.1400	0.15	0.985	0.17[b]
54229.1	6147	9	1.74E+08	0.1350	0.13	0.669	0.50[b]
	14857	9	2.84E+06	0.0033	-1.48	0.011	
	16553	9	3.43E+07	0.0435	-0.36	0.132	
	17437	11	3.43E+07	0.0380	-0.34	0.132	
	19071	9	1.61E+06	0.0023	-1.63	0.006	
	19442	13	3.23E+06	0.0034	-1.32	0.012	
	20534	11	1.40E+06	0.0019	-1.65	0.005	
	23235	9	5.79E+06	0.0108	-0.97	0.022	
	25209	9	5.88E+05	0.0013	-1.90	0.002	
	26159	9	1.15E+06	0.0026	-1.58	0.004	
54958.6	6147	9	2.26E+08	0.1710	0.23	0.734	
	14857	9	1.05E+07	0.0118	-0.93	0.034	
	16553	9	2.63E+07	0.0320	-0.49	0.085	-0.13[b]
	17437	11	2.67E+07	0.0285	-0.47	0.087	-0.09[b]
	19071	9	2.58E+06	0.0036	-1.44	0.008	
	19442	13	9.91E+05	0.0010	-1.85	0.003	
	20534	11	4.83E+06	0.0061	-1.13	0.016	
	20780	9	4.44E+06	0.0068	-1.17	0.014	
	23235	9	4.07E+06	0.0073	-1.14	0.013	
	23955	11	7.21E+05	0.0011	-1.87	0.002	
	29341	9	4.32E+05	0.0012	-1.93	0.001	
56376.6	6147	9	4.05E+07	0.0289	-0.54	0.43	
	14857	9	9.81E+06	0.0102	-0.99	0.104	
	16553	9	2.00E+06	0.0023	-1.64	0.021	
	19071	9	5.49E+06	0.0071	-1.15	0.058	
	19442	13	7.40E+06	0.0070	-1.01	0.079	
	20534	11	1.10E+07	0.0129	-0.81	0.117	
	20780	9	6.55E+06	0.0093	-1.03	0.07	
	23235	9	1.97E+06	0.0032	-1.49	0.021	
	23955	11	1.77E+06	0.0025	-1.52	0.019	

	25209	9	2.19E+06	0.0041	-1.39	0.023	
	26159	9	3.03E+06	0.0060	-1.22	0.032	
	29341	9	4.63E+05	0.0011	-1.94	0.005	
	33911	11	4.94E+05	0.0015	-1.75	0.005	
58891.7	6147	9	2.29E+07	0.0148	-0.83	0.086	
	14857	9	7.30E+07	0.0678	-0.17	0.274	-0.05[b]
	16553	9	1.67E+07	0.0167	-0.78	0.062	
	17437	11	2.56E+07	0.0223	-0.57	0.096	
	19071	9	5.92E+07	0.0671	-0.17	0.222	-0.12[b]
	19442	13	2.01E+07	0.0166	-0.63	0.075	
	20534	11	1.22E+07	0.0125	-0.82	0.046	
	20780	9	2.43E+07	0.0301	-0.52	0.091	
	26929	11	5.38E+06	0.0079	-1.02	0.02	
	29341	9	1.91E+06	0.0039	-1.41	0.007	
	30633	9	8.68E+05	0.0020	-1.71	0.003	
	33911	11	2.95E+06	0.0071	-1.07	0.011	
60219.1	14857	9	1.56E+07	0.0136	-0.87	0.135	
	17437	11	2.11E+06	0.0017	-1.68	0.018	
	19071	9	1.71E+07	0.0182	-0.74	0.149	
	19442	13	2.05E+06	0.0016	-1.65	0.018	
	20780	9	3.57E+07	0.0413	-0.38	0.31	-0.12[b]
	23235	9	2.16E+07	0.0284	-0.55	0.188	
	23955	11	1.89E+06	0.0022	-1.59	0.016	
	25209	9	4.65E+06	0.0068	-1.17	0.04	
	26159	9	2.08E+06	0.0032	-1.49	0.018	
	26929	11	1.43E+06	0.0019	-1.64	0.012	
	29341	9	5.09E+06	0.0096	-1.02	0.044	
	31100	11	1.50E+06	0.0027	-1.50	0.013	
61240.8	6147	9	8.78E+06	0.0052	-1.28	0.034	
	14857	9	1.52E+07	0.0127	-0.90	0.058	
	16553	9	4.08E+07	0.0368	-0.43	0.156	
	17437	11	6.40E+07	0.0500	-0.22	0.244	
	19071	9	4.55E+07	0.0460	-0.34	0.174	
	19442	13	5.40E+06	0.0040	-1.26	0.021	
	20534	11	9.40E+06	0.0085	-0.99	0.036	
	20780	9	3.04E+07	0.0334	-0.48	0.116	
	23235	9	2.66E+07	0.0332	-0.48	0.102	
	25209	9	5.93E+06	0.0082	-1.09	0.023	
	29341	9	2.82E+06	0.0050	-1.30	0.011	
61589.5	14857	9	1.79E+07	0.0148	-0.83	0.058	
	16553	9	8.12E+07	0.0720	-0.14	0.263	
	17437	11	3.45E+07	0.0265	-0.50	0.111	

	19442	13	2.67E+07	0.0193	-0.57	0.086	
	20534	11	5.85E+07	0.0521	-0.20	0.189	-0.15[b]
	20780	9	4.10E+06	0.0044	-1.35	0.013	
	23235	9	5.93E+07	0.0725	-0.14	0.192	
	23955	11	6.78E+06	0.0072	-1.06	0.022	
	31100	11	3.84E+06	0.0062	-1.13	0.012	
	33911	11	3.41E+06	0.0067	-1.10	0.011	
62966.5	14857	9	1.17E+08	0.0910	-0.04	0.447	
	16553	9	1.28E+07	0.0107	-0.97	0.049	
	17437	11	1.23E+07	0.0089	-0.97	0.047	
	19071	9	8.17E+06	0.0076	-1.12	0.031	
	20534	11	1.23E+07	0.0102	-0.91	0.047	
	20780	9	6.14E+06	0.0062	-1.21	0.023	
	25209	9	4.65E+07	0.0586	-0.23	0.177	
	26929	11	2.37E+07	0.0274	-0.48	0.091	
	33911	11	1.25E+07	0.0222	-0.57	0.048	

([a]) NIST [1]

([O]) Results from literature, other work (b and c)

([b]) Quinet et al , 2010 [18]

([c]) Lennertsson et al, 2011 [16]

4.4 References

1. NIST: http://physics.nist.gov/cgi-bin/ASD/energy1.pl
2. A. E. Karamida and T. Shiria, Compilation of wavelengths, energy levels, and transition probabilities for W I and W II, *J. Phys. Chem. Data*, **35** , 423 (2006)
3. J. O. Ekberg, R. Kling, and W. Mende, *Phys. Scr.* **61**, 146 (2000)
4. D. D. Laun and J. Res, *Nat. Bur. Stand. Sect. A* **68**, 207 (1964)
5. R. Kling, J. O. Ekberg, and M. Kock, J. *Quant. Sectrosc. Radiat. Transfer* **67**, 227 (2000)
6. R. Schnabel, M. Schulz-Johnning, and M. Kock, *Eur. Phys. J. D* **4**, 267 (1998)
7. H. Nilsson et al, *Eur. Phys. J. D* DOI: 10.1140/epjd/e2008-00131-2 (2008)
8. R. Schnabel, M. Schultz-Johanning, and M. Kock, Eur. Phys. J. D **4**, 267 (1998)
9. M. Kwiatkowski, F. Naumann, K. Werner, and P. Zimmermann, *Phys. Lett. A* **103**, 49 (1984)
10. M. Henderson, R.E. Irving, R. Matulioniene, L.J. Curtis, D.G. Ellis, G.M. Wahlgren, and T. Brage, *Astrophys. J.* **520**, 805 (1999)
11. M. Shultz-Johanning, R. Schnabel and M. Kock, *Eur. Phys. J. D* **5**, 341 (1999)
12. A. Lenef, *IEEE Cong. Rec. –Abstr*. Int. Conf. Plasma Science **241** (1999)
13. C. H. Corliss, and W R Bozman, *Nat. Bur. Stand. (US)* **53** (1962)
14. H. U. Obbarius, and M Kock, *J. Phys. B* **15**, 527 (1982)
15. J. F. Wyart, and J. Blaise, *Physica Scripta* **42**, 209 (1990)
16. T. Lennartsson, H. Nilsson, R. Blackwell-Whitehead, L. Engstrom and S. Huldt, *J. Phys. B* **44** 245001 (2011)
17. L. J. Curtis, chapter-17 in "*handbook of atomic, molecular, and optical physics*." by Drake, W F Gordon, Springer Science & Business Media, (2006)
18. P. Quinet, V. Vinogradoff, P. Palmeri, and E. Biemont, *J. Phys. B*, **43**, 144003 (2010)
19. J. P. Desclaux, *Compt. Phys. Commun*, **9**, 31 (1975)

20. C. A. Nicolaides and D. R. Beck, *Chem. Phys. Lett*. , **36**, 79 (1975)
21. D. R. Beck F-value code, unpublished
22. M. H. Abdalmoneam and D. R. Beck, *J. Phy. B* 48, 105001 (2015)
23. D. R. Beck and Z. Cai, *Phys. Rev. A* **41**, 301 (1990)

5 Summary and Future Work

In this study the relativistic configuration interaction (RCI) has been used to produce atomic data for three positive ions, Ni II, V II, and W II. The RCI is an Ab initio computational methodology and it had been modified a little by shifting the diagonal matrix elements. This shift was done in two ways. The simple way was to compare the RCI energy values of the excited atomic levels to the experimental ones and to use the difference to produce the value of the shift. This is a semi empirical method that had been used in previous RCI studies. The other method for producing the values of the shift was to isolate specific electronic configurations and do study them with pure ab initio RCI calculations, then using these results to produce the values for the shift. The configurations that has been isolated and studied separately were those that have big matrix size, quite large energy effect, and almost negligible effect on other atomic properties (e.g. electric and magnetic moments). Although the separate runs took long time, this method of shift is very systematic and has improved the RCI results. Another improvement in the computational method was the interpolations of the bound and continuum states calculations to include all ranges on energy starting from the ground state to infinity. This was implemented in the Ni II study.

We calculated atomic electric moments of Ni II, Hyperfine structure constants of V II, and lifetime and oscillator strength of W II.

Improving the W II oscillator strength and branching fractions is a good next step. It will support the validity of the lifetimes that appear in this study. Also, it will reduce the unsatisfactory disagreement between the calculated and experimental oscillator strength and branching fractions. Another future project will be studying the hyperfine structure of other transition atoms and or ions using the same methodology that has been used in studying V II. The computational methods that have been used to calculate the electric moments on Ni II were very detailed and valuable and they were done for the first time. They can be applied to more complicated ions, for example Th II, but this will require cooperation with some experimental group. In case it happens, it will be great addition to the scientific literature.

6 Appendix

6.1 Cowan's Method and Code

Cowan's semi-empirical methodology is used by both experimenters and computationalists who wish to "quickly" obtain properties of "all" the observed [1] energy levels with known configurational labeling. A description of the method is given in Cowan's book [2], accompanying the source code [3], and an article by Quinet et al extending the treatment to a rare earth ion, Tm II [4].

6.1.1 The steps in the process are essentially these:

(1) Use observation to choose the configurations used to create the radial functions. The Hamiltonian used for them is a non-relativistic one, which may include the mass-variation with velocity and Darwin terms from the low-Z Pauli approximation. The radial equation is of the Hartree-Fock Slater type, i.e. the exchange effects are averaged and become part of the potential [5]. Effectively, one is obtaining radials which optimize the average energy [6]. With the configuration's radials established, the two particle electrostatic F^k and G^k integral values and some approximation for the spin-orbit effects are computed. Two particle effects [7] may be incorporated in the spin-orbit constant following Blume and Watson [8]. Using the non-relativistic operators, and the one particle low Z Pauli operators for the Hamiltonian, matrix elements between all levels belonging to the configuration, with fixed J and parity are set up. For example, the electrostatic portion of the energy arising $1s^2$ 2s 2p is E_{avg}-G^1 (2s, 2p)/6 for the ^3P and E_{avg} + G^1 (2s, 2p)/2 for the ^1P. The spin-orbit contribution for J=1 would be [9]

$$\langle\, {}^3P_1 | f(s_0) |\, {}^3P_1 \rangle = -A(r); \qquad \langle\, {}^1P_1 | f(s_0) |\, {}^1P_1 \rangle = 0 \qquad (A.1)$$

$$\langle\, {}^3P_1 | f(s_0) |\, {}^1P_1 \rangle = \sqrt{2}\, A(r), \qquad A(r) \cong \frac{1}{r}\frac{dV(r)}{dr} \qquad (A.2)$$

In equation (A.1) having this matrix element equal to zero mean that the diagonal matrix element has zero spin orbit effect.

, V(r) being the potential. Energy contributions from the closed sub-shells are included in E_{avg}, which has a known, simple structure [6] .Cowan in Appendix F [2] uses Racah algebra to produce the atomic structure. RCI [10] does so by dealing with determinantal pairs.

(2) Once the radial functions for all the configurations have been obtained, and the intra-configurational matrix elements have set up, one lets levels belonging to different configurations interact. These off-diagonal matrix elements will involve a more general electrostatic radial integral known as a R^K integral. Any non-orthogonality effects are assumed negligible. For example, the interaction between $1s^2$ 2s 2p and $1s^2$ 3d 4f would require R^2 (2s, 2p; 3d, 4f) and R^3(2s,2p;4f,3d), N.B. $F^k(x, y) = R^k(x, y; x, y)$ and $G^k(x, y) = R^k(x, y; y, x)$

(3) The full matrix is diagonalized, and its energy levels are compared with observation. One does not expect a good match, because (i) many relativistic effects are missing (ii) exchange is included only approximately and (iii) almost all correlation effects are missing. We now come to the "heart of the method"- all the energy parameters E_{avg}, F^k, G^k, R^k and spin-orbit constants are varied in a least-squares iterative manner to get the best fit to the observed energy levels possible. While there are many parameters-possibly 50 or more for each J, parity, based on previous work some trends seem well established. For example, rescaling the F^k, G^k, and R^k integrals using a 0.85 factor normally works well in the majority of cases. See discussion by Cowan [2] on pages 464-7 and beyond. A list of rescaling factors is commonly included in papers using the Cowan method [e.g.4].

(4) Assessment. The energy fit to experiment can be quite good- as close as 100 cm^{-1} on average for a hundred levels. The main outputs are the wavefunctions for each level which are used to evaluate like oscillator strengths (see chapter-4, W II) and hyperfine structure (see chapter-3, V II). These results seem to be useful at least in a semi-quantitative manner. The real weakness of the procedure, in addition to requiring a lot of data, is that it lacks formal justification. A priori prediction of whether it will be successful in any particular new case depends solely on prior results on similar systems and the user's skills.

(5) Possible future justification of the method. Our work with shifts used to correct diagonal matrix elements for missing correlation effects can be used to partially justify some of the scaling appearing in the Cowan method. However, we have not yet been able to formally justify (or identify) the source of scaling in the off-diagonal matrix elements. On p.464 Cowan remarks that p (ns) is perturbed by p (ms) (m > n) in such a way as to narrow the gap between ^1P,^3P for p (ns).This may be helpful in reducing the spacing between the $3d^4$ and $3d^3$ 4s ^3G_J levels in V II (by adding more virtual s (= *v*s) via $3d^3$ *v*s ^3G_J (see section 5, V II), "*v*" is for a virtual sub-shell.

References

1. Physics.nist.gov/PhysRevData/ASD/levels_form.html
2. R. D. Cowan, "*The Theory of Atomic Structure and Spectra"*, Univ.Ca. Press (1981), Chapters 8 and 16
3. https://www.tcd.ie/Physics/people/Cormac.McGuinness/Cowan/Cowan source code with instructions for the user
4. P. Quinet, P. Palmeri and E. Biemont, J. Quant. *Spect. Rad. Trans*. **62**, 625(1999)
5. F. Herman and S. Skillman, "*Atomic Structure Calculations*", Prentice -Hall (1963)
6. Slater, "*Quantum Theory of Atomic Structure*", Volume II, Mc Graw Hill,(1960)
7. H. A. Bethe and E. E. Salpeter," *Quantum Mechanics of One- and Two-Electron Atoms*", Academic Press, P 181, (1957)
8. M. Blume, A. J. Freeman and R. E. Watson, *Phys. Rev*. *A* **134**, 320 (1964)
9. E. U. Condon and G. H. Shortley, "*The Theory of Atomic Spectra"*, Cambridge. p.268 and p.159, (1963)
10. D. R. Beck, RCI code (unpublished)

6.2 Relativistic Hyperfine Structure Formula used in RCI code [1]

6.2.1 Introduction

The hyperfine structure (HFS) operators are taken from the work of Lindgren and Rosen [2]. For N electrons, the HFS Hamiltonian can be written as

$$H_{HFS} = \sum_{K} T^{a} \,.\, M^{a}$$

$$,T^{a} = \sum_{i} t^{a}(i), \quad and \quad M^{a} = \sum_{i=1}^{N} m^{a}(i) \qquad (B.1)$$

"a" designates a tensor of rank "a" . Odd values of "a" are magnetic terms, e.g. a =1 is a magnetic dipole and even values of "a" are electrostatic terms, e.g. a = 2 for the electric quadrupole. "T" designates the electronic part of the operator and "M" designates the nuclear part. Only the electronic part is evaluated in Atomic Computations.

6.2.2 Coupling Scheme

In the RCI computations which are developed by Beck and used throughout his research group the coupling scheme is chosen as follows; the neutron and proton nuclear spins are coupled together to form the total angular momentum "$\vec{I}$" , and the spins of the electrons are coupled together to form the total electronic angular momentum "$\vec{J}$ ". $\vec{I}$ *and* $\vec{J}$ are then coupled to form the total angular momentum of the system, "$\vec{F}$" .

The electron-nuclear states are labeled $|\, I\ J\ F\ M_F\rangle$ and their matrix elements can be written as;

$$\left\langle IJFM_F \middle| H^{a}_{HFS} \middle| \grave{I}\grave{J}\grave{F}\grave{M}_F \right\rangle = (-1)^{2J-F\grave{-}I+J}\ \delta_{F\grave{F}}\ \delta_{M_F \grave{M}_F} * \langle I \| M^{a} \| \grave{I} \rangle \langle J \| T^{a} \| \grave{J} \rangle \begin{Bmatrix} I & J & F \\ \grave{J} & \grave{I} & a \end{Bmatrix} \qquad (B.2)$$

Where { } is a Wigner 6j symbol [3]. $\langle \ \| \ \ \| \ \grave{} \ \rangle$ is a reduced matrix element which appears when the Wigner-Eckart theorem [3] is used to remove the dependence on the azimuthal quantum numbers. For example, the nuclear reduced matrix element is given by

$$\langle I\ I | M^{a}_{O} | I\ I \rangle = \begin{pmatrix} I & a & I \\ -I & 0 & I \end{pmatrix} \langle I \| M^{a} \| I \rangle \qquad (B.3)$$

Where the stretched matrix element (i.e. the one with the highest possible value of the azimuthal quantum number) appearing on the left hand side is usually available [4] from experiment, and the ( ) is a Wigner 3j symbol [3]. a=1 is for the magnetic dipole operator and a=2 for the electric quadrupole operator. These are the two largest operators (unless they equal to zero) and they are the only ones used in this work (beside the electric dipole operator). Here only the diagonal case is of interest, that's $\grave{I} = I \; and \; \grave{j} = J$.

6.2.3 Results for Magnetic Dipole

The magnetic dipole operator is frequently written as $A(\vec{I}\,.\,\vec{J})$ for the diagonal matrix elemnt, and expectation value of this operator is

$$\langle A\,(\vec{I}\,.\,\vec{J}\,)\rangle \;=\; \frac{A}{2}\,[\,F(F+1) - \,I(I+1) - \,J(J+1)] \qquad (B.4)$$

Experimentally "A" is given in units of MHz, A is a scalar and its matrix element carries all required information other than spin so it ends up a simple number. From equations B.2 and B.3and expanding the 6j symbol [3], "A" can be written as

$$A = \; - \frac{\mu_I}{I\,J}\,\langle J\,J|\grave{T}_O|J\,J\rangle \qquad (B.5)$$

Where μ_I is the expectation value of M_O^1 in the stretched state, i.e. the nucleus magnetic dipole moment in nuclear magneton units [4].

6.2.4 Results for Nuclear Quadrupole

The nuclear Quadrupole contribution to the diagonal HFS energy (by using eq. B.2) can be written as;

$$B\;K_q \;=\; - \frac{3\;Q\;K_q}{4\,J(2J-1)I\;(2I-1)}\,\langle J\,J|\,\textstyle\sum_K r_K^{-3}\;\;C_O^2\,(K)|J\,J\rangle \qquad (B.6)$$

Where the quadrupole moment is defined to be:

$$\frac{eQ}{2} \;\equiv\; \langle I\;I|M_O^2|I\;I\rangle \qquad (B.7)$$

$$C_O^K = \sqrt{\frac{4\pi}{2K+1}}\;\;Y_{KO} \qquad (B.8)$$

$$K_q = \frac{1}{6}(-1)^{I+J+F}\begin{Bmatrix} J & I & F \\ I & J & 2 \end{Bmatrix} * \sqrt{2I(2I-1)(2I+2)(2I+1)(2I+3)} * \sqrt{2J(2J+1)(2J+2)(2J+3)(2J-1)} \tag{B.9}$$

And

$$K_q = K(K+1) \quad , \quad K = F(F+1) - I(I+1) - J(J+1) \tag{B.10}$$

, the equivalence is only strictly valid if the part independent of "F" is dropped.

6.2.5 Matrix Elements for one electron HFS operator

$$H_{HFS} = ec\,\vec{\alpha}\,.\vec{A}_N - e\,\varphi_N = \sum_{a>0} t^a\,.m^a \tag{B.11}$$

$$\vec{A}_N = -\frac{i\,\mu_O}{4\pi}\sum_a r^{-a-1}\left(\vec{l}\,C^a\right).m^a \tag{B.12}$$

The electronic part can be reduced to:

$$t^a = -2i\;\frac{\mu_O}{4\pi}\,\frac{\mu_B}{a_0}\sqrt{\frac{a+1}{a}}\;r^{-a-1}\;\{\vec{\alpha}\,C^a\}^a \tag{B.13}$$

, $ec = 2\,\mu_B/\alpha a_o$, a_o is Bohr radius.

6.2.5.1 Magnetic Dipole

The final "standard" result for the magnetic dipole is then:

$$\langle n\,\kappa\,m_j|t_Q^1|\grave{n}\;\grave{\kappa}\;\grave{m}_j\rangle = \frac{2\,\mu_o}{4\pi}\,\frac{\mu_B}{\alpha\,a_o}(-1)^{m_j+\frac{1}{2}}\sqrt{(2j+1)(2\grave{j}+1)}\;(\kappa+\grave{\kappa}) * \begin{pmatrix} j & j' & 1 \\ \frac{-1}{2} & \frac{1}{2} & 0 \end{pmatrix}\begin{pmatrix} j & j' & 1 \\ -m_j & m_j' & Q \end{pmatrix}\int_0^\infty dr\,r^{-2}\,[P_{n\kappa}\,Q_{n'\kappa'} + Q_{n\kappa}\,P_{n'\kappa'}] \tag{B.14}$$

"κ" is Kappa that gives the angular momentum, $\kappa = \left|J \pm \frac{1}{2}\right|, \kappa \neq 0$.

6.2.5.2 Electric Quadrupole Hyperfine Operators

$$t^a = \frac{-e}{4\pi\epsilon_0}\, r^{-a-1}\, C^a(\theta,\varphi) \qquad (B.15)$$

The final result is given by

$$\langle n\,\kappa\, m_j | t_Q^a | n'\,\kappa'\, m_j' \rangle$$
$$= (-1)^{(a-m_j+\frac{1}{2}-j-j')} \sqrt{(2j+1)(2j'+1)} \begin{pmatrix} j & j' & a \\ \frac{1}{2} & \frac{-1}{2} & 0 \end{pmatrix} \begin{pmatrix} j & j' & a \\ -m_j & m_j' & Q \end{pmatrix} *$$
$$\left(\frac{-e}{4\pi\,\epsilon_0}\right) \int_0^\infty dr\, r^{-a-1} \left[P_{n\kappa}\, P_{n'\kappa'} + Q_{n\kappa}\, Q_{n'\kappa'}\right] \qquad (B.16)$$

P, and Q are the major and minor radial components, $\kappa = \pm \left| j + \frac{1}{2} \right|$

6.2.5.3 Contributions from the Closed Shells

Core contributions to the HFS involve the sum

$$\sum_{m_j=-j}^{+j} (-1)^{-m_j} \begin{pmatrix} j & j & a \\ -m_j & m_j & 0 \end{pmatrix} \quad a > 0 \qquad (B.17)$$

, which equals to zero.

6.2.6 Units

HFS units can be confusing. Calculations are done in atomic units. Experimental constants "A" and "B" and given in MHz and nuclear moments are given in nuclear magnetons, $\mu_N \equiv \frac{e\,\hbar}{2M}$ [4], "Q" is given in barns.

References

1. D. R. Beck, RCI code, unpublished
2. I. Lindgren and A. Rosen, "*Case Studies in Atomic Physics*", Volume 4, M. R. C. Mc Dowell and Mc Daniel, eds, North Holland (1974), especially pps. 161-2 and 168-9
3. A. R. Edmonds," *Angular Momentum in Quantum Mechanics*", Princeton (1957)
4. G. H. Fuller and V. W. Cohen*, Nucl. Data Tables A* **5**, 433 (1969)
5. D. R. Beck, "*Atomic Relativistic Many Body Theory*", Book Draft for Springer Verlag, unpublished

6.3 Shift

Shift of the diagonal matrix element refers to adding (or subtracting) an exact amount of energy to a specific vector(s) during the process of calculating the total wavefunction by the RCI program. In this study shift has been used to replace some double (and higher order) excitations (i.e. all the single excitations were directly represented in the energy matrix and thus in the total wavefunction). Determining the energy for the shift and the usefulness of the shift is discussed below, see [1-2] for more details.

In order to appreciate the usefulness of the shift we can consider a case with two reference configurations ψ_1 and ψ_2. Using the second order perturbation for these two functions the energy lowering is

$dE(2) = H^2(1,2) / [H(1,1) - H(2,2)]$

In the case of no correlation H(1,1) and H(2,2) can be energetically close, so the denominator is small and dE(2) is large. If only H(1,1) is correlated and H(2,2) is not then the magnitude of the denominator can be considerably larger (e.g. ~ 0.5 – 1.0 eV), which will dramatically reduce dE(2). So the only way to get accurate dE(2) is to equivalently correlate the two reference functions.

In practical cases of more than one reference configurations the equivalent correlation of all references may be computationally expensive. For example; consider the case of V II with three reference configurations; $3d^4$, $3d^3$ 4s, and $3d^2$ $4s^2$. A double excitation like $3d^2$ to vf^2 contributes about 0.3 eV to the $3d^4$ reference. So it is an energetically important correlation and it should be equivalently added to the three references. This will result in these new configurations;

a. $3d^2$ vf^2 (a double excitation from the $3d^4$ reference)
b. 3d 4s vf^2 (a double excitation from $3d^3$ 4s reference)
c. $4s^2$ vf^2 (a double excitation from $3d^2$ $4s^2$ reference).

On the other hand if we look at the $3d^3$ 4s and a correlation to the $3d^4$ through the single excitation of 3d to 4s then a configuration (b) will be considered as a triple excitation from $3d^4$ ($3d^3$ to 4s vf^2). Similarly; $3d^2$ $4s^2$ can be considered as a double excitation from

the $3d^4$ and the configuration (c) will be a quartet excitation from $3d^4$. So the equivalent inclusion of vf^2 to the three references implies on in-equivalent correlation to the first reference, as it will include the single, double and triple excitations. To avoid this it is better to include vf^2 correlation through shifts.

Another case in which the method was so useful was the study of Ni II Rydberg states in order to compute different polarizabilities of Ni II [3]. For Rydberg configurations like $3d^8$ np (n = 4 -14) .The RCI Rydberg wavefunctions used for the RESIS matrix elements all involve transition probabilities. To make them accurate, the relative positioning of nearly degenerate Rydberg levels is important, as is the proper radial-angular behavior of the Rydberg electron. Most correlation for these levels is in the Ni III core, with a much lesser amount arising from the core-Rydberg electron interaction. This implies with the possibility to replace core correlation (e.g. $3d^2$ to vf^2, 3p 3d to *v*d *v*f, etc.) with a shift of the diagonal matrix elements for the reference function (e.g. for $3d^8$ ($^{2S+1}L_{J\text{-core}}$) $4p_j$ J_{total}=5/2).

To obtain the shifts associated with the core energy, we compare our single configuration energies $3d^8$ ($^{2S+1}L_{J\text{-core}}$) using our Ni II radial functions with the NIST [4] Ni III ($^{2S+1}L_J$) observed energy levels. The difference is used to shift our Ni II $3d^8$ ($^{2S+1}L_{J\text{-core}}$) np_j J_{total} diagonal energy matrix elements. This method is quite useful due to the simplicity of the Rydberg levels. For the energetically lower most Ni II levels, the shifts are adjusted (to a small extent) to match the observed [4] Ni II spectrum. This adjustment represents the effect of core-Rydberg correlation (which decreases at higher energies) on the position of energy levels.

Determining the required energy for shift is done through separate runs. Each run includes one reference and one correlation configuration. After obtaining the energy contribution due to a specific correlation to a specific reference only the relative energy effect is included in the wavefunction to represent the relative shift of one (or two) reference to another one. This method in determining the shift is used in cases of having more than one reference configurations. Another way to determining the energy of the shift is comparison with experimental data when available. In this case the energies of the excited levels are compared to the experimental values and the energy difference is added as a shift. This method is used when having only one reference configuration. This

energy difference (~ 10^{-3} eV) represents the contribution due to triple and quadrupole excitations. If the experimental energies are not available then this step is skipped.

The shift method has been developed basing on computational experience gained by Beck over four decades [5, 6]. The shifts that are obtained through matching experimental energies are useful for obtaining good oscillator strengths values. A huge advantage of using shift was the possibility of computing atomic properties that need accurate inclusion of so many correlations including the core excitations. The matrix size is limited to specific number of vectors; the more correlation is added the faster that space is used up. Even an $n10^6$ x $n10^6$ matrix will not be enough to include all possible excitations. So it is better to use the matrix space for the correlations that contribute to the different atomic properties and to replace the correlations that effect only on the total energy by shift, see chapter-3 for more details.

References

1. M. H. Abdalmoneam D. R. Beck, *J. Phys. B* **48**, 105001 (2015)
2. D. R. Beck, *J. Phys. B* **45**, 225002 (2012)
3. M. H. Abdalmoneam and D. R. Beck, *J. Phys. B* **47** 085003 (2014)
4. National Institute of Science and Technology, NIST, atomic data basis http://physics.nist.gov/PhysRefData/ASD/levels_form.html
5. D. R. Beck and C. A. Nicolaides, *Phys. Letts. A* **61**, 227 (1977)
6. D. R. Beck, and D. Detta, *Phys. Rev. A* **48**, 182 (1993)

6.4 Quantities and units in Atomic Physics

6.4.1 Electronic Configurations and Coupling Schemes:

The quantum numbers which denote the energy states for an atom are mainly those of the outer most electrons. Those quantum numbers are (n*, l, s, and J*) principle, orbital, spin and total angular momentum. All electrons in the outer most shells couple together and final L, S, and J are given to the whole configurations as $^{2s+1}L_J$.

L = 0, 1, 3, 4, 5, 6, 7…

Symbol S, P, D, F, G, H, I, K…..

6.4.1.1 Russell-Saunders (L-S) Coupling:

In several-electron configurations, especially simple spectra cases, the interactions between electrons is such that spins of individual electrons "s" combine together to form on single spin for the whole configuration "S". The same happens with orbital angular momentum, single "*l*" combine to give one "L". Then the total angular momentum "J" is the resultant of S and L. good for low to medium Z.

$S = \sum s$, $|l_1 - l_2| \leq L \leq |l_1 + l_2|$, $|L - S| \leq J \leq |L + S|$

6.4.1.2 (j, j) Coupling

In this case the spin-orbit interaction for each electron is much larger than the interaction between different electrons. So that *j's* of individual electrons combine together to form the resultant J. Good for highly ionized high Z (atomic number).

$|l_\nu - s_\nu| \leq j_\nu \leq |l_\nu + s_\nu|$ $\quad |j_\nu - j_\mu| \leq J \leq |j_\nu + j_\mu|$

The RCI code allows these two coupling mechanisms and it also allows intermediate coupling, that's not purely LS or J-J, where the computation itself determines the type of coupling.

6.4.2 Units

Quantity	Unit (au)	Conversion factors
Energy	Hartree	27.21 eV 219474.63 cm^{-1}
Transition probability	s^{-1}	s^{-1}
Electric dipole	$a_0^2\ e^2$	$8.478 \times 10^{-30}\ m^2\ C^2$
Electric quadrupole	$a_0^4\ e^2$	$2.013 \times 10^{-79}\ m^4\ C^2$
Magnetic dipole	$\mu_B^{\ 2}$	$8.601 \times 10^{-47}\ J^2T^{-2}$

References

1. Bacher, Robert Fox, and Samuel Abraham Goudsmit. *Atomic energy states*. Greenwood Press (1968).
2. Drake, Gordon WF, ed. *Springer handbook of atomic, molecular, and optical physics*. Springer Science & Business Media (2006).

6.5 Computer time and Resources

Our recourses are two PCs with 2.5 GHz AMD processors. The required time for computation includes preparing a few input files manually and many other files are prepared automatically. Preparing the angular momentum sections usually takes few seconds for those electronic configurations that have matrix size smaller than 1K x 1K. Angular momentum sections of more complicated configurations are done on several steps in the BCB calculation method. The time needed for each step is a few seconds but more human time is needed in this case. The main step and the core of the calculations is producing the radials (or the complete wavefunctions). This is the RCI run; a full matrix size of 20 K x 20 K takes about 55 minutes. Calculating the transition probabilities and oscillator strength in done in the next step of calculations and it take a few seconds.

6.6 Publications

6.6.1 Published papers

1. Marwa H Abdalmoneam and Donald R. Beck ,“ Magnetic dipole and electric quadrupole hyperfine constants for V II $3d^4$, $3d^3$ $4s$ and $3d^2$ $4s^2$ J=1-5 States ”, J. Phys. B **48** ,105001. (2015).
2. Marwa H Abdalmoneam and Donald R. Beck , “ Dipole and Quadrupole Polarizabilities of Ni II and Parameters of an Effective Potential for Ni I Rydberg States ”, J. Phys. B: At. Mol. Opt. Phys. 47 085003 (2014)

6.6.2 Presentations

1. Donald Beck and Marwa Abdalmoneam, “Relativistic configuration interaction lifetimes and transition probabilities for W II”, DAMOP, K1.5, 2012

http://meetings.aps.org/link/BAPS.2012.DAMOP.K1.5

2. Donald Beck and Marwa Abdalmoneam, “Role of d^{n-1} s configurations in hyperfine structure (HFS) of d^n levels in transition metal atoms and ions: Application to V II, DAMOP, D1.40, 2014

http://meetings.aps.org/link/BAPS.2014.DAMOP.D1.40

3. Marwa Abdalmoneam and Donald Beck, “ Dipole and quadrupole polarizabilities of Ni II and parameters of an effective potential for Ni I Rydberg states”, DAMOP, d1.51, 2014

http://meetings.aps.org/link/BAPS.2014.DAMOP.D1.51